Being Excited by Lanthanide Coordination Complexes: Aqua Species, Chirality, Excited-State Chemistry, and Exchange Dynamics

David Parker,* Rachel S. Dickins, Horst Puschmann, Clare Crossland, and Judith A. K. Howard

Department of Chemistry, University of Durham, South Road, Durham, DH1 3LE, U.K.

Received October 9, 2001

Contents

* To whom correspondence should be addressed. Fax: +(0)191 3844737. E-mail: david.parker@dur.ac.uk.

I. Introduction

Over the past 10 years there has been a resurgence of interest in the coordination chemistry of lanthanide complexes in aqueous solution. Excitement in this work may be related to an enhanced appreciation of the rich functionality of the ground and excited states of lanthanide complexes. The high-spin paramagnetism and long electronic relaxation time of Gd^{3+} has made it pre-eminent among contrast agents for magnetic resonance imaging (MRI).[1,2] Related complexes of Dy and Tm—with much shorter electronic relaxation times—are effective NMR shift reagents.[3] The controlled modulation of Lewis acidity across the series is allowing the development of complexes exhibiting phosphatase activity,[4] while the redox activity of cerium, samarium, and europium may be expected to allow the development of further selective oxidants and reductants.

Lanthanide complexes in solution exhibit a well-defined luminescence which is characterized by narrow emission bands, large Stokes' shifts, and long excited-state lifetimes. Europium and terbium complexes possess excited-state lifetimes in aqueous solution of up to 5 ms and emit in the red and green; they have been used as probes in fluoroimmunoassays[5,6] and show considerable promise in luminescence imaging and as sensors for certain bioactive ions.[7] The near-IR emission from the excited state of Nd^{3+}, Yb^{3+}, and Er^{3+} is less long-lived, but complexes of these ions offer much promise as probes in vivo as tissue is relatively transparent to incident light with a wavelength of around 1000 nm.

In this review we have set out to highlight the complexation chemistry of lanthanide ions in aqueous solution that has caused us and others to progress from a state of 'getting excited' [8] in 1996 to 'being excited' in 2002! In the past few years several excellent reviews have appeared detailing aspects of contrast agent structure and solution dynamics,[1,2,12] biomedical and NMR applications,[1,2,9] complex design features,[10] thermodynamic aspects of complex formation,[1,11] the development of luminescent lanthanide complexes operating in aqueous media,[5,6,12] and the diagnostic and therapeutic uses of lanthanide−texaphyrin and −porphyrin complexes.[14,15] Here we have set out to review only lanthanide complexes which are water soluble. We highlight structural aspects of the lanthanide−water bond by a comprehensive analysis of the Cambridge Structural Database (CSD) of all published species in coordination number 9,

10.1021/cr010452+ CCC: $39.75
Published on Web 05/21/2002

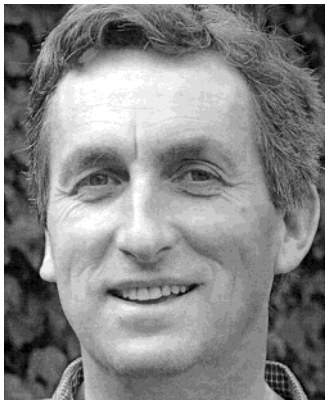

David Parker is a native of the Northeast of England and received three degrees from Oxford University, studying asymmetric catalysis for his D.Phil. degree with John Brown. After a NATO postdoctoral fellowship with Jean-Marie Lehn in Strasbourg, he was appointed as a Lecturer at the University of Durham in 1982. Promotion to Senior Lecturer and soon afterward a Chair in Chemistry (1992) was followed by a period serving as Head of Department. His research interests currently embrace many aspects of tailored metal complexes and their conjugates from sensors and diagnostic agents to therapeutics. The author of over 250 papers and patents, he has received several awards and prizes, most recently the inaugural IBC Award in Supramolecular Science and Technology.

Rachel S. Dickins received her B.Sc. degree in Chemistry at the University of Durham in 1994 and stayed on to study for her Ph.D. degree with David Parker. She devised several new series of emissive chiral lanthanide complexes, examining the selectivity of their interaction with anions. In 1997 she took up a position as a Research Scientist at Organon in Lanark, Scotland, where she became familar with modern approaches to library synthesis. She returned to Durham two years later and was awarded a Royal Society Dorothy Hodgkin Fellowship in 2000 to study new aspects of magnetic resonance shift and relaxation agents.

possessing between one and nine bound water molecules, focusing on $q = 1$, 2, and 9 systems. In addition, we have sought to update aspects of inter- and intramolecular exchange processes, summarize advances in magnetic resonance spectroscopy, and review the developments in the excited-state chemistry of luminescent lanthanide complexes. Throughout there is an emphasis on chiral systems, and although there is necessarily a degree of overlap with some of the recent reviews cited above, the intention is to provide an update and where appropriate focus on literature published in the period 1994−2001.

II. Structural Analysis of Nine Coordinate Aqua–Lanthanide Complexes

Much of the current research into the chemistry of lanthanide complexes is carried out in the solution

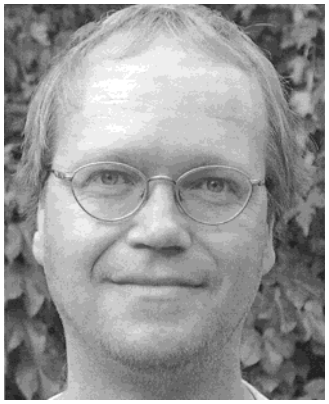

Horst Puschmann completed his B.A. degree in Chemistry at the University of Oxford in 1992, where he was involved in the synthesis of potentially useful Gd-complexing ligands. A move to the other side of the world saw him working for his Ph.D. degree with David Weatherburn at Victoria University of Wellington in New Zealand, focusing on trinuclear carboxylato complexes of first-row transition metals. Much of this work involved X-ray structural analysis, and he became more and more interested in this field so that he eventually took a research position with Judith Howard at the University of Durham. He has recently joined the research group of David Parker, focusing on structural aspects of lanthanide chemistry.

Clare Crossland received her M.Sci. degree in Chemistry in 2001 from the University of Durham. During her final year undergraduate project, she undertook a database analysis of aqua metal ion species, part of which has been used as the basis for section I of this article. She is currently studying for her Ph.D. degree with John S. O. Evans at Durham on solid-state oxy–sulfide materials.

Judith Howard is the Professor of Structural Chemistry at the University of Durham, a position she has held since 1991. Her research interests embrace X-ray and neutron crystallography at ultralow temperatures and under pressure and include high-resolution charge density studies. After working at Oxford for her D.Phil. degree with Dorothy Hodgkin O.M., she was appointed to the staff at Bristol University, where she established a significant crystallography group within the Inorganic Chemistry Department of F. G. A. Stone. She has gained several awards, including a CBE for 'services to science' and is currently an EPSRC Senior Research Fellow.

state—and rightly so. It is the properties of these complexes in aqueous solution that are of great interest scientifically, medically, and therefore commercially.

However, exact information about conformation, bond distances, and bond angles within a complex can only be obtained from the solid state through diffraction techniques. Furthermore, potentially important interactions between the complex and its environment in solution—and specifically the interaction with solvent water molecules—may be probed through the study of the solid-state structure.

Of specific interest in this review is the geometric 'makeup' of nine-coordinate lanthanide complexes where there is at least one ligating water molecule present. With respect to MRI contrast agents, those in which the number of bound water molecules is either one or two ($q = 1$ or 2) are of particular interest. A closer examination of the other limiting case, where $q = 9$, i.e., the nona-aqua complexes, has also been undertaken. These complexes may be regarded as representing the 'model situation' where no other ligand effects are present except for those ascribed to water molecules.

A. Source of Data

All data relevant to this discussion were obtained from the Cambridge Structural Database (October 2000 release).[16] The search strategy employed, the actual search queries, as well as the full search results are available in electronic form at http://www.dur.ac.uk/dp.group/supplementary.htm.

B. Complexes with Nine Coordinated Water Molecules ($q = 9$)

The metal−water bond distances for all water ligands in nine-coordinate lanthanide aqua ions in the CSD are summarized in Figure 1, showing the variation of the M−O distances sorted for each lanthanide ion.

Along the lanthanide series there is a decrease in the average length of a metal−water bond. This trend corresponds to the decreasing metallic radius of the lanthanide ion. In 36 of the known lanthanide nona-aqua ion structures there are two distinct metal−water bond lengths in a particular aqua ion. Each of the structures in which this trend is seen has the same crystallographic space group, $P6_3/m$, and in every case the anion is either ethyl sulfate ($EtOSO_3^-$) or triflate ($CF_3SO_3^-$). Structures that have a chemically more complex counterion do not crystallize in the $P6_3/m$ space group. These form crystals with lower symmetry space groups, and the metal−water bond lengths in these aqua ions vary over a wider range of values.

For aqua ions containing a given metal atom there is a variation in the length of metal−water bonds. This is expected for structures in which the coordination environment of the water ligands is different, but even structures that have the same geometry around the metal atom (and thus the same coordination environment of the ligands) have different

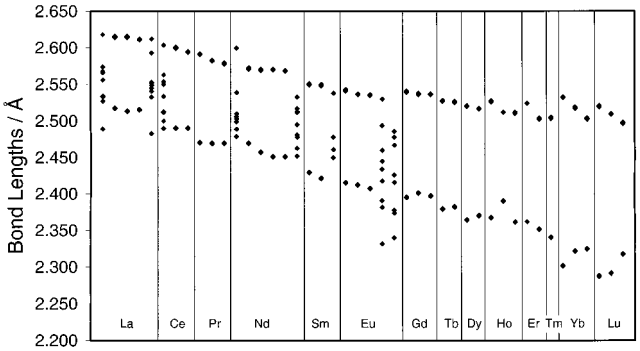

Figure 1. Metal−water bond lengths in lanthanide nona-aqua ions sorted by the metal involved.

metal−water bond lengths. This is seen in the two ytterbium complexes, CSD reference codes BUVYEW01[17] and ESULYB (Chart 1).[18] The crystal structures of both of these complexes have been determined at 295 K and are in the $P6_3/m$ space group. The arrangement of the ligands around the metal center is the same in each case. In BUVYEW01 the counterion is triflate and the two metal−water bond lengths are 2.302(3) and 2.532(3) Å. In ESULYB, which has an ethyl sulfate counterion, the bond lengths are 2.322(3) and 2.517(3) Å. This suggests that the length (and strength) of the metal−water bonds in lanthanide aqua ions is not determined solely by the coordination environment. The counterion and arrangement of molecules in the crystal must also be important. In particular, the counterion, which appears to affect the length of metal−water bonds, may play an important part in the water exchange process.

C. Complexes with Two to Eight Coordinated Waters ($q = 2$–8)

There are a total of 41 entries in the CSD for compounds containing two coordinated water molecules. For all but one compound (AFACND) the two distances to the water molecules are almost the same: in 18 of the complexes the longer distance is less than 1% longer, in 13 it is between 1% and 2% longer, and in 10 complexes it is found to be between 2% and 5% longer. In AFACND (Chart 1),[19] however, it is reported to be 19% longer: 2.444(4) and 2.922(3) Å, respectively. The compound is a dimeric, fluoroacetate-bridged Nd complex. There are six other complexes of this carboxylato-bridged type with a similar geometric arrangement of the ligands in the CSD, and in none of them is the longer bond elongated by more than 0.8%.

Eighty eight compounds in the CSD are lanthanide complexes with three coordinated water molecules, 37 have four molecules of water, 25 have five, 10 have six, 5 have seven, and only 1 has eight water molecules bound to a lanthanide ion where $n = 9$. The largest difference between the longest and shortest distance to the water molecule is exhibited in PUBVOX,[20] where the elongation is as much as 20%. The distance to this water molecule in this peculiar Sm complex is 2.885(3) Å, which is particularly long.

Chart 1

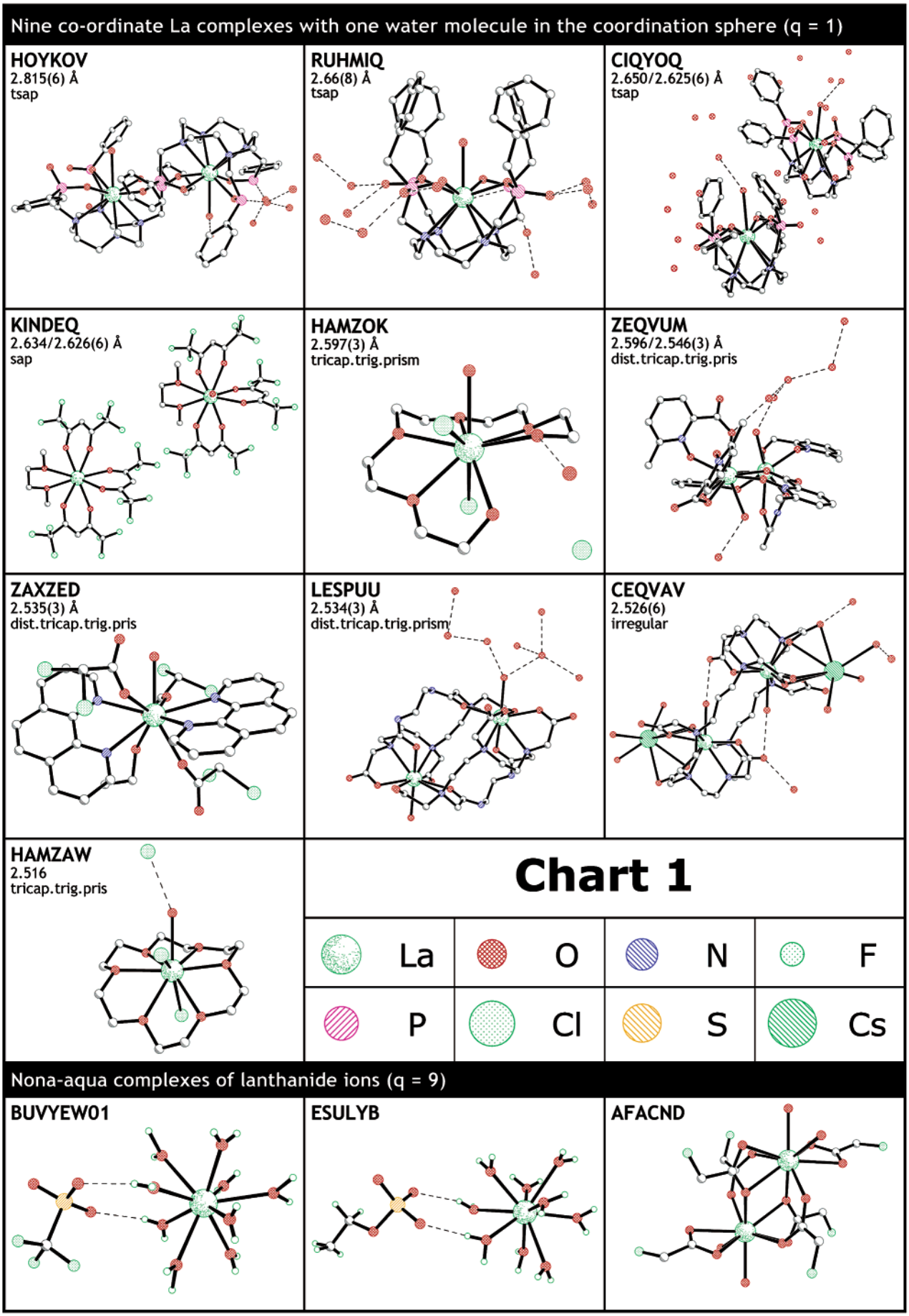
Nine co-ordinate La complexes with one water molecule in the coordination sphere (q = 1)
HOYKOV
2.815(6) Å
tsap
RUHMIQ
2.66(8) Å
tsap
CIQYOQ
2.650/2.625(6) Å
tsap
KINDEQ
2.634/2.626(6) Å
sap
HAMZOK
2.597(3) Å
tricap.trig.prism
ZEQVUM
2.596/2.546(3) Å
dist.tricap.trig.pris
ZAXZED
2.535(3) Å
dist.tricap.trig.pris
LESPUU
2.534(3) Å
dist.tricap.trig.prism
CEQVAV
2.526(6)
irregular
HAMZAW
2.516
tricap.trig.pris
Chart 1
La
O
N
F
P
Cl
S
Cs
Nona-aqua complexes of lanthanide ions (q = 9)
BUVYEW01
ESULYB
AFACND

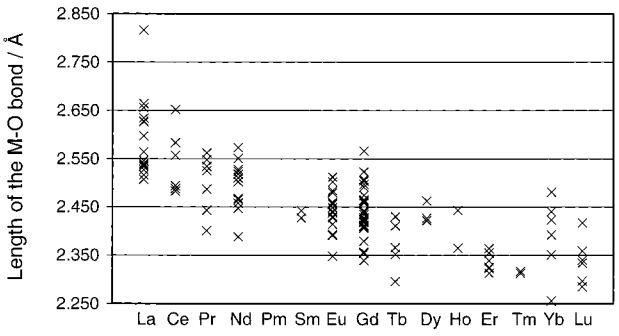

Figure 2. Distances from the metal atom to the coordinated water molecule for all structures in the CSD that contain a nine-coordinate lanthanide ion with only one coordinated water molecule ($q = 1$).

D. Complexes with One Coordinated Water Molecule ($q = 1$)

There are 129 structures in the CSD that contain a nine-coordinate lanthanide ion with a single coordinated water molecule; all the lanthanide metals are represented except promethium. Several factors have been considered in order to try and find out what determines the metal−water bond lengths in these complexes. These include the type of donor atoms in the ligands, the number of coordination sites in the ligand, the crystallographic space group, and the geometry of the lanthanide coordination sphere. In Figure 2 the metal−water bond lengths for these complexes are summarized.

Across the lanthanide series the expected general trend is for the metal−water bond length to decrease. This is found and corresponds to the decreasing atomic radius of the lanthanide metal ion.[23] In addition, there is also some variation in metal−water bond length for different structures containing the same metal ion. For example, in complexes of lanthanum, the metal−water bond length ranges from 2.507 to 2.816 Å, a variation of 0.309 Å. For complexes containing cerium, the difference is even greater (0.370 Å) with bond lengths ranging from 2.483 to 2.853 Å. For the smaller lanthanides, the range of metal−water bonding distances is smaller than that for lanthanum and cerium. For example, with gadolinium the bond length differences fall within a range of 0.227 Å, while europium−water bond lengths range over 0.164 Å. A comparison of the variation in metal−water bond lengths for both nona-aqua ions and nine-coordinate complexes with one coordinated water molecule is provided in Table 1.

For each of the complexes studied only the relevant part of the coordination sphere was considered, namely, the metal ion, the oxygen atom in the coordinated water molecule, and the four atoms that make up the face of the square antiprism capped by the water molecule (Figure 3). Several parameters were determined for each complex as follows: the position of the coordinated water molecule, O_w, relative to the plane defined by the four ligand oxygen atoms, O_L; an artificial centroid, X, placed in the center of the plane of the four ligand oxygen atoms, the angles between the centroid water vector, $X-O_w$, and the centroid ligand atom vector, $X-O_L$, for each of the four ligand atoms; the metal centroid distance, Ln−X, and centroid water distance, $X-O_w$, for each complex. These parameters can be analyzed to show how the water molecule changes position relative to the plane of oxygen atoms as the metal−water distance increases.

Table 1. Mean Metal−Water Bond Lengths and the Average Deviation from the Mean Bond Length of Metal−Water Bond Lengths in Nine-Coordinate Lanthanide Complexes with One Coordinated Water Molecule and in Nona-aqua Ions of the Lanthanides

	nona-aqua ions			nine-coordinate complexes		
		metal−water bond length/Å			metal−water bond length/Å	
metal	no.	mean	average deviation from mean	no.	mean	average deviation from mean
La	5	2.550	0.037	16	2.593	0.059
Ce	3	2.529	0.042	7	2.587	0.094
Pr	3	2.508	0.051	7	2.500	0.048
Nd	6	2.495	0.044	12	2.494	0.041
Sm	3	2.468	0.043	2	2.435	0.008
Eu	5	2.442	0.050	21	2.444	0.028
Gd	3	2.445	0.062	31	2.439	0.040
Tb	2	2.430	0.065	5	2.371	0.040
Dy	2	2.418	0.067	4	2.434	0.015
Ho	3	2.421	0.064	2	2.404	0.039
Er	2	2.409	0.070	7	2.340	0.018
Tm	1	2.395	0.073	2	2.315	0.002
Yb	3	2.383	0.090	6	2.391	0.058
Lu	3	2.354	0.061	7	2.323	0.045

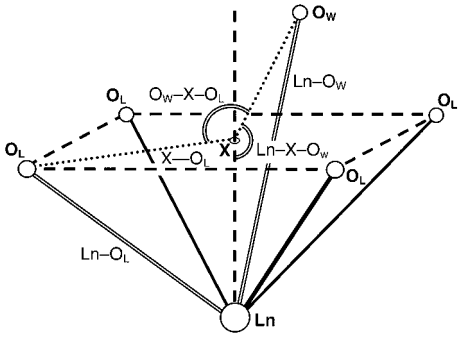

Figure 3. Diagram showing the part of the complex used when comparing the position of coordinated water in different complexes.

There were four lanthanum complexes in the CSD with octadentate ligands and a square-antiprismatic geometry. The variation of the O_w-X-O_L bond angles with the distance of the coordinated water oxygen atom from the centroid, $X-O_w$, is shown in Figure 4.

For the lanthanum and cerium complexes studied, as the water molecule gets further away from the plane of oxygen atoms, the variation in the O_w-X-O_L angles (indicated by the spread of points for a particular $X-O_w$ distance) increases. This means that for complexes with long metal−water bonds, the $X-O_w$ vector is no longer normal to the plane. This is confirmed by considering how the angle $La-X-O_w$ changes as the centroid−water distance increases. As the distance increases, the $La-X-O_w$ angle decreases, i.e., it gets further away from being 180°, Figure 5.

The same trends are seen for the three complexes of cerium that were studied. This change in the position of the coordinated water molecule may

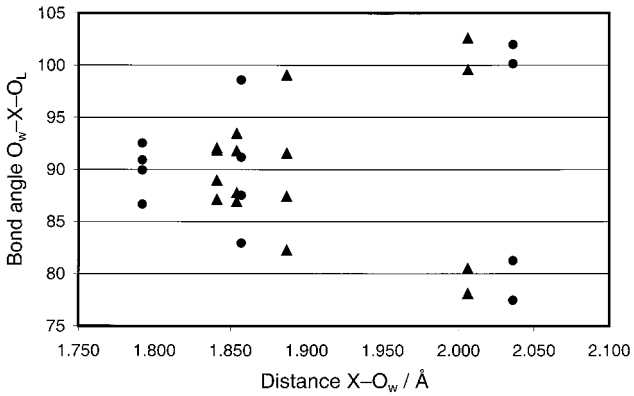

Figure 4. Variation of the angle between the centroid−water vector, X−O_w, and the centroid−ligand vector, X−O_L, as the centroid−water distance, X−O_w, changes. Lanthanum complexes are denoted by triangles and Cerium complexes by filled circles.

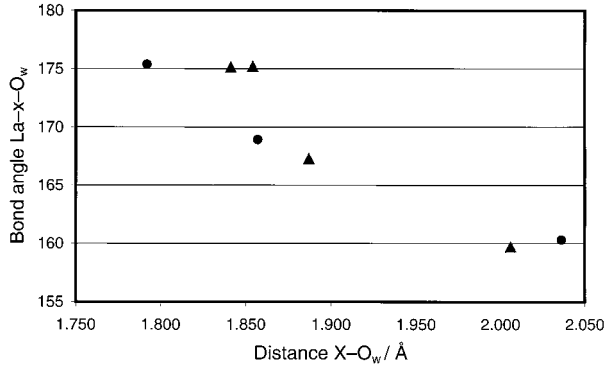

Figure 5. Variation in M−centroid−water angle, La−X−O_w, as the coordinated water molecule moves further away from the plane of oxygen atoms. Triangles refer to La complexes and filled circles to Ce complexes.

indicate that there is a significant interaction between the coordinated water molecule and the ligand. This can be further investigated by considering what causes the variation in the metal−water bond length.

The study of lanthanum and cerium complexes with very long metal−water bonds suggests that the most significant factor in determining their metal−water bond lengths is the coordination geometry of the metal center and the steric interactions between the water molecule and other atoms in the ligand. The change in metal−water distance with geometry is confirmed by a wider study of other lanthanide complexes. The data in Table 2 show the metal−water bond length for several lanthanum complexes and the corresponding geometry around the metal atom.

There is a clear correlation between the coordination geometry around the lanthanum ion and the length of the metal−water bond. The longest bonds are found in twisted square-antiprismatic complexes. It is likely that in these complexes the arrangement of the ligating atoms restricts the approach of the water molecule to the metal center. The oxygen atom in the water molecule cannot get close to the metal atom without buttressing atoms in the ligand, giving rise to steric repulsion. In the tricapped trigonal prismatic geometry, the water molecule is able to get closer to the metal center without encountering such

Table 2. Variation of Metal−Water Bond Length with the Coordination Geometry for Nine-Coordinate Lanthanum Complexes with One Coordinated Water Molecule

CSD refecode	M−H_2O distance/Å	geometry of lanthanum center
HOYKOV[21]	2.815(6)	twisted square antiprism
RUHMIQ[22]	2.66(8)	twisted square antiprism
CIQYOQ(A)[24]	2.650(6)	twisted square antiprism
KINDEQ(A)[25]	2.634(6)	square antiprism
CIQYOQ(B)[24]	2.625(6)	twisted square antiprism
KINDEQ(B)[25]	2.626(6)	square antiprism
HAMZOK[26]	2.597(6)	tricapped trigonal prism
ZEQVUM(A)[27]	2.596(3)	distorted tricapped trigonal prism
ZEQVUM(B)[27]	2.546(3)	distorted tricapped trigonal prism
ZAXZED[28]	2.535(3)	distorted tricapped trigonal prism
LESPUU[29]	2.534(2)	distorted tricapped trigonal prism
CEOVAV[30]	2.526(6)	irregular polyhedron
HAMZAW[26]	2.516(4)	tricapped trigonal prism

steric interactions with the ligand. For the other lanthanide ions (Ce−Yb), crystal field variations across the series may perturb the analysis. Such effects are most pronounced when the water molecule occupies an axial coordination site (see sections IV.C and VI.A).

Examination of the $q = 1$ series has also shown that there is no obvious variation of metal−water bond length with ligand denticity. There is just as much variation in the metal−water bond length for complexes with octadentate ligands as there is in complexes with eight monodentate ligands. The increased rigidity of the ligand does not appear to restrict the bond lengths.

E. Concluding Remarks

The factors that influence the metal−water bond length in nine-coordinate lanthanide complexes are complicated. The nature of the metal ion and its coordination geometry are important, as is interaction between the coordinated water molecule and hydrogen-bond acceptor groups in the ligand. For complexes with long bonds, the geometry is such that there is usually more interaction between the water molecule and atoms in the ligand than there is in complexes with shorter metal−water distances.

More work is needed in this area. The small number of complexes where structural data are available is certainly the limiting factor in reaching firm conclusions. In particular, systematic studies involving only one variable are badly needed: keeping the counterion constant and varying the metal, keeping the ligand constant and varying the metal, and keeping the metal constant with a varying counterion—this sort of experimental data is bound to return valuable information about the structure−solution properties relationship.

A first step in this direction has very recently been reported.[270] Crystal structures of the mono-aqua complexes of DOTMPhA (Chart 2) with a common triflate counterion and common SAP geometries have been solved for Ce, Pr, Eu, Gd, Dy, and Yb. While the variation of ligand O−Ln and N−Ln distances faithfully follow the ionic radius change,[23] the Ln−OH_2 distances do not (Figure 6). The Ln−OH_2 distances were found to vary with the crystal form

Chart 2

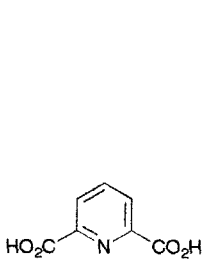

DPA

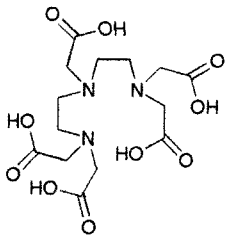

DTPA

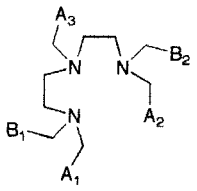

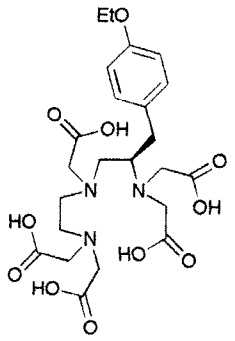

EOB-DTPA

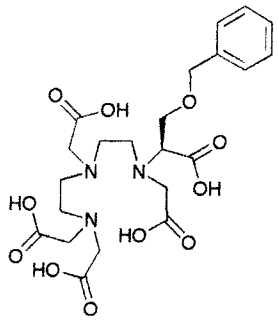

BOPTA

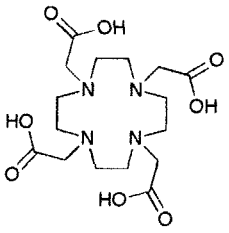

DOTA

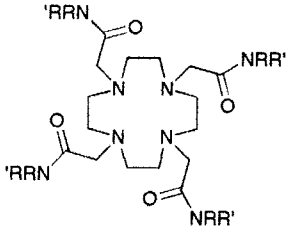

R = R' = H : DOTAM
R = Me, R' = H DTMA
R = R' = Me DOTTA

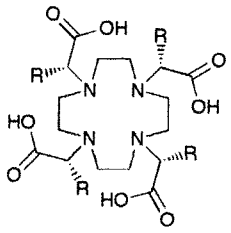

R = Me DOTMA
R = $CH_2CH_2CO_2H$ gDOTA

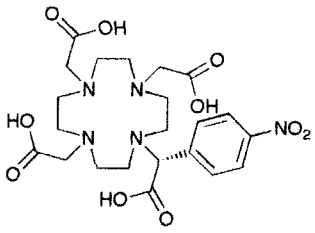

DOTA-pNB

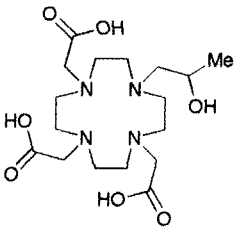

HPDO3A

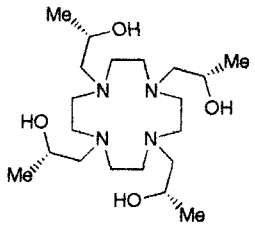

(SSSS)-THP

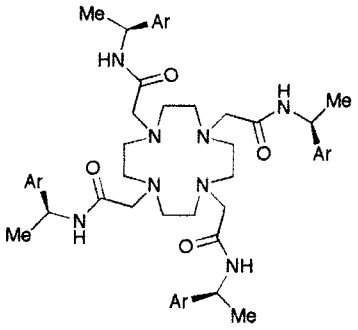

Ar = Ph DOTMPhA
Ar = 1-Np DOTMNpA

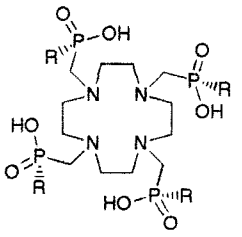

R = Me DOTMP
R = Bn DOTBP
R = Et DOTEP
R = Ph DOTPhP
R = OCH_2CF_3 DOTFEP

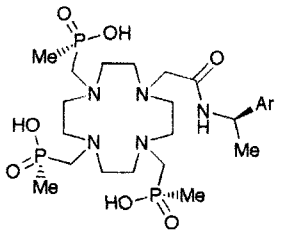

Ar = Ph (S)-DO3MPPhA
Ar = 1-Np (S)-DO3MPNpA

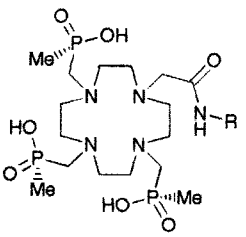

R = Me DO3MPMA

adopted and the degree of solvation of the complex and were also sensitive to variation of the anion, e.g., NO_3^-, ClO_4^-, and $CF_3SO_3^-$. Complexes where the bound water acted as a hydrogen-bond donor to the oxygen of a second sphere water possessed shorter $Ln-OH_2$ bonds than those in which the bound water

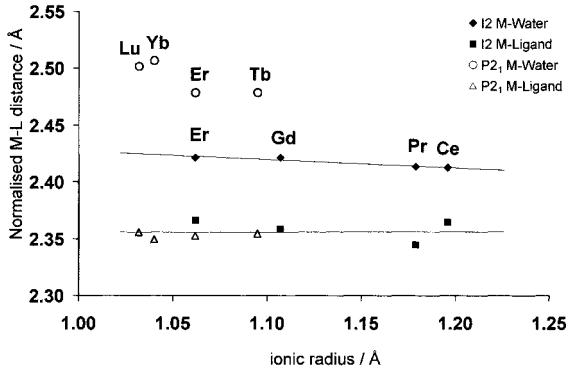

Figure 6. Variation of Ln−OH_2 and Ln−O (ligand) distances in complexes of DOTMPhA (Chart 2).

served as a hydrogen-bond acceptor. Such observations, coupled with the slowness of the measured dissociative water exchange rate (section IV.C) at Gd/Eu compared to Yb (500 times faster) or Ce/Pr (100 times faster) suggest that the position of the transition-state structure may vary from 'late' for the smaller Ln ions (longer bond) to early for the central ions (ground-state stabilized).

III. Chirality of Lanthanide Complexes in Aqueous Solution

A. Static Analysis of Stereoisomerism

The stereoisomerism associated with lanthanide complexes is relatively well understood and has been documented in a number of recent reviews.[1−3] A brief description of the possible solution isomers of representative classic chiral systems is presented here. The ratio of isomers observed in solution is dependent on a large number of factors. These include the nature of the lanthanide ion, solvent, temperature, pressure, concentration, and the type of counterion, in addition to the concentration of added salt and, of course, the ligand structure.[1−3,31−33] Exchange processes, allowing the interconversion of isomeric species, are described in detail in section IV.

1. Acyclic Ligands

When a tridentate ligand such as pyridine-2,6-dicarboylate (DPA) (Chart 2) binds to a lanthanide ion, an anionic tris chelate complex is formed. The ligands arrange around the lanthanide in a three-bladed 'propeller-like' manner and can form a left- or right-handed helix about a 3-fold symmetry axis. The two enantiomeric species formed are denoted Λ or Δ and are present as a racemic solution in water at room temperature.

The octadentate coordination of DTPA, involving ligation of three nitrogens and five monodentate carboxylate oxygens, results in the formation of two enantiomeric species. These chiral "wrapping" isomers, $\lambda\lambda$ and $\delta\delta$, are distinguished by the helicity of the C−C ethylene bond relative to the Ln^{3+}−N−N plane and may interconvert through a shuffling of the acetate groups accompanied by a flip of the diethylenetriamine backbone. The central nitrogen atom in DTPA is therefore chiral when coordinated as a result of this helicity. Nitrogen inversion in the diethylenetriamine backbone is inhibited upon binding to the Ln(III) ion. Therefore, unsymmetrical substitution will render the terminal nitrogens chiral upon chelation and consequently increase the number of possible stereoisomers. For example in bis(amide) derivatives where $A_1 = A_2 \neq B_1 = B_2$ (Chart 2), the two terminal nitrogens become chiral upon complexation and give rise to four diastereomers (these have been termed nonsystematically 'cis', 'trans', 'syn', and 'anti'),[1,2] each of which can exist in the two "wrapping" isomer forms giving rise to eight possible isomers (four enantiomeric pairs) (Figure 7). In cyclic DTPA−bisamides, the steric constraints of the tether render the 'trans' and 'anti' isomers sterically unfavorable and only the 'cis' and 'syn' exist in the two 'wrapping isomer' forms.

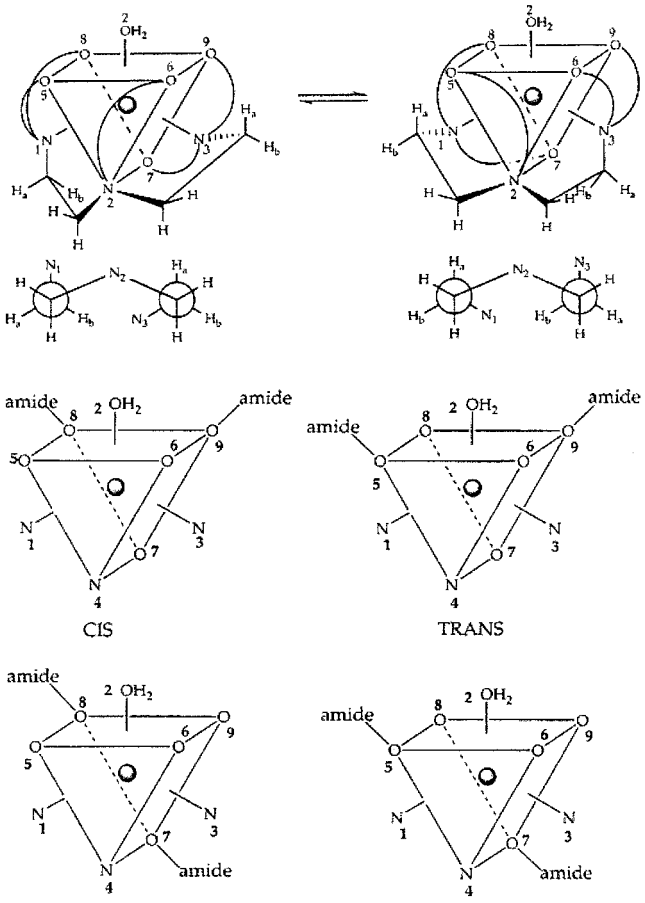

Figure 7. Two 'wrapping' isomers of $[LnDTPA]^{2-}$ complexes (upper), and the four possible diastereoisomers conformations of [LnDTPA-bisamides] in a tricapped trigonal prismatic arrangement.

In Ln complexes of BOPTA ($A_1 = B_1 = B_2 \neq A_2$), the terminal and central nitrogens are chiral. The presence of a stereogenic center (in A_2) coupled with the two 'wrapping isomers' gives rise to 16 possible stereoisomers. Derivatization of the diethylenetriamine backbone, e.g., EOB-DTPA (Chart 2), renders the central nitrogen chiral upon complexation. Two chiral centers and the two wrapping isomers result in eight possible stereoisomers, which reduces to four diastereomers when the ligand is enantiopure.

2. DOTA and Derivatives

In lanthanide complexes of DOTA, the four ethylenediamine groups adopt gauche conformations giv-

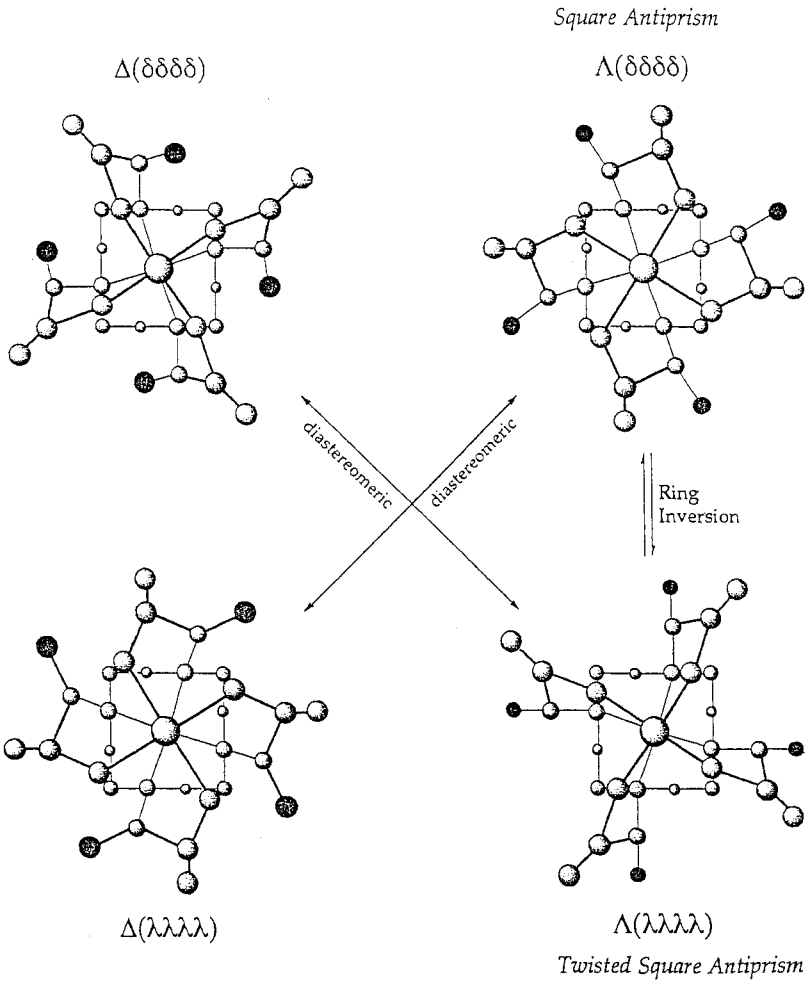

Figure 8. Schematic representation of the four C_4-symmetric diastereoisomeric [LnDOTA]$^-$ complexes in which there is an arbitary α-substituent of common configuration. Interconversion of SAP and TSAP diastereomers by arm rotation is sterically inhibited in such systems.

ing rise to two macrocyclic ring conformations, *λλλλ* and *δδδδ*. There are also two possible arrangements for the acetate arms, Λ or Δ, resulting in four possible stereoisomers, existing as two enantiomeric pairs. The stereoisomers adopt either a capped square-antiprismatic (CAP) geometry with a twist angle ~40° (Λ(*δδδδ*) and Δ(*λλλλ*)) or a twisted SAP geometry (TSAP) with twist angle ~30° (Δ(*δδδδ*) and Λ(*λλλλ*)) (Figure 8). The isomers may interconvert in solution by ring inversion (*λλλλ* ↔ *δδδδ*) or arm rotation (Λ ↔ Δ). Either process alone exchanges between monocapped SAP and twisted SAP geometries, while both processes combined in succession or in concert result in exchange between enantiomeric pairs. The isomer ratio is dependent on the Ln ion, temperature, pressure, and concentration of added salts.[31−33] For the larger lanthanides, La^{3+}−Nd^{3+}, the twisted square antiprism (TSAP) is favored, whereas the SAP is the major species observed for smaller lanthanides, Sm^{3+}−Er^{3+}.[31,32]

Ligand structure also affects the isomer ratio. Introduction of four symmetrically distributed (*RRRR*/*SSSS*) substituents α to the ring N, e.g., DOTMA and TCE-DOTA, or one substituent DOTA-pNB renders each of the isomers depicted in Figure 8 diastereomeric. The absolute configuration at the stereogenic carbon center determines the favored helicity (Δ or Λ) of the complex. Only two diastereomers are observed in aqueous solution with TSAP geometries dominating for the central Ln ions.[34−36] In contrast, introduction of a single chiral center *β* to the ring N, e.g., HP-DO3A, does not appear to favor a particular helicity, and for [YHPDO3A], multiple isomers are observed in solution.[37] Introduction of four symmetrical-disposed chiral centers *β* to the ring nitrogen, as in (*SSSS*)-THP, however, results in preferential formation of one out of the four possible diastereomers in solution.[38]

The tetraamides DOTAM, DTMA, and DOTTA behave similarly to DOTA and exist as two diastereomeric species in aqueous solution, the TSAP form being favored as the steric demand (i.e., the bulk of the amide substituents) at the metal center increases.[34,39−44] A chiral center *δ* to the ring nitrogen, e.g., DOTMPhA, imparts considerable conformational rigidity, inhibiting arm rotation. This results in the exclusive formation of one diastereomer in solution (out of a possible four). The configuration of the chiral center again determines the helicity of the pendant arms and also the macrocyclic ring conformation (i.e., *R* and *S* at carbon producing SAP geometries Λ(*δδδδ*) and Δ(*λλλλ*), respectively).[45,46]

Lanthanide complexes of phosphinates generate a chiral center at P on coordination. Six isomers are

possible (*RRRR*/*SSSS*, *RRRS*/*SSSR*, *RRSS*, *RSRS*), and each can have the two ring conformations and pendant arm helicities generating 24 isomers (16 diastereomers) and 8 enantiomeric pairs. For DOTBP and DOTMP, such is the steric demand that >90% of one major species is observed in solution, existing as an enantiomeric pair in the TSAP geometry (*RRRR*-Λ-($\lambda\lambda\lambda\lambda$) and *SSSS*-Δ-($\delta\delta\delta\delta$)).[22,47] However, complexes of the tetraphenyl analogue, DOTPhP, and the fluorinated ethyl ester analogue, DOTFEP, exist as a fairly random mixture of stereoisomers in solution.[48,49] Replacement of a phosphinate arm with a carboxamide, e.g., DO3MPMA, results in 32 possible isomers (*RRR*/*SSS*, *RRS*/*SSR*, *RSR*/*SRS*, *RSS*/*SRR* with respect to P). One enantiomeric pair predominates in aqueous solution with a suggested TSAP geometry.[50,51] Introduction of a chiral center in the carboxamide moiety, e.g., DO3MPPhA and DO3MPNpA, renders each of the 32 isomers diastereomeric. For the Eu complex, only two isomers were observed in aqueous solution in a ratio dependent on the size of the chiral group (2:1 for DO3MPPhA and 4:1 for DO3MPNpA), with suggested TSAP geometries in which the P−Me groups are directed away from the macrocycle; there is a preferred *RRR*/*SSS* configuration at P.[51] The remote chiral group again acts as a stereodifferentiating moiety and favors a particular pendant arm helicity and ring conformation.

B. Chiroptical Spectroscopy

1. Natural Circular Dichroism and Circularly Polarized Luminescence

Chiral lanthanide complexes are amenable to study by circular dichroism, CD (the differential absorption of left and right circularly polarized light), and more particularly circularly polarized luminescence, CPL (the differential spontaneous emission of left and right circularly polarized light). The application of such chiroptical methods has been surveyed in a number of reviews.[52−60] Chiroptical properties of lanthanides are particularly sensitive to ligand coordination geometry and stereochemistry, electronic state structure, and the interactions between a complex and its environment. Natural CD and CPL are only exhibited by systems displaying some element of chirality which may be reflected in the chiral arrangement of ligands, a chiral conformation, or the presence of stereogenic centers in the coordinating ligands.

Whereas CD reflects ground-state structure, CPL probes the structure of the excited state.[53] Generally a high concentration of lanthanide complex is required for CD studies as most 4f−4f transitions are parity forbidden and have very low molar absorptivities. This may pose problems due to possible oligomerization[61] occurring or where there is a necessity to study dilute solutions, for example, in bimolecular lanthanide complexes. CPL however combines instrument sensitivity with structure selectivity and may be carried out on dilute solutions. The greatest sensitivity is observed for Tb^{3+} ($^7F_J \leftarrow ^5D_4$) and Eu^{3+} ($^7F_J \leftarrow ^5D_o$) and to a lesser extent Sm^{3+} ($^6H_J \leftarrow ^4G_{5/2}$), Yb^{3+} ($^2F_{5/2} \leftarrow ^2F_{7/2}$), and Dy^{3+} ($^6H_J \leftarrow ^4F_{9/2}$) systems. It is common to report CD and CPL results in terms of an absorption dissymmetry factor g_{abs} (eq 1) and an emission dissymmetry factor g_{em} (eq 2) where ϵ_L, ϵ_R, I_L and I_R, are molar absorption coefficients and emission intensities for left- and right-handed circularly polarized light.

$$g_{abs}(\lambda) = \frac{2(\epsilon_L - \epsilon_R)}{(\epsilon_L + \epsilon_R)} \quad (1)$$

$$g_{em}(\lambda) = \frac{2(I_L(\lambda) - I_R(\lambda))}{(I_L(\lambda) + I_R(\lambda))} \quad (2)$$

This may be related to the rotatory strength R_{ab} associated with the given transition (between arbitrary states a and b), which is the product of the electric $|P_{ab}|$ and magnetic-dipole $|M_{ba}|$ transition moment vectors modified by the angle between them, τ_{ab} (eq 3).

$$R_{ab} = |P_{ab}||M_{ba}| \cos \tau_{ab} \quad (3)$$

It can be shown that—for axially symmetric systems—the emission dissymmetry factor, g_{em}, may also be approximated by eq 4, in which D_{ab} is the electric-dipole strength of the given transition which approximates to the square of $|P_{ab}|$.[62,63]

$$g_{em}(\lambda) = \frac{4R_{ab}}{|D_{ab}|} \approx \frac{4|M_{ba}|}{|P_{ab}|} \cos \tau_{ab} \quad (4)$$

Thus, lanthanide complexes may show large dissymmetry factors in those magnetic-dipole-allowed transitions which have weak electric-dipole character, while the most intense CPL transition will tend to be both magnetic- and electric-dipole allowed. With the exception of europium(III) complexes, the large number of possible transitions between different *J* states renders chiroptical spectra complex for most lanthanide systems. Indeed, a full exploitation of structural studies awaits further analysis of spectral−structure correlations.[79] Herein we discuss CD and CPL spectra exhibited by some recently reported lanthanide complexes in aqueous solution.

Mirror-image CD spectra arising from the chiral ligand have been reported for the enantiopure europium complexes of (*RRRR*)-Λ- and (*SSSS*)-Δ-DOTMNpA in aqueous methanol solution.[64,65] Insight into the solution structure of the complexes was ascertained from the CD spectrum, as strong exciton coupling between the naphthyl chromophores was displayed, characterized by a bisignate profile around 222 nm (e.g., g_{abs} (219) = -6×10^{-3}, g_{abs} (229) = $+3 \times 10^{-3}$ for (*R*)-Λ-[EuDOTMNpA]. Given that the amplitude of exciton coupling is maximal when the dihedral angle between the two chromophores is ca. 70° and tends to zero as the angle approaches 0° or 180°, the naphthyl chromophores must be in a near orthogonal relationship to one another in solution. The constitutionally isomeric 2-Np-substituted Eu complexes showed no exciton coupling[67] nor did the analogous 1-quinolyl systems.[66] Circular dichroism associated with f−f transitions in lanthanides in a

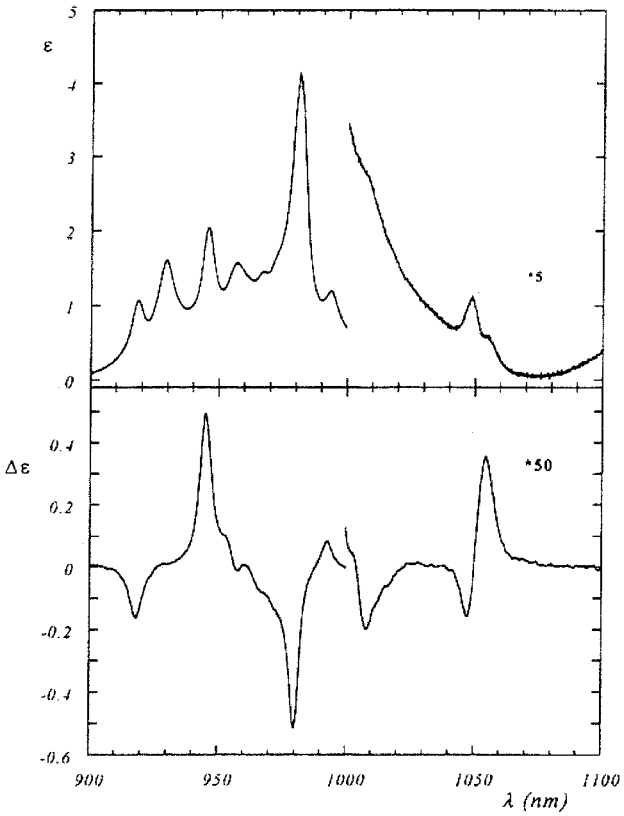

Figure 9. Near-IR absorption (upper) and CD spectra of $[YbDOTMA]^-$ (H_2O, 0.16 M) showing several of the allowed transitions from $^2F_{7/2} \rightarrow {}^2F_{5/2}$.

chiral environment is rather weak and difficult to observe. However, near-IR CD from ytterbium, centered around 980 nm associated with the magnetic-dipole-allowed $^2F_{5/2} \leftarrow {}^2F_{7/2}$ transition, has been reported recently (Figure 9). The chiral C_4-symmetric Yb^{3+} complex of DOTMPhA and DOTMBrPhA (Charts 2 and 3) gave rise to an observable CD signal ($g_{em}^{995} = 0.18$) with rich associated fine structure, although due to band overlap and the presence of up to 12 transitions no interpretation was attempted.[46,68] However, the form of the CD and CPL spectra were remarkably sensitive to the nature of the axial donor ligand. Salvadori et al. also reported CD from (*RRRR*)-[YbDOTMA] in water ($g_{abs}^{946} = +0.25$), which exists as two diastereomeric complexes in solution ($\Lambda(\lambda\lambda\lambda\lambda)$ and $\Lambda(\delta\delta\delta\delta)$).[69] Several well-resolved components were observed between 1095 and 920 nm with line widths below 10 nm (Figure 9). A tentative assignment of the transitions was made, and the sign sequence of the dichroic bands was regarded as a direct consequence of the Λ-configuration.

Circularly polarized luminescence of Tb^{3+} and Eu^{3+}, as substitutional replacements for calcium and iron (less reasonably), has been utilized to probe the structural conformational and coordination environment of several calcium-binding proteins and a series of iron-binding transferrins.[70−72] Lanthanide complexes of the C_4-symmetric chiral tetraamide ligands, e.g., DOTMPhA and DOTMNpA, exhibit well-defined CPL in aqueous solution that efficiently modulates the frequency of the emitted light by variation of the lanthanide ion. For example, CPL in the near-IR (ca. 980 nm) was observed for Yb^{3+} complexes of DOTMPhA and DOTMBrPhA.[67,73] Although very weak, near-IR CPL was also observed from a related Nd^{3+} chiral complex incorporating a porphyrin moiety as a sensitizing group.[73,74] The corresponding Dy^{3+} complexes of DOTMPhA are only weakly luminescent due to efficient vibrational quenching. However, strong CPL was observed for the $^4F_{9/2} - {}^6H_{11/2}$ transition ($g_{em}^{657} = +0.35$, $g_{em}^{607} = -0.41$ for (*R*)-[DyDOTMPhA].[14] Likewise, such Eu^{3+} complexes also gave rise to well-defined CPL ($g_{em}^{590} = -0.12$, $g_{em}^{595} = +0.18$ for (Λ-[EuDOTMNpA]).[64,65,67] The related Tb^{3+} complexes are much more emissive than the corresponding Yb, Dy, and Eu examples, and intense circularly polarized emission (e.g., $g_{em}^{548} = +0.27$ for Δ-[TbDOTMPhA] was observed[45,46,75] for several tetraamide complexes. Enantiomeric complexes gave rise to mirror image CPL spectra (Figures 10 and 11). This provides a means of modulating the polarization of the emitted light through choice of the appropriate helicity of the lanthanide complex which, in turn, is controlled by the absolute configuration at the remote chiral carbon center (*R* gives $\Lambda(\delta\delta\delta\delta)$ and *S* gives $\Delta(\lambda\lambda\lambda\lambda)$. The efficiency of the process is dependent on the nature of the lanthanide and the precise transition observed.

Although there are very few useful reports of spectra−structure correlation from CPL spectra, some structural information is beginning to be ascertained.[41,76] The Eu^{3+} and Tb^{3+} complexes of DO3MPPhA and DO3MPNpA (Chart 2) exist as two diastereomers, in ratios of 2:1 and 4:1, respectively.

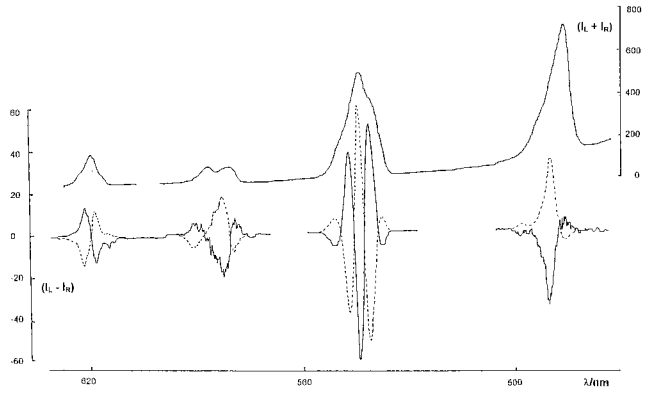

Figure 10. Total emission (upper) and circularly polarized luminescence spectra for (SSSS)-Δ-[TbDOTMPhA]$^{3+}$ (solid line) and the (RRRR)-enantiomer (dashed line) (293 K, H_2O/MeCN, 2 mM dm^{-3}, λ_{exc} 255 nm).

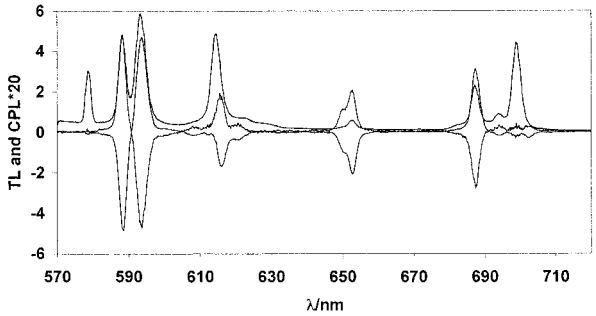

Figure 11. Total emission (upper) and circularly polarized luminescence spectra (×20) for (SSS)-Δ-[EuDO3Phphen-Me]$^{4+}$ (positive sign at 616 and 588 nm) and its enantiomer (H_2O, pH 5.5, 293 K, λ_{exc} 365 nm).

Chart 3

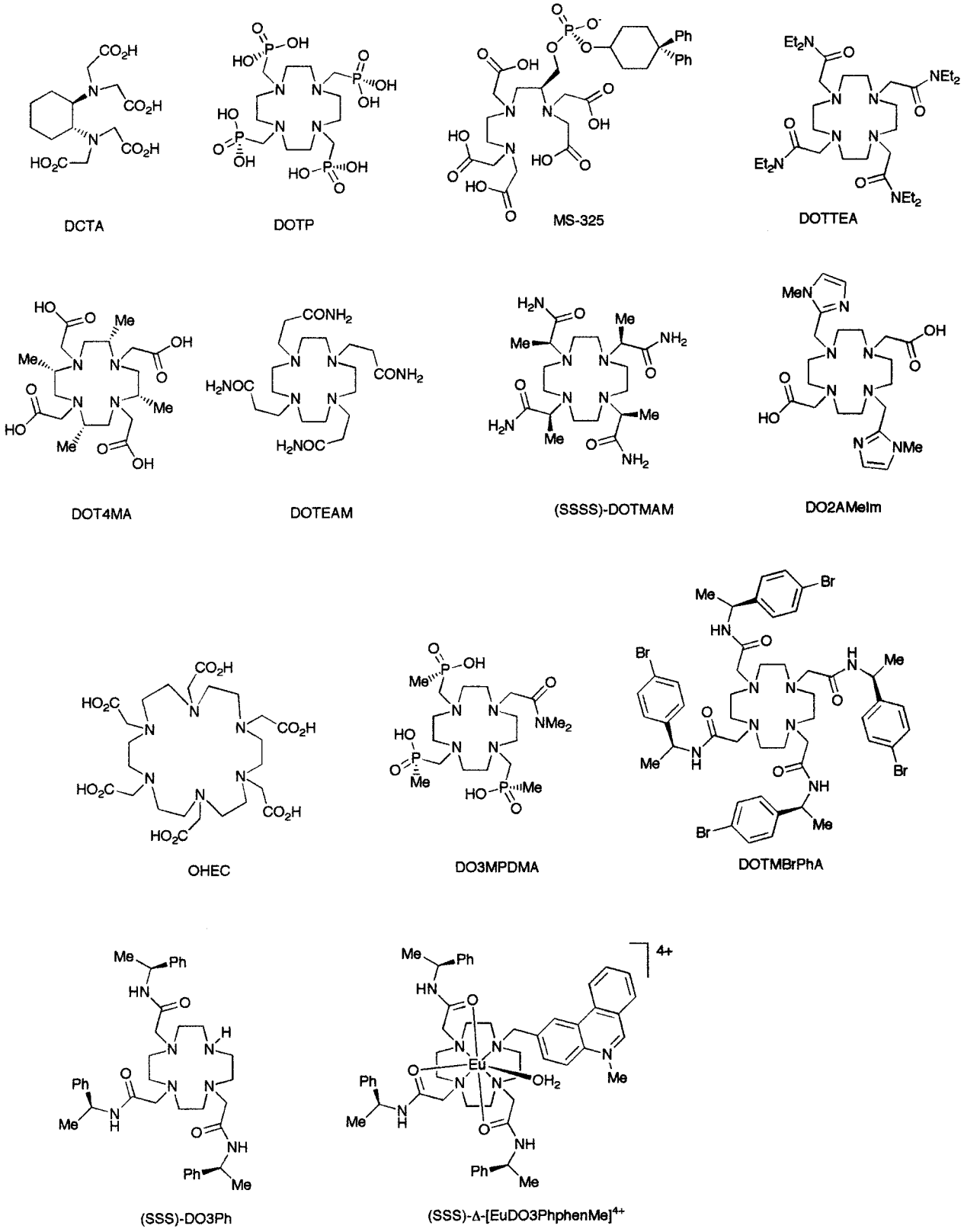

The sign and magnitude of the CPL is determined by helicity about the lanthanide center. Therefore, if the two diastereoisomers have identical ring conformations and the same layout of the pendant arms, the observed CPL will be due to contributions from both isomers. If the two diastereomers have enantiomeric ring conformations and pendant arm layout, then the CPL from the major isomer will cancel out that of the minor. As the ratio of the major to minor isomer is greater for DO3MPNpA and the observed disymmetry factors and CPL spectra were almost identical for the two complexes, this strongly suggests the two diasteromers have the same macrocyclic ring conformation and pendant arm helicity and therefore

differ only in the configuration at each of the three stereogenic P centers.[76]

CPL has recently been used to signal anion binding at a coordinately unsaturated chiral lanthanide complex[77,78] [EuDO3Ph]$^{3+}$ and [EuDO3PhphenMe]$^{4+}$. The binding of carbonate was studied in particular, and changes in the form of the CPL spectra were consistent with formation of a chelated carbonate complex, possibly with a different helical twist about the lanthanide.[78]

A series of conformationally rigid, structurally homologous lanthanide complexes, based on DOTA, has been recently studied to deduce important factors determining characteristics of CPL spectra.[79] The nature of the ligand field and in particular the polarizability of the axial donor group were shown to play dominant roles. The local helicity at the lanthanide center determines the angle between the magnetic and electric-dipole transition moment vectors and hence the rotatory strength associated with a given transition, (eq 3). The CPL is predicted to follow a sin 4θ dependence on the twist angle θ between the N_4 and O_4 planes and hence to be a maximum for square-antiprismatic complexes at a twist angle of $\pm$22.5 and zero at 0° and 45°. Finally, the degree of conformational mobility of the complex determines the time-averaged helicity around the Ln ion. This, in turn, affects the rotatory strength of a transition and must also be considered. Thus, the highest g_{em} values have been observed to date for those square-antiprismatic complexes which are conformationally locked on the emission time scale.

2. Induced CD and CPL

CD may be observed from a racemic mixture on the addition of an external chiral species (Pfeiffer effect). This induced circular dichroism (ICD) is a result of enantioselective complexation. For example, Meskers reported ICD in the electronic Nd^{3+} transitions (700−800 nm) from a racemic aqueous solution of [Nd(DPA)$_3$]$^{3-}$, which exists as two interconverting enantiomeric forms (Λ and Δ), following addition of vitamin B12 derivatives.[80,81] The ICD can yield information on the enantioselectivity of the association process, and the observed Pfeiffer effect was attributed to an excess of the Λ-[Nd(DPA)$_3$]$^{3-}$ outer-sphere complex.[80]

Induced CD has recently been utilized to probe the interaction of enantiopure lanthanide complexes containing a phenanthridine moiety [LnDO3PhphenMe][44] with some self-complementary dodecamer oligonucleotides.[82] A positive ICD was observed in the phenanthridinium chromphore with both Δ- and Λ-Ln complexes, supporting an intercalative binding interaction in which the local helicity around the chromophore was determined by the handedness of the nucleic acid. At the same time the right-handed oligonucleotide underwent distinctive changes in local helicity and pitch which were sensitive to the handedness of the lanthanide complex and the nature of the lanthanide ion.

Nonracemic excited states can be generated from racemic ground states through enantioselective excited-state quenching which may occur following the addition of a chiral acceptor to a racemic donor lanthanide complex.[59] CPL has thus been used to monitor the enantioselective luminescence quenching of racemic [Ln(DPA)$_3$]$^{3-}$ complexes by a variety of chiral acceptors such as metalloproteins,[81,83,84] vitamin B12 derivatives[81,84−86] transition-metal complexes,[87,88] and dicopper trefoil knots.[89] This has provided an insight into the stereochemistry and structure of the acceptor and has probed active sites. Information regarding the stability of the diastereomeric complexes, relationship between molecular structure and enantioselectivity, chiral discrimination in the energy-transfer reaction, and the elucidation of the mechanism of energy transfer may also be ascertained from such studies. Future applications may involve the study of enantioselectivity in the luminescence of metal-containing membrane proteins.[84]

Excitation of a racemic solution with circularly polarized light may result in preferential absorption of light by one enantiomer to produce an enantiomeric excess in the excited electronic state. As long as the rate of racemization is slower than the emission lifetime, CPL will be observed. The measurement of CPL from racemic mixtures is not only dependent on the emission dissymmetry factor, $g_{em}^{R}(\lambda)$, but also on the differential absorption of the circularly polarized light in the excitation process $g_{abs}^{R}(\lambda')$ (where R denotes a particular enantiomer and λ' is the excitation wavelength). Therefore, the observed emission dissymmetry factor following excitation with left circularly polarized light, for example, is given by the product of the two dissymmetry factors (eq 5), and as a result the technique is limited to transitions associated with large dissymmetry ratios.[36,37]

$$g_{em}'(\lambda)\text{obs} = (1/2)g_{abs}^{R}(\lambda')g_{em}^{R}(\lambda) \qquad (5)$$

Riehl and co-workers carried out such circularly polarized excitation studies (CPE) on racemic aqueous solutions of Ln(DPA)$_3^{3-}$ (where Ln = Sm^{3+}, Eu^{3+}, Tb^{3+}, Dy^{3+})[57,59,92] and phosphinate macrocyclic complexes of Eu^{3+}, Dy^{3+}, and Tb^{3+} (DOTBP, DOTMP, DO3MPDMA).[90,93] Richardson et al. also studied such [Eu(DPA)$_3$]$^{3-}$ complexes with CPL to ascertain the solvent and temperature dependence of the enantiomer interconversion ($\Lambda \leftrightarrow \Delta$) rates in solution.[91] Comparison of the CPL spectra from a series of complexes may provide structural information. For example, CPL observed from Tb^{3+} complexes of these three phosphinates suggested that the solution structure of the complexes was very similar. However, the Eu^{3+} complexes exhibit quite different CPL spectra, corresponding to undefined structural differences between the complexes. The CPL intensity from these Tb^{3+} complexes was stronger than the corresponding Eu^{3+} complexes, which is surprising and contrary to predictions based upon f−f transition selection rules,[62,63] suggesting differences in the emitting state structures of the Eu^{3+} and Tb^{3+} complexes.[90]

IV. Exchange Dynamics

Details of dynamic exchange processes for lanthanide complexes have been subdivided into four

groups here. First, kinetic studies of complex formation and dissociation pathways are considered followed by a survey of intramolecular dynamic processes. The exchange of water molecules and of water protons bound or close to the lanthanide center is detailed separately followed by a summary of other intermolecular exchange processes, involving either water substitution or noncovalent binding of the entire complex, driven either by electrostatic or hydrophobic effects.

A. Complex Association and Dissociation

Details of the methods used and the results obtained in monitoring the rate of lanthanide complex formation of dissociation in aqueous media have been thoroughly surveyed recently elsewhere.[1,2] A brief update follows here. In assessing the kinetic stability of $[GdDTPA]^{2-}$, the role of endogenous Cu^{2+} and—more importantly—Zn^{2+} ions has been quantified.[94] This cation-mediated pathway is likely to compete in vivo with the better-defined acid-catalyzed dissociation process which is more significant at lower pH. These results confirm earlier hypotheses concerning the importance of acid- and cation-mediated dissociation pathways,[95−97] based on the in vivo biodistribution of ^{153}Gd- or ^{90}Y-radiolabeled complexes. Of course, monoanionic and charge neutral complexes are much less sensitive to such a cation-mediated dissociation mechanism.[96,98] The pH dependence of the kinetics of dissociation of MS-325 has been studied with the aid of a radioisotope of europium to scavenge free ligand.[99] Under these conditions, MS-325 was found to be 10−100 times more kinetically inert than $[GdDTPA]^{2-}$, although this study did not consider the importance of the significant cation-mediated dissociation pathway.

The rates of formation and dissociation of the tetraphosphonate $[GdDOTP]^{5-}$ and its tetra-*O*-butyl ester have been studied by relaxometric and spectrophotometric methods.[100] In the association step, loss of a nitrogen-bound proton is involved in the rate-limiting step, while acid-catalyzed dissociation was slower for the less anionic tetrabutyl ester complex. Further reports of the kinetic stability of heptadentate and octadentate ligands based on cyclen have appeared,[101,102] while the rate constants characterizing formation of lanthanide complexes of DCTA have been shown, as expected, to increase with increasing atomic number.[103]

B. Intramolecular Ligand Exchange Processes

The static stereochemical analysis of chiral lanthanide complexes has been discussed in section III. Several stereoisomeric species may be formed in aqueous solution upon binding of acyclic or cyclic ligands, and processes for their interconversion are considered here and related to complex structure. The understanding of these dynamic processes is most advanced for complexes of macrocyclic ligands, especially those based on cyclen (1,4,7,10-tetraazacyclododecane). The archetypal ligand in this series is DOTA, which forms four stereoisomeric complexes on lanthanide binding. These isomers are defined by the sign of the torsion angles about the axially symmetric NCCN (typically ±60°) and pendant arm NCCO groups (near ±30°). Thus, two pairs of enantiomeric complexes exist which may interconvert by arm rotation or by a ring inversion process, (Scheme 1). The rate of the cooperative ring inversion process ($\delta\delta\delta\delta \rightarrow \lambda\lambda\lambda\lambda$) has been measured by ^{13}C NMR line shape analysis for certain La complexes,[39,104−106] by ^{1}H-EXSY, or by selective magnetization-transfer methods, (Table 3). Given the likely error associated with the measurements, it is clear that for a range of differently substituted cyclen complexes (Charts 2 and 3), the rate of ring inversion is apparently independent of the complex structure and occurs with a free energy of activation of ca. 60 (±3) kJ mol^{-1} at 298 K. The rate of ring inversion is slowed—on the NMR time scale—by introduction of one or more substituents at carbon on the 12-membered ring. Thus, in the monomethyl or C_4-distributed tetramethyl DOTA lanthanide complexes, e.g., DOT4MA, the ring inversion process is frozen.[232] Indeed, when a phenyl group is directly attached to one of the ring carbons, the ring mobility is so drastically inhibited that it was apparently not possible for the ring in the complex to adopt the minimum energy [3333]-conformation, and a much less-stable, higher energy conformation[232] was populated instead.

Scheme 1

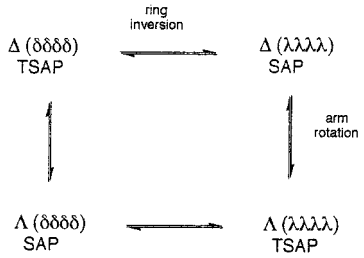

The rate of arm rotation about the principal axis is very sensitive to the nature and steric demand of the donor group on the pendant arms. Thus, comparing the rate of arm rotation in $[Eu(DOTA)]^{-}$, $[Eu(DOTAM)]^{3+}$, and $[Eu(DTMA)]^{3+}$, the values of k_{ex} (298 K) vary from 78 to 1700 to 670 s^{-1}.[32,33,107] More significantly, the introduction of one or more substituents, α to the ring nitrogen (e.g., DOTMAM, gDOTA, DOTA-pNB), leads to a freezing out of this motion on the NMR time scale, allowing ring inversion to be studied separately.[108,109,111] This behavior negates the idea put forward[110] that the dissociative water exchange process is strongly coupled to such ligand motion. The motion of arm rotation is also apparently very slow in the series of phosphinate and phosphonate complexes, which generally lack a capping water molecule.[111] For simple alkyl and benzylphosphinate complexes (e.g., DOTMP, DOTBP)[47,22] the predominant solution species is a C_4-symmetric species (*RRRR*/*SSSS* at each stereogenic phosphorus) with a twisted square-antiprismatic structure; i.e., a $\Lambda(\lambda\lambda\lambda\lambda)$ and $\Delta(\delta\delta\delta\delta)$ enantiomeric pair. No evidence was found for racemization at P (requiring dissociation of the P−O bond to La) nor for arm rotation (interconverting the diastereotopic NCH_2 (methylene) protons on the arm) between 0 and 60 °C. For the

Table 3. Kinetic Data for Ring Inversion in C_4-Symmetric Macrocyclic Lanthanide Complexes

complex	ref	$\Delta G^{\#}$ (kJ mol^{-1})[a]	T/K	k_{ex} (s^{-1})[c]	comment[b]
La(DOTA)$^-$	104	60.7	278	23	^{13}C NMR line shape
La(DOTTEA)$^{3+}$	105	58.8	298	300	^{13}C NMR
La(DOTEAM)$^{3+}$	39	58.9	298		^{13}C NMR
La(DO2AMeIm)	106	62.6	298	107	^{13}C NMR
Eu(DOTA)$^-$	32,33		298	35	^{1}H-EXSY
Yb(DOTA)$^-$	107	61.2	298		^{1}H-EXSY
(R)-Eu(gDOTA)$^{5-}$	108		293	45(M→m) 11(m→M	arm rotation frozen; ^{1}H-MT
Eu(DTMA)$^{3+}$	109	62.2	298	80(M→m) 430(m→M)	^{1}H-MT and 2D-EXSY
Eu(DOTMAM)$^{3+}$	109	59.5 62.5	298	230(M→M) 70(m→M)	arm rotation frozen; ^{1}H-MT

[a] Typical error is ±2.5 kJ mol^{-1}. [b] MT is magnetization transfer. [c] M and m refer to square-antiprismatic (SAP) and twisted square-antiprismatic (TSAP) isomeric structures.

analogous P−Ph phosphinates, (DOTPhP) however, a mixture of six diastereoisomers was observed by ^{31}P NMR analysis in water, which were assigned to differing chiralities at P, with the *RRRS* isomer slightly preferred.[24] A similar pattern of behavior was defined for the trifluoroethylphosphinate lanthanide complexes (DOTFEP),[112] with steric interactions between adjacent phosphorus groups suggested to determine the solution distribution of isomers. A complex distribution of isomers was also evident for monoamide derivatives of DOTPhP,[21] whereas with the P−Me phosphinate analogues, one preferred isomer had been observed earlier by ^{31}P and ^{1}H NMR analysis.[113] That these complexes do not undergo significant arm rotation was also suggested by VT-NMR analysis of the Eu complexes of the related chiral monoamide ligands DO3MPPhA and DO3-MPNpA (Chart 2). Out of 32 possible diastereoisomeric species, two nonexchanging diastereoisomers were observed in a 2:1 and 4:1 ratio, respectively, differing in configuration at phosphorus (*SSS* or *RRR*) but with the same helicity for the pendant arms and the macrocyclic ring—these two elements of chirality being determined by the configuration of the chiral amide center.[51] A further example of the steric inhibition of arm rotation has been suggested for the lanthanide complexes of the chiral tetraamide ligands, DOTMPhA and DOTMNpA. In this case, the sterogenic center at carbon is δ to the ring N but determines the helicity (Δ/Λ) of the complex, an *S*-configuration at carbon giving a Δ-helicity in a preferred square-antiprismatic complex geometry. This isomeric species predominates across the series,[46,67,68] and CD, CPL, and solution NMR studies suggest that Δ/Λ interconversion remains slow on the Eu/Tb emission (millisecond) and NMR time scales, favoring their use as chiral probes for nucleic acid structure.[82] Concerted arm rotation is also believed to be the salient dynamic process occurring in lanthanide complexes of expanded polyazamacrocyclic-substituted ligands. Thus, with the dimeric Y^{3+} complex of the octa(aza-acetate), OHEC (Chart 3), ^{1}H-ROESY studies indicated an interconversion between a centrosymmetric major isomer and an asymmetric minor isomer (ΔG_{300} 65 kJ mol^{-1}) that may well involve rotation of the acetate groups.[114]

The situation with acyclic ligands (e.g., DTPA and its substituted variants) is more complex and less well-defined. Two recent reviews have summarized our current understanding.[1,115] In the parent, DTPA complexes of Pr, Eu, and Yb, δ/λ interconversion of the NCCN chelates (k_{ex} [278 K] = 265, 360, and 4300 s^{-1}, respectively) is accompanied by a 'shuffling' of the bound acetate groups (equilibrating two acetate arms) and leads to a change in complex helicity.[116] Much slower processes, leading to racemization at the terminal ligand nitrogen centers, have been identified at elevated temperatures and are more evident in the behavior of the related DTPA-bisamide analogues.[117,118] Two diastereoisomeric complexes of (*S*)-EOB-DTPA have been examined by NMR and HPLC: exchange is very slow (pH 9, 298 K, $t_{1/2}$ > 545 days) but was acid-catalyzed, suggesting that a process involving decomplexation of one or more of the ligating donors was occurring,[119] possibly related to racemization of the central N atom.

Scheme 2

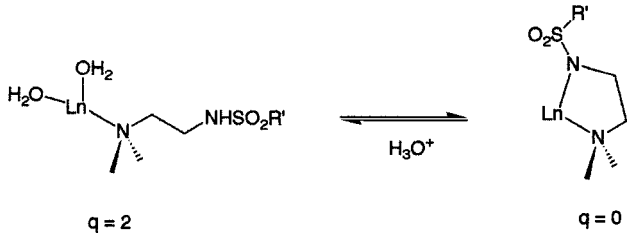

Deliberate modulation of on/off donor ligation has been achieved through pH control of sulfonamide binding to a Eu, Gd, or Tb center.[120−122] Thus, in more acidic media, protonation of the sulfonamide nitrogen (Scheme 2) occurs leading to formation of a mono- or diaqua species with an enhanced relaxivity (Gd) or reduced luminescence (Eu, Tb). At higher pH, the sulfonamide N binds, displacing the water molecules giving species with enhanced luminescence or reduced relaxivity. Control over the pH range (pH 5.5−8) where this process occurs is readily achieved through variation of the substituent R′ that, in turn, determines the electron density at the nitrogen center. An analogous process involving intramolecular carboxylate ligation (7 ring chelate) has been defined in the same systems. Such pH-dependent modulation of the lanthanide hydration state has already found application in a sol−gel-based pH sensor[123] and offers much promise in the quest for practicable pH-modulated contrast agents in MRI.[120]

C. Water and Proton Exchange

Here we consider the interchange of the lanthanide-bound water molecule, its associated hydrogens, or exchange of labile ligand protons. Traditionally the most reliable method for studying the water exchange process has been a VT-^{17}O NMR study of gadolinium complexes, measuring the transverse oxygen relaxation rate as a function of temperature following by data-fitting to the analysis promulgated by Swift and Connick.[124] Such methods have been reviewed[1−3] and give values for the *mean* water exchange rate of kinetically active species. Given that water exchange is usually fast with respect to the intramolecular interconversion of isomeric species, then additional information is required to define the salient kinetically active species involved. Independent measurement of the rate of the exchange process for chemically distinct species has very recently been achieved by ^{1}H and ^{17}O NMR methods for selected slow-exchanging complexes involving *direct* NMR observation of the bound water proton[34,44,125,126] or oxygen.[110,126] For those cases where water or proton exchange is fast with respect to the NMR time scale, then it is prudent to examine independently the distribution of complex species by NMR, absorption, or luminescence methods. In this respect, considerable caution must be exercised. For example, although absorption spectroscopy is ideal from the time scale viewpoint (subpicosecond!), the analysis of the absorption spectra of Eu complexes in certain cases relies upon a questionable assumption. The frequency of the weak, nondegenerate $^7F_o \rightarrow {}^5D_o$ transition for a Eu^{3+} species is sensitive to the nature of the ligand donors and complex geometry. However, the oscillator strength of that transition is also very sensitive to complex symmetry and the local ligand field. Several analyses have assumed, for example, that a pair of eight- and nine-coordinate Eu complexes will give rise to two $^7F_o \rightarrow {}^5D_o$ transitions for which the sum of their band intensities is constant. This assumption—first validated experimentally by Jorgensen and Tananaeva in 1971 for $[Eu(EDTA)]^-$ for the equilibrium between $q = 2$ and 3 species[128,129]—has been assumed by others for different systems.[130,131] However, complexes of Eu in which the ligand has a low steric demand (DTPA, DOTA) are usually nine-coordinate, so that alternative explanations may need to be considered, such as the presence of two aquated isomeric species of differing structure and local symmetry giving rise to distinct $^7F_o \rightarrow {}^5D_o$ transitions of different relative intensity.[132,133]

1. Direct NMR Observation of Bound Waters

In the Eu, Yb, and Pr complexes of the macrocyclic 12-N_4-based tetraamide ligands DOTAM,[44,110] DTMA,[34,109] and DOTMPhA[126] (Chart 2), the predominant solution species is a regular square-antiprismatic structure with a bound water molecule that is in slow exchange with 'bulk' water on the NMR time scale. Thus, in aqueous acetonitrile or in water itself, the rate of water exchange is sufficiently slow that the bound water may be observed by ^{1}H NMR, e.g., for $[Ln(DOTMPhA)]^{3+}$ at ca. +80 ppm (Eu, 235 K, MeCN/H_2O), +325 ppm (Yb, 233 K, MeCN/H_2O),[68] and −130 ppm (Pr, 233 K, MeCN/H_2O). The water protons in the minor isomeric twisted square-antiprismatic species of DOTAM and DTMA resonate to lower frequency for Eu complexes, allowing the rates of water exchange to be monitored separately for each species by magnetization-transfer or line shape analyses (see section B, below). Parallel observations using ^{17}O NMR have been reported[127,110] with the bound oxygen in the square-antiprismatic $[Eu(DOTMGly\text{-}Et)]^{3+}$ complex, for example, resonating 897 ppm to lower frequency of the bulk water signal[127] at 298 K (Chart 4).

2. The Role of Complex Geometry

These NMR studies have revealed the pre-eminent role of complex structure and geometry in determining water exchange rates. Kinetic data for water exchange, determined by ^{17}O NMR methods in structurally analogous gadolinium complexes, are collated in Table 4, together with related measurements made on slow-exchanging species by ^{1}H NMR methods. The most important conclusion revealed is that dissociative water exchange in the twisted square-antiprismatic isomers occurs between 50 and perhaps up to 500 times faster than in the isomeric square-antiprismatic structures. For the series of anionic complexes related to DOTA (top five entries in Table 4), the rate of water exchange correlates directly with the proportion of the twisted square-antiprismatic structure, suggesting a common limiting exchange rate of ca. 2×10^7 s^{-1} (298 K). That this rate is independent of complex structure in this short series is consistent with a late transition-state structure for the dissociative water interchange process.[108] Further support for this premise is provided by data for (*S*)-$[Gd(THP)]^{3+}$—as the triflate salt[135]—which exists in aqueous solution as >95% of the TSAP structure. A rate of 2×10^7 s^{-1} (298 K) was also measured here by ^{17}O NMR methods, notwithstanding the tripositive charge on the complex. In the series of neutral complexes based on DO3A (bottom 6 entries, Table 4), the mean rate of exchange is relatively constant (ca. 2×10^6 s^{-1}, 298 K) and is consistent with the predominance of a regular square-antiprismatic structure undergoing relatively slow water exchange in solution.

For the series of cationic complexes of the central Ln^{3+} ions, the slowness of the exchange rate of the SAP isomeric structures accords with the idea of an early transition-state structure for dissociative interchange. Such complexes exhibit a dependence of water exchange rate on the nature of the counteranion,[42,136] as revealed by ^{17}O NMR and relaxometric studies, with the more chaotropic anions (e.g., $I^- > Br^- > Cl^-$) giving rise to faster exchange. Evidently the nature of the anion—as well as the complex cation—plays a key role in defining the second sphere of hydration around these complexes, and the local structure of the second hydration sphere around the $Ln-OH_2$ moiety must be important in defining water exchange dynamics, (see section II.E).

3. Second Sphere of Hydration

The presence of the second sphere of hydration has been revealed through recent crystallographic studies

Chart 4

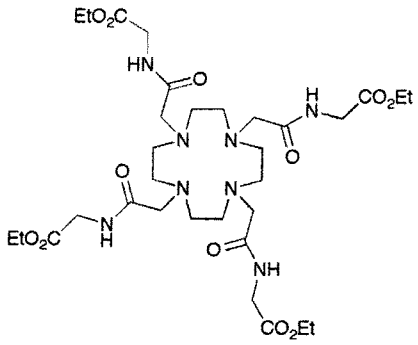

DOTMGlyEt

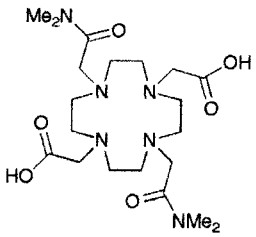

DO2ADMA

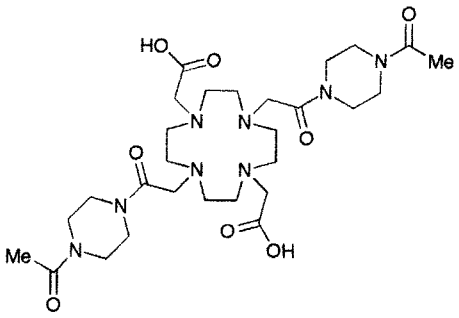

DO2AAPA

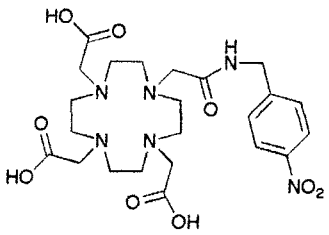

DO3AABNO2

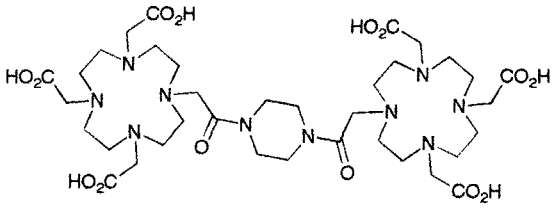

pip(DO3A)$_2$

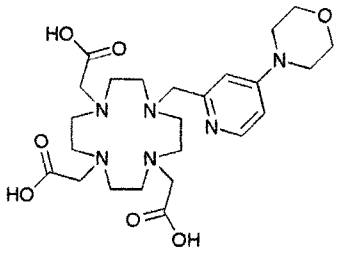

morpyDO3A

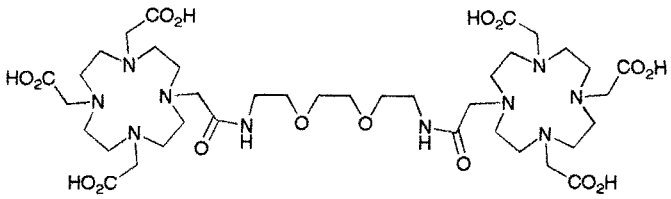

oxaen(DO3A)$_2$

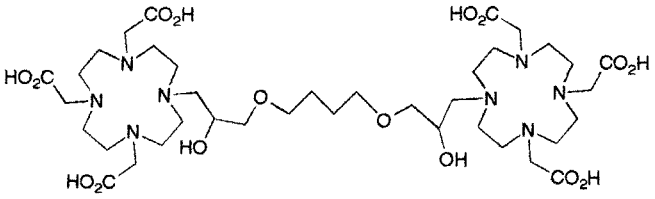

OB(HPDO3A)$_2$

(see section II) and its importance demonstrated by a series of relaxometric (Gd) and luminescence (Eu, Tb, Yb) studies. The structures of two representative Yb complexes (Figure 12) have revealed the location of the bound (primary), second-sphere and outer-sphere water molecules.[126,144] In the case of the cationic complex $[Yb(DOTMPhA)]^{3+}(CF_3SO_3)_3$, the second-sphere oxygen is 3.6 Å away from the Yb ion and is hydrogen-bonded to the bound water. In the anionic complex $[Yb(DTPA)]^{2-}$, the second water is 4.2 Å away, acts as a hydrogen bond donor to a ligand carboxylate oxygen and forms part of a 'linear' chain of hydration. These two examples have lent credence to the hypothesis that second-sphere waters may contribute significantly to the relaxivity of Gd complexes.[145] The nature of the well-defined second sphere of hydration in $[Yb(DOTMPhA)]^{3+}$ may also be an important factor in its 500-fold faster water exchange rate compared to the Eu analogue (section II.D),[270] for which X-ray analyses have yet to reveal the presence of such a second sphere of solvation.[46,67] In addition, these results support the idea that closely diffusing (i.e., second-sphere) water molecules may quench the $^5D_0$, $^5D_4$, or $^2F_{7/2}$ excited states of Eu, Tb, and Yb, respectively, by a vibrational energy-transfer process[146,147] which as for proton relaxivity is a function of r^{-6} (r is the Ln−HX separation). Indeed, a good correlation has been found for a series of complexes that includes several monoamidetriphosphinate complexes (DO3MPMA, Chart 5: first sphere $q = 0$ from ^{17}O NMR; one major solution species only by ^1H, ^{31}P NMR analysis), between the average hydration state q ($0 < q < 1.2$) determined by luminescence, and the Gd−H distance determined by fitting NMRD analyses so as to allow for second-sphere contributions.[8,50] Where fractional q values are obtained by such analyses, a well-defined second hydration sphere is strongly suggested and nonintegral hydration states for lanthanide ions in solution are then entirely reasonable. The pure outer-sphere ($q = 0$) and single inner-sphere ($q = 1$) cases may then be regarded as limiting cases, with nonintegral values being determined by the hydrophobicity of local substituents and the number, nature, and location of hydrogen-bond acceptors in the ligand.[7,8,147]

Table 4. Comparison of Mean Rates of Water Exchange (298 K, ^{17}O NMR) for Macrocyclic Lanthanide Complexes, Highlighting the Effect of Complex Stereochemistry

complex	distance[e] Ln−OH_2 (Å)	k_{ex}^{298} (s^{-1}) (values for [M] or (m) isomers are in parentheses)	isomer ratio of Eu analogue (SAP/TSAP) or (M/m)	ref
[GdDOTA]$^-$	2.46(Gd)	4.1×10^6(24×10^6)	4.7[b]	134
[GdDOTMA]$^-$		14.7×10^6(31×10^6)	0.41[b]	9
(*RRRR*)-[GdgDOTA]$^{5-}$	2.43(Gd)	15.4×10^6(22×10^6)	0.40[b]	108
(*RRRS*)-[GdgDOTA]$^{5-}$		9.0×10^6(21×10^6)	2.3	108
(*RSRS*)-[GdgDOTA]$^{5-}$		3.5×10^6(20×10^6)	4.7	108
(*SSSS*)-[GdTHP]$(CF_3SO_3)_3$	2.51(Eu)	(19×10^6)	<0.1	135
[GdDOTAM]$(CF_3SO_3)_3$	2.44(Eu)	0.05×10^6[c]	4.5	34,136
[GdDTMA]$(CF_3SO_3)_3$	2.46(Gd)	0.06×10^6[c]	5	34
[GdDOTTA]$(CF_3SO_3)_3$		0.13×10^6[c]	0.5	34
[GdDO2ADMA]Cl		[0.74×10^6](74×10^6)	1.30	137
[GdDO2AAPA]Cl		[0.42×10^6](330×10^6)	1.28	137
[GdDO3ABNO$_2$]		1.6×10^6	>8[d]	138
[Gd$_2$pip(DO3A)$_2$]		1.5×10^6	>8[d]	139
[Gd$_2$oxaen(DO3A)$_2$]		1.4×10^6	>8[d]	139
[GdHPDO3A]	2.50(Gd)	2.9×10^6	1.4	141,140
[GdmorpyDO3A]	2.40(Gd)	2.7×10^6	2	142
[Gd$_2$OB(HPODO3A)$_2$]		1.0×10^6	n.d.	143

[a] For the square-antiprismatic isomer. [b] Value represents the mean value of the corresponding Eu and Tb complexes determined by ^1H NMR at 298 K; data is recorded with $k_{ex}^M \sim 5 \times 10^5$ s^{-1} and (twisted antiprism) $k_{ex}^m = 2 \times 10^7$ s^{-1}. [c] Direct observation of individual isomeric exchange rates on Eu analogues in MeCN/H_2O gives for m and M [Eu−DOTAM]$^{3+}$, $k_{ex}^m = 5 \times 10^5$ s^{-1}, $k_{ex}^M = 9 \times 10^3$ s^{-1}; m/M[Eu−DTMA]$^{3+}$: $k_{ex}^m = 3.6 \times 10^5$ s^{-1}, $k_{ex}^M = 8 \times 10^3$ s^{-1}. These rates are for the triflate salts, and the rate of exchange is faster with more chaotropic counterions (e.g., OAc^-, Br^-). [d] Estimated by analogy with related EuDO3A-monoamide complexes. [e] Note the absence of any significant correlation between the Gd−water bond length and the water exchange rate in this series; here there are too many variables at work determining this distance (ligand/geometry changes). For an example where the bond length may be related to the water exchange rate, see ref 270.

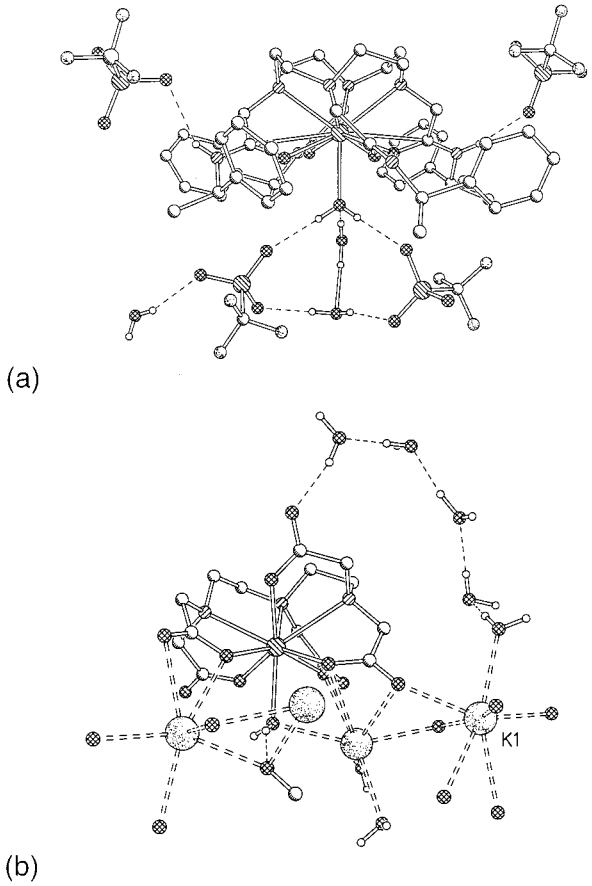

Figure 12. X-ray crystal structures of (a) [YbDOTMPhA-(H_2O)]$(CF_3SO_3)_3$·$4H_2O$ (120 K), and (b) K_2[YbDTPA(H_2O)]-0·$8H_2O$ (173K) showing the first, second and outer-sphere water molecules.

4. Diaqua Systems

Less attention has been paid toward the behavior of $q = 2$ complexes as they tend to be less kinetically stable, exhibit reduced thermodynamic stability, and may undergo chemical exchange of one or both of the bound water molecules by anions or proteins (see section IV.D). Data for the rate of water interchange by ^{17}O NMR methods are collated in Table 5, for Gd complexes of hexa- and heptadentate ligands (Chart 5).[148−153] In the case of [GdHOPO$(H_2O)_2$], the ligand is hexadentate and fairly rapid water exchange ($k_{ex} = 7 \times 10^7$ s^{-1}, 298 K) occurs via an associative mechanism.[149] Relatively fast exchange has also been defined for [Gd(PDTA)$(H_2O)_2$], although a switch in mechanism was observed from Gd to Yb as the fairly rapid associative interchange process (Gd) changed to a much slower dissociative one (250 times slower and a positive $\Delta V^{\#}$ for Yb).[152] With the heptadentate ligands, exchange probably occurs via a dissociative process (at least for the central Ln^{3+} ions) and is fastest for the stable complex [Gd(aDO3A)$(H_2O)_2$],[153] for which anion binding by carbonate and protein binding in serum is suppressed by the introduction of carboxypropyl substituents. Indeed, the relatively high relaxivity of this Gd complex ($r_{1p} = 12.3$ mM^{-1} s^{-1}, pH 7.2 in serum, 65.6 MHz, 293 K) suggests a substantial second-sphere contribution, associated with the solvation of the ionized proximate carboxylates. This may also be the case for the rather insoluble Gd complexes of TPAA (Chart 5) in which the observed high relaxivity (13.3 mM^{-1} s^{-1} 60 MHz, 298 K) was interpreted in terms of a mixture of $q =$ 2 and 3 species,[278] although a large second-sphere contribution may also explain this value.

5. Prototropic Exchange: pH, Ion Pair, and Anion Effects

The exchange of protons in a lanthanide complex—either of a bound water molecule or of relatively acidic ligand hydrogens—is subject to acid or base catalysis. Potentiometric titrations for the cationic Eu and Gd complexes of DTMA revealed pK_a values,

Chart 5

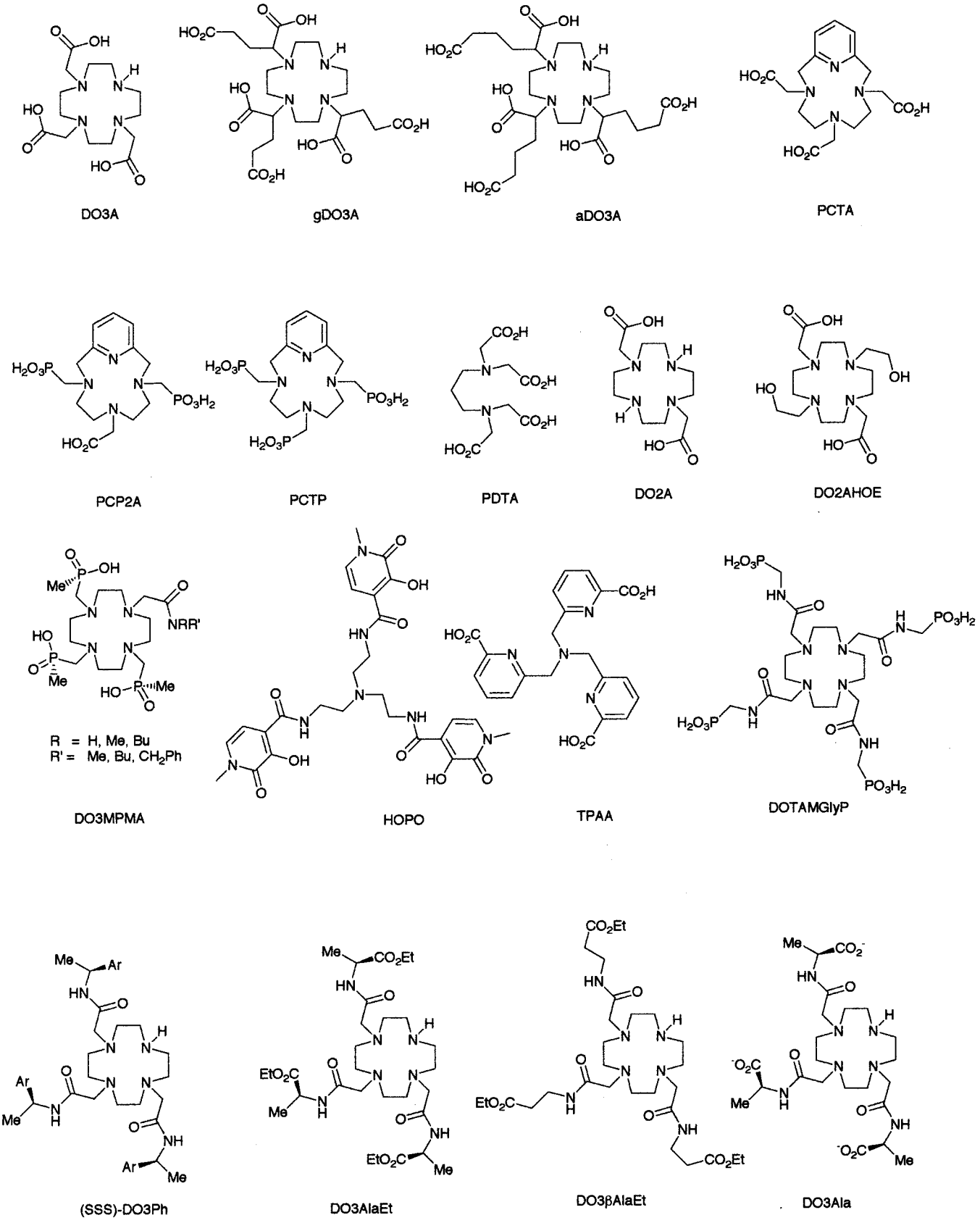

associated with deprotonation of the bound water, of 7.3 and 7.9 (0.1 M NMe_4ClO_4, 298 K), respectively,[34,42,43,101] which are similar to the value of 7.5 reported for $[EuDO2AHOE(H_2O)]^+$.[41] For systems where water exchange is slow on the NMR time scale and for which $\tau_m > T_{1m}$ in eq 6 (defining paramagnetic proton relaxivity, r_{1p}, where c is the complex concentration, τ_m the water exchange lifetime, and T_{1m} the water proton longitudinal relaxation time), measurements of the pH dependence of proton re-

Table 5. Rates of Water Exchange in Di-aqua Gadolinium Complexes (298 K, ^{17}O−VT-NMR Analyses)

complex	k_{ex} (10^6 s^{-1}) (298 K)	comment	ref
[GdDO3A][a]	6.25	water displaced by HCO_3^- or protein	148
$[GdaDO3A]^{3-}$	33	relaxivity (20 MHz, 298 K) is 12.3 mM^{-1} s^{-1}	153
[GdHOPO]	70	eight-coordinate, associative exchange	149
$[GdPCP2A]^-$	16	no change in phosphate buffer	151
[GdPCTA][b]	14		148
$[GdPDTA]^-$	100	rate reduces Gd→Yb as I_A mechanism switches I_D	130

[a] In comparison, $[GdDO2A(H_2O)_3]^+$ undergoes dissociative exchange with $k_{ex} = 10 \times 10^6$ s^{-1}.[152] [b] The Gd complexes of the heptacoordinate ligands, PCTP, and the [13]-ring analogue possess only one bound water molecule and undergo fast (associative) exchange, k_{ex} (298 K) = 170 and 125 × 10^6 s^{-1}, respectively.[148,150]

laxivity allow these prototropic processes to be examined.

$$r_{1p} = \frac{cq}{55.6}\left(\frac{1}{T_{1m} + \tau_m}\right) \quad (6)$$

Thus, with $[Gd(DTMA)(H_2O)]^{3+}$, base catalysis of the exchange of the bound water proton was observed with a second-order rate constant of 1.4 × 10^{10} M^{-1} s^{-1}, leading to an enhanced proton relaxivity in basic media.[34,42] Similar observations have now been reported for a series of cationic Gd complexes.[125,127,154] Moreover, in a tetraphosphonate complex with a cationic core, protonation of the terminal phosphonate groups in [Gd(DOTAMGlyP)] facilitated proton exchange, giving rise to a pH-dependent relaxivity profile around ambient pH.[125] A similar effect[127]—this time intermolecular in nature—has been noted following addition of a large excess of sodium phosphonate to $[Gd(DOTAMGlyEt)]^{3+}$.

The coordination of a secondary amide carbonyl or an alcohol OH group to a lanthanide ion enhances the susceptibility of the NH/OH protons to undergo rapid H/D exchange.[8,146] Even the NCH_2CO_2 methylene protons of bound carboxymethyl groups undergo H/D exchange at elevated temperatures, facilitating the synthesis of ^2H-labeled lanthanide complexes.[147,155] The onset of amide deprotonation is signaled by an enhanced water proton relaxivity and has been observed for several complexes.[34,156,157] Such behavior may be compared to the quenching effect of amide NH protons on Eu luminescence, observed when measuring the radiative rate constant for depopulation of the ^5D_o excited state in H_2O and D_2O.[147] Prototropic exchange between bulk water and shifted amide NH or Ln-bound OH protons may occur at a rate which is comparable to their chemical shift separation. Under these conditions, saturation-transfer methods may be used that allow the definition of a new type of contrast agent, based on magnetization transfer (MT).[229] Thus, presaturation of the bound water signal in 'slowly exchanging' Eu complexes can lead to up to an 80% change in the intensity of the bulk water resonance. As exchange between Ln−water and Ln−amide protons may also be pH-dependent, the MT contrast agents may be used to report tissue pH directly through changes in the intensity of the bulk water signal.[230,231]

The case with acid catalysis of proton exchange is rather less well-defined. For $[Gd(DOTA)(H_2O)]^-$, the water exchange rate is 10 times slower in 1 M HCl than in neutral media but the proton relaxivity is higher than expected based on the τ_m modulation.[158] For the cationic complexes, such as $[Ln(DTMA)]^{3+}$, the increase in proton relaxivity observed in acidic media was very sensitive to the nature of the counteranion.[34] Such behavior is consistent with the acid-promoted break up of ion pairs. The $[LnL(OH_2)(X)_3]$ complexes can be considered to involve a 'solvent-separated intimate ion pair' (see Figure 12). Addition of more acid also leads to enhanced anion concentrations whose presence may lead to a marked labilization of the second hydration sphere. Related evidence for the importance of tight ion pairs in aqueous media has come from NMR observations of the association of the polyanionic complex $[EuDOTP]^{5-}$ with the *N*-methylglucaminium or $[Co(en)_3]^{3+}$ cation—leading to spectral resolution of the diastereoisomeric salts.[159,160] Similarly, for $[Tm(DOTP)]^{5-}$ addition of the enantiopure complex Δ-(SSSS)-$[La(THP)]^{3+}$ leads to ^{31}P and ^{13}C NMR discrimination of the Tm−phosphonate enantiomers, the cationic complex serving as a—rather poor—aqueous chiral solvating agent[161] (see section VI for further examples).

D. Intermolecular Ligand Exchange

In this short section we consider the substitution of a bound water molecule at the Ln center and noncovalent binding processes involving lanthanide complexes in aqueous solution. Exchange of the primary ligand—akin to complex dissociation—is not considered. More detailed analyses of the interaction of Ln complexes with proteins have recently been reviewed[1,162] and are not considered further here.

1. Water Substitution

In nine-coordinate complexes possessing one bound water molecule, the bound water is generally very difficult to substitute in aqueous media, even though it may be undergoing dissociative exchange with bulk water at a rate of $>10^7$ s^{-1} at 298 K. Only addition of excess fluoride has been shown to displace the water,[163] e.g., for $[EuDOTMPhA]^{3+}$ and partially for $[Eu(DOTA)(H_2O)]^-$. In the fluoride-bound species, the complex seemed to adopt a preferred twisted square-antiprismatic structure possibly formed via the TSAP mono-aqua species. The water molecules in $q = 2$ or 3 complexes are usually readily displaced by addition of ligating anions, especially chelating species (e.g., lactate, citrate, malonate, succinate).[78,154,164,269] Such reactions may be monitored by following the enhancement of luminescence emission intensity and lifetime as bound water molecules efficiently quench the excited state of, e.g., Yb^{3+}, Nd^{3+}, Eu^{3+}, and Tb^{3+} species. In the case of Eu complexes, the change in

Scheme 3

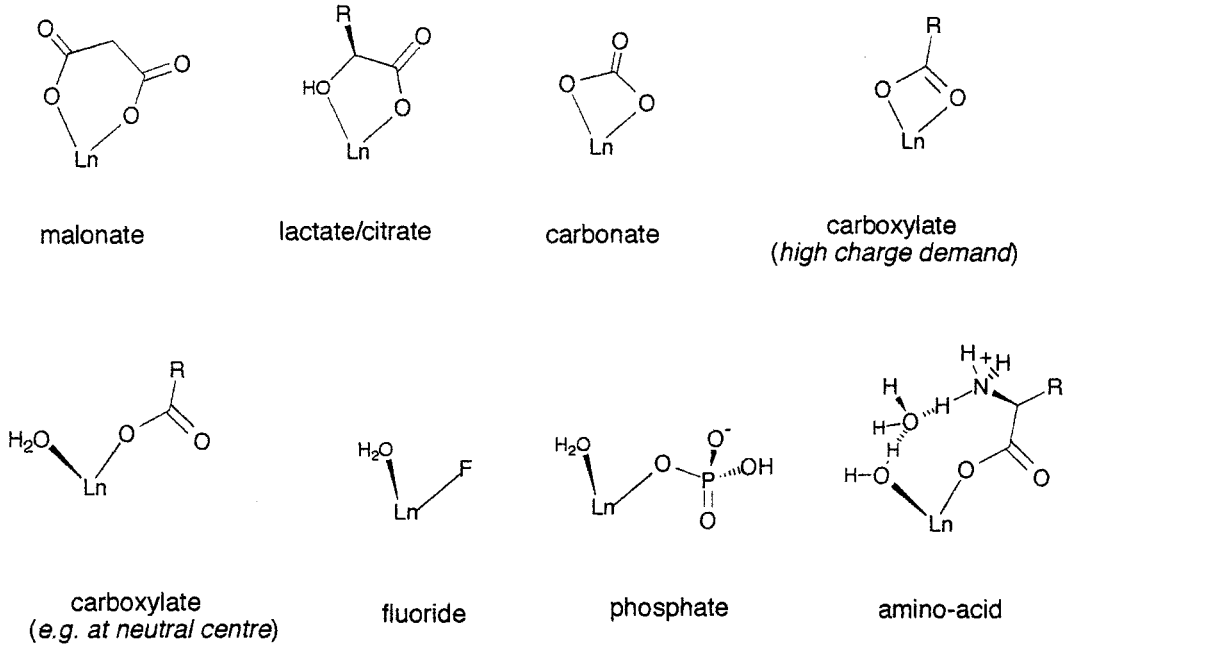

the form of the emission spectrum also characterizes this process (see section V), and for analogous Gd complexes, relaxivity measurements as a function of effective anion concentration are very informative.[165] This has been demonstrated for the binding of carbonate to $[Gd(DO3A)(H_2O)_2]$—a process distinguished by its pH sensitivity over the range 6−10.[134,165] Binding of carbonate leads to more emissive Eu complexes and Gd complexes of lower relaxivity. Complexation of HCO_3^- is suppressed in the analogous carboxyalkyl-substituted complexes, $[Ln(aDO3A)]^{5-}$ and $[Ln(gDO3A)]$,$^{5-}$ in the latter case as a consequence of competitive intramolecular carboxylate ligation.[120]

Coulombic attraction enhances anion binding affinity to the positively charged Ln center in related complexes, e.g., $[Ln(DO3Ph)]^{3+}$, $[LnDO3AlaEt]^{3+}$, [Ln(DO3βAlaEt)], and [Ln(DO3Ala)], (Chart 5). The structures of ternary anion adducts of $[Ln(DO3Ph)]^{3+}$ in particular have been defined by luminescence, ^{17}O and ^1H NMR, and relaxometric studies (Scheme 3).[78] Displacement of one of the bound waters by hydrogenphosphonate results in a mono-aqua complex in which the water exchange rate increased from 8×10^5 s^{-1} (298 K, triflate salt−diaqua species) to 5×10^7 s^{-1} (Figure 13). The chelation of lactate and citrate to $[LnDO3MPhA]^{3+}$ has been substantiated by crystallographic analyses[166] of the bound adduct (Scheme 3). For monocarboxylate donors, the binding affinity was significantly lower. There is some evidence that the less basic carboxylate oxygen of amino acids may be bound in a similar manner to give $q = 1$ complexes, with the presence of a well-defined second-sphere molecule suggested by relaxometric studies.[167]

2. Non-Covalent Binding

In the bis(*m*-boroxyphenylamide)Gd DTPA complex (Chart 6, DTPA-bisBPh), the boronic acid functionalities bind reversibly to fructosamine residues of

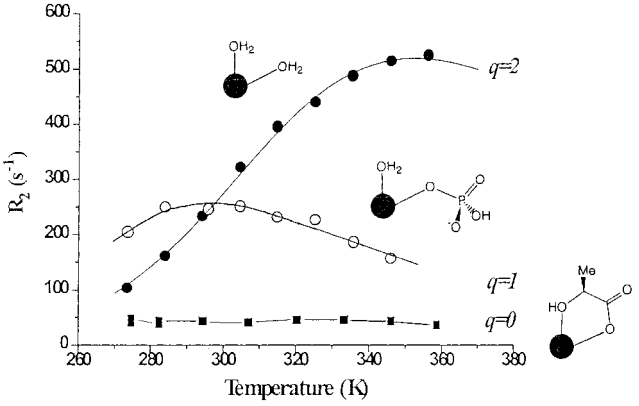

Figure 13. Temperature dependence of the ^{17}O NMR (9.4T) transverse relaxation rate for $[GdDO3Ph(H_2O)_2](CF_3SO_3)_3$ in water ($k_{ex} = 8 \times 10^5$ s^{-1}, 298 K) in the presence of a 10-fold excess of Na_2HPO_4 ($k_{ex} = 5 \times 10^7$ s^{-1}, 298 K) and with sodium lactate ($q = 0$), highlighting the faster exchange of the phosphate-bound complex.

oxygenated glycated human haemoglobin. Two complexes interact with one haemoglobin tetramer ($K_D = 1 \times 10^{-5}$ and 4.6×10^{-4} M), and the affinity was significantly higher than that for the deoxy derivative. Unusually, the complex serves as an allosteric effector by stabilizing the high-affinity state of human haemoglobin. Binding has been proposed to occur at the 2,3-diphosphoglycerate binding site involving formation of an N−B bound moiety at His residues of two different β chains.[169] Conversely, it has been shown by ^{11}B and ^1H NMR that borate interacts with the *cis*-diol residues in the bis-glucamide complex of [LnDTPA-bisGlu],[168,170] forming a 1:1 intramolecular complex involving the 3,4-diol group.

Hydrophobic binding of size-matched aryl or alkyl residues in aqueous media is a feature of the complexation behavior of β and γ-cyclodextrins. The benzyl groups of benzyloxyproprionate derivatives of DOTA and DTPA are included by β-CD, leading to a relaxivity enhancement for the Gd complexes.[171]

Chart 6

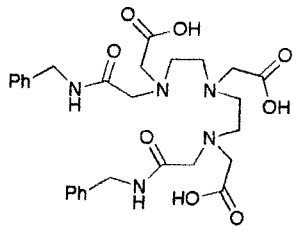

DTPA-BBA

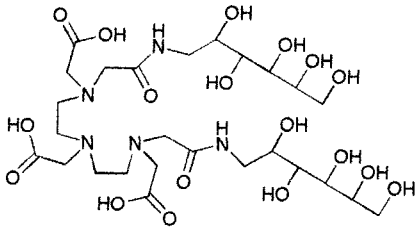

DTPA-bisGlu

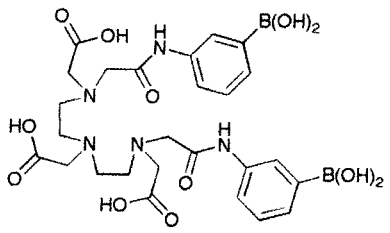

DTPA-bisBPh

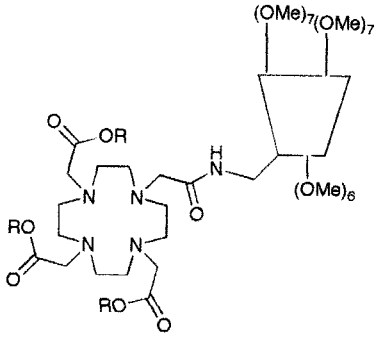

DO3AAMMeCD

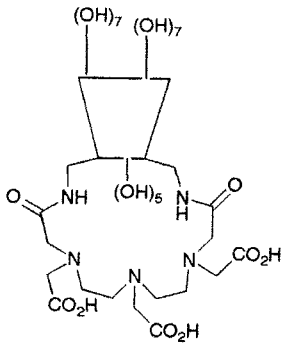

DTPA-bisAMCD

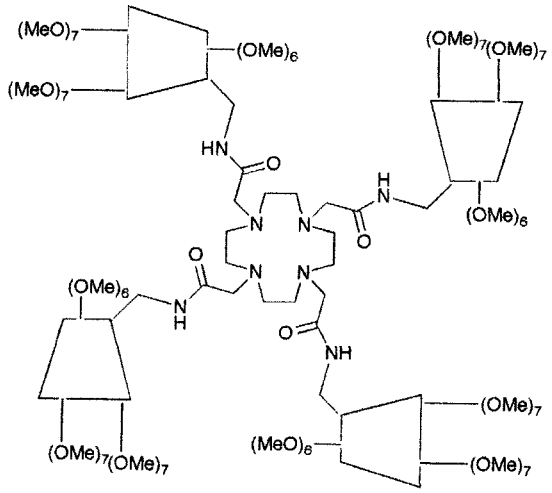

DOTAMMeCD

Weak complexes have been defined also for [Tm(DOTP)]$^{5-}$ [172] and [Tm(DOTA)]$^{-}$ [173] with γ-cyclodextrin. The solubility of [Gd(DTPA-BBA)] in aqueous solution is enhanced by addition of the pharmaceutically well-tolerated hydroxypropyl-β-cyclodextrin.[174] Mono- and polysaccharides themselves tend not to bind Ln^{III} aqua species significantly in competitive aqueous media. The racemic tris(2,6-pyridine dicarboxylate) complexes of Eu and Tb ($Ln(DPA)_3$) are $q = 0$ species in water, and circularly polarized luminescence studies have revealed that the formation of weakly bound diastereoisomeric adducts with a variety of sugars—although perturbing the racemic equilibrium —involves a purely 'outer-sphere' process.[175]

A cyclic DTPA—bisamide ligand has been grafted onto an A,D-disubstituted β-cyclodextrin to yield DTPA—bis AMCD.[176−178] The emission from the charge-neutral terbium adduct is sensitized following binding of naphthalene or durene inside the CD cavity. Similar behavior has been defined for the terbium complexes of the per-O-methylated mono- and tetra-CD ligands DO3A—AMMeCD and DOTA-MMeCD.[179] Sensitization in the presence of 2-Me-naphthalene and *p-tert*-butylbenzoate with [TbDOTAMMeCD] was demonstrated, but the slowness of the energy-transfer step from the excited aryl triplet to the rather distant Ln ion renders the process sensitive to competitive oxygen quenching, limiting the scope of this noncovalently triggered luminescence process. Enhancement (due to an increase in τ_r for the complex) of the relaxivity of [GdDO3AAMMeCD] was observed following addition of MS-325, which has been shown to bind to the parent β-CD with an affinity of 8×10^4 M^{-1} (Chart 3). A 6-fold larger enhancement was found with a cholic-acid-appended Gd complex, the increase also ascribed to this 'supramolecular' effect.[179]

V. Excited-State Chemistry

In this short section, salient excitation and quenching processes are considered[180] (see also the review by Bünzli and Piguet in this issue[181]), together with recent developments in our understanding of information concerning complex structure and dynamics that can be gleaned from static and time-resolved[182] measurements of luminescence. In addition, examples are described in which the intensity, lifetime, or polarization of lanthanide emission is rendered sensitive to the local ionic or chiral environment by perturbation of the singlet, triplet, or lanthanide excited states that are populated following absorption of light.[7,8]

A. Excitation and Quenching

The lanthanide excited state may be directly populated by absorption of light, but the very low molar absorption coefficients associated with parity-forbidden f—f transitions ($\epsilon < 1$ M^{-1} cm^{-1} commonly) necessitates the implementation of laser excitation.

Scheme 4

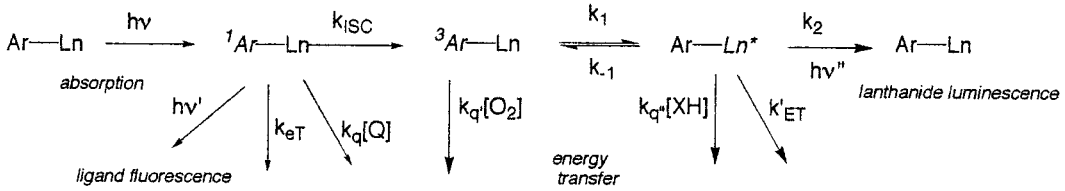

Tunable dye lasers allow $^5D_o \leftrightarrow {}^7F_o$ excitation of Eu (580 nm), and the $^7F_6 - {}^5D_4$ transition in Tb^{3+} species can be populated using an argon laser.[7] The $^7F_1 \rightarrow {}^5D_2$ and $^7F_o \rightarrow {}^5D_2$; transitions of Eu have also been excited using the weaker argon laser lines at 472.7 and 465.8 nm.[92,90]

Direct excitation of the near-IR emitting Ln^{3+} ions (Er^{3+}, Nd^{3+}, Yb^{3+}) may be achieved using an optical parametric oscillator.[183] Sensitization of lanthanide luminescence (Scheme 4) may be achieved by incorporating a suitable chromophore into the ligand structure. Ideally such a chromophore should absorb light efficiently (large ϵ) at a suitable wavelength and possess a fast intersystem crossing to the triplet state, allowing its efficient population. The relatively high energy of the most likely acceptor levels on Eu^{3+}/Tb^{3+} (17 200 and 20 400 cm^{-1}) means that the triplet excited state should be above 22 000 cm^{-1}, otherwise competing, thermally activated, back energy transfer occurs. This restricts the range of chromophores to those with a high triplet energy and therefore a small $S_1 - T_1$ energy gap if excitation is to be achieved in the range 330−430 nm.[184,185] Examples include substituted coumarin,[183] phenanthridines,[184] tris-bipyridylcryptates,[186] acyclic terpyridyls,[187] aryl-substituted calixarenes,[188] *m*-terphenyls,[189] acridones,[190] and aryl ketones.[191] Highly emissive complexes of β-diketonates (λ_{ex} 430 nm) have also been reported, but the Ln^{3+} complexes are usually hydrolytically unstable.[192,193] For the near-IR emitters (e.g., the Yb^{3+}-luminescent $^2F_{5/2}$ excited state is at 10 200 cm^{-1}), this restriction is lifted and a far wider range of sensitizing chromophores (e.g., eosin, fluorescein, phenanthridines, porphyrins) has been—or will be—identified.[74,194−196] The feasibility of multiphoton excitation of the sensitizing ligand in these Ln conjugates has been demonstrated. Using a pulsed Ti−sapphire laser, excitation around 776 nm has led to the sensitized emission of selected Eu complexes via a two-photon excitation process.[268]

The ease of reduction of the Eu^{3+} ion in its complexes with poly-aza ligands (typically at around −1.1 V) means that competitive deactivation of the singlet excited state of the chromophore by a photoinduced electron-transfer (PET) process often limits the overall emission quantum yield. This PET process has been suppressed by raising the oxidation potential of the sensitizing chromophore,[184] e.g., in azatriphenylenes[197,280] and in 6-substituted phenanthridines and *p*-substituted aromatics[67,198] possessing an electron-withdrawing group.[123]

To avert ligand exchange processes in aqueous media and engender high kinetic and thermodynamic stability of the primary complex, the same basic ligand systems that have been developed for use in targeted radiotherapy or as radiosensitizers[14,15,199,200] and in contrast agent research[1,2] are of interest in the excited-state chemistry of emissive Ln complexes. Examples of such complexes (a selection is given in Chart 7) reveal the preponderance of DOTA- and DTPA-based ligands, echoing the situation for the in vivo applications.[13,74,82,185,198,201]

Deactivation of the luminescence from excited Ln^{3+} ions in solution occurs by a vibrational energy-transfer process, involving high-energy vibrations of water molecules—both bound and closely diffusing—or of ligand oscillators.[147] Quenching by OH oscillators may be minimized by using octa- or nonadentate ligands ($q = 1 \rightarrow 0$), although amide and amine NH oscillators may also quench efficiently in certain cases.[202] For excited Er^{3+} ($^4I_{13/2}$), Nd^{3+} ($^4F_{3/2}$), and Yb^{3+} ($^2F_{5/2}$) species, much longer lifetimes have been found in inorganic matrices,[203−205] highlighting the efficient quenching by C−H oscillators[189]—in addition to the much larger effect associated with NH and OH vibrational quenching.[148,183] The effect of distance on the efficiency of vibrational deactivation follows an approximate r^{-6} dependence. For an OH oscillator that is 2.9 Å from a Ln^{3+} ion, the effect can be assumed to be 100% efficient (i.e., a typical Ln water proton distance from crystallographic analyses of aqua species: section II). Then at a distance of 3.6 Å, the process may be calculated to be 25% efficient and 8% at 4.5 Å.[180] These distances approximate to second- and outer-sphere hydration values (section III.C) and highlight the quenching effect of unbound water molecules. As a consequence, an improved method for assessing the hydration states of Eu, Yb, and Tb complexes has emerged, accounting for the effect of exchangeable XH oscillators and of closely diffusing waters,[147,180] In a revision of the earlier procedure,[206] based on the assumption that quenching by O−D and N−D oscillations is negligible, eqs 7 and 8 are operative (x is the number of oxygen-bound amide NH groups). Values of q should still be treated with caution (±20%) as the empirical correction terms are a function of complex hydrophobicity and were calibrated for relatively hydrophilic complexes.

$$q^{Eu} = 1.2[(k_{H_2O} - k_{D_2O}) - (0.25 + 0.07x)] \quad (7)$$

$$q^{Tb} = 5[(k_{H_2O} - k_{D_2O}) - 0.06] \quad (8)$$

A critical assessment of this process has been described, together with a collation of examples,[147,180] reporting the radiative rate constants for emission in H_2O and D_2O.

B. Emission Characteristics

Only Eu^{3+} species give rise to relatively simple emission spectra as the luminescent ^5D_o excited state

Chart 7

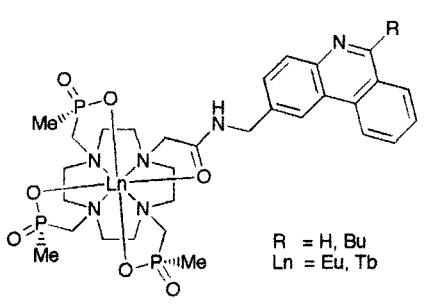

[LnDO3MPphen]

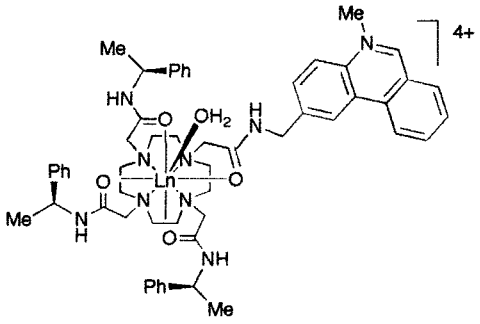

(SSS)-Δ-[LnDO3PhAM-phenMe]$^{4+}$

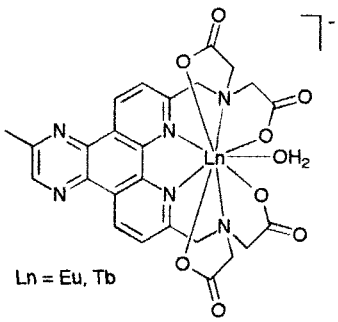

[LnTATRIPHENTA]$^{-}$

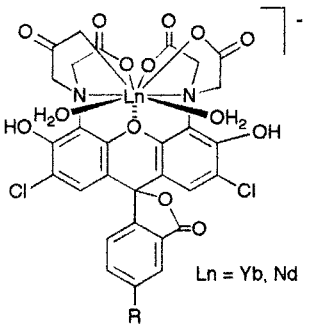

[LnFX]$^{-}$

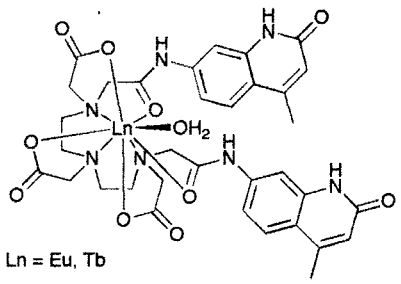

[LnDTPA-AmCOU]

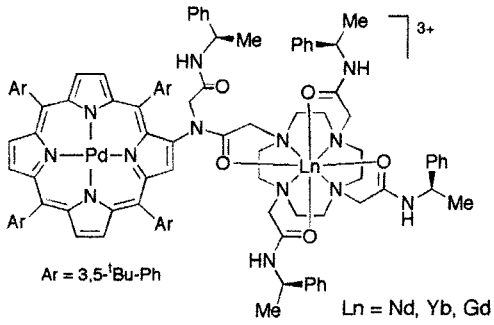

(S-SSS)-Δ-[LnDO3Ph-PdP]$^{3+}$

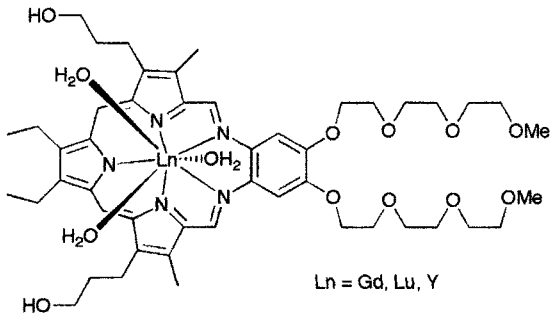

[Ln-TEX]$^{2+}$

is nondegenerate.[207,208] For the highest energy $^5D_o-{}^7F_o$ emission band at 580 nm, one component is expected for each chemically distinct species that is not undergoing exchange on the millisecond time scale. Laser excitation of this transition may be monitored at 591 ($\Delta J = 1$) or 614 nm ($\Delta J = 2$), and each Eu^{3+} species will give rise to a unique excitation spectrum whose intensity is a function of complex concentration. The use of pulsed laser excitation allows the measurement of Eu^{3+} excited-state lifetimes, which are characteristic of each complex. Such behavior has been used in the development of a spectroscopic method for determining Eu^{3+} stability constants in aqueous solution,[209,210] based on competition between two ligands, for one of which stability and speciation has been established. Following laser excitation at 579−581 nm, the excitation intensity of each species is measured using time-resolved methods if their excited state lifetimes are sufficiently different or if emission intensities (e.g., at 614 nm, $\Delta J = 2$) of the two species differ at the excitation wavelength, using non-time-resolved methods. The values of formation constants obtained agree well with measurements made by potentiometric methods.[209]

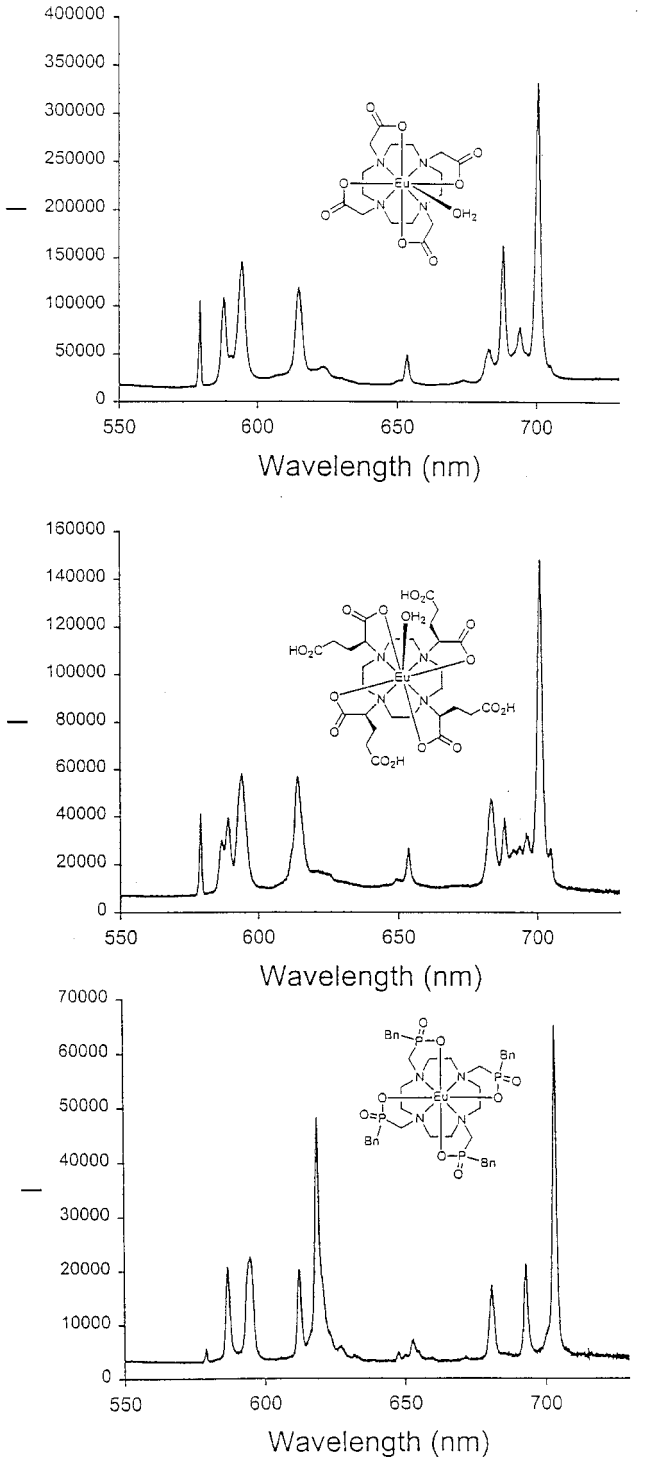

Figure 14. Europium luminescence emission spectra for axially symmetric $[EuDOTA(H_2O)]^-$ (upper) with a 4:1 ratio of SAP/TSAP isomers; (*RRRR*)-$[EugDOTA(H_2O)]^{5-}$ with a 1:4 ratio of SAP/TSAP isomers, and (lower) (*RRRR*)-$[EuDOTPB]^-$ (>95% TSAP, $q = 0$), highlighting differences in the hypersensitive $\Delta J = 2$ and 4 manifolds, centered around 615 and 690 nm, respectively.

The dynamics of ligand exchange reactions may also be examined by time-resolved luminescence. The time dependence of Ln^{3+} emission is a function of the rate of chemical exchange relative to the de-excitation rate. When the chemical exchange rate is similar to the rate of luminescent decay (eq 9), the time-dependence of the observed luminescence can be

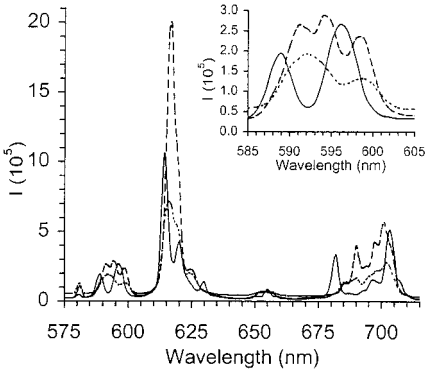

Figure 15. Changes in the Eu emisison spectrum of $[EugDO3AMeoS]^{3-}$ at pH 9.93 (line), 5.49 (large dashes), and 3.00 (small dashes), highlighting the presence of 3 solution species (λ_{exc} 397 nm): see Schemes 2 and 5.

defined precisely.[182,211−213] Such methods may attract increasing attention to monitor water exchange reactions at Eu/Tb in cationic complexes on the millisecond time scale or at Yb/Nd in the microsecond lifetime regime.[126]

$$\mathrm{LnL} + \mathrm{L}' \underset{k_{-1}}{\overset{k_1}{\rightleftharpoons}} \mathrm{LnL}' + \mathrm{L} \qquad (9)$$

$$\mathrm{LnL} \xrightarrow{k_{em}} \qquad \mathrm{LnL}' \xrightarrow{k'_{em}}$$

The formally forbidden $\Delta J = 0$ transition in Eu^{3+} emission may gain intensity through *J*-mixing (e.g., in C_n, C_{nv} symmetry),[211] and its oscillator strength in general is sensitive to the ligand field and symmetry.[62] The intensity of the magnetic-dipole-allowed $\Delta J = 1$ transition is relatively independent of coordination environment: two transitions are allowed if the complex possesses a C_3 or C_4 axis and three in complexes of lower symmetry. For the hypersensitive $\Delta J = 2$ and 4 transitions, the intensity[62] is very sensitive to the ligand field, especially the nature and polarizability of the axial donor—if present.[279] Thus, the Eu emission spectrum can be considered as a fingerprint of the Eu coordination environment. Selected examples (Figure 14) showing C_4-symmetric Eu complexes highlight this aspect.

As an example of the manner in which the Eu emission spectra signal the different structure of exchanging species, consider the competition between pH-dependent sulfonamide ligation and intramolecular carboxylate binding (Figure 15). Sulfonamide ligation is associated with an increase in intensity of the bands at 681 and 614 nm, whereas carboxylate association is signaled by intensity changes at 617 nm and by distinctive changes in the form of the $\Delta J = 1$ manifold (Scheme 5). The pH dependence of these emission spectral variations ($I_{em} = 614$ nm) mirrored exactly the variation of proton relaxivity in the analogous Gd complexes.[120] Furthermore, the ratio of $\Delta J = 2/\Delta J = 1$ bond intensities serve as a useful parameter for monitoring changes in species distribution. This ratio is independent of complex concentration and has been used analytically.[78,120,123] Factors determining the polarization of emission in chiral Ln^{3+} complexes have also been surveyed[63,79] and discussed in section III.

Scheme 5

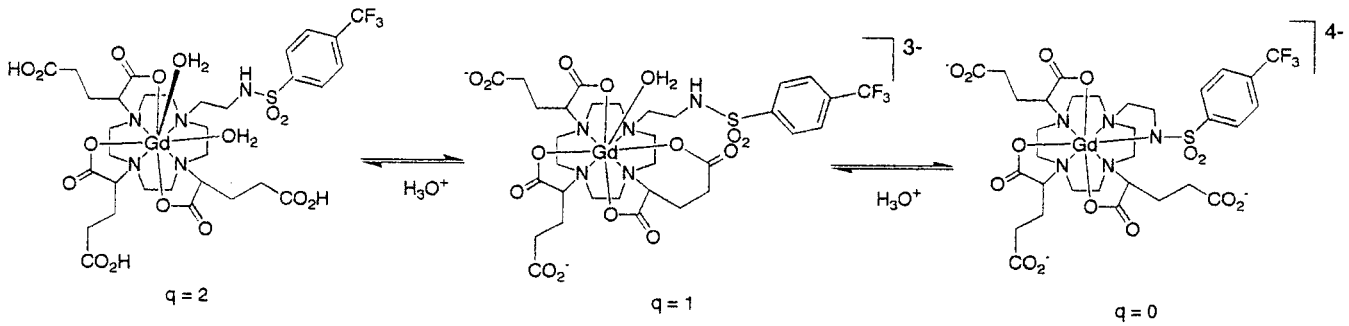

C. Responsive Luminescent Systems

Consideration of the photophysical scheme defining sensitized lanthanide luminescence reveals three 'windows of opportunity' to achieve modulation of the Ln^{3+} emission (Scheme 3). The first involves perturbation of the singlet excited state, wherein quenching involving electron- or charge-transfer processes may be altered by a binding process of the Ln complex. Suppression of intramolecular photoinduced electron transfer following protonation of the ligand constitutes a simple example[214,218] and has been demonstrated in the pH sensitivity of emission from [Tb(TERPYAMEt)]$^{+}$ (Charts 8 and 9) involving protonation of the tertiary amine groups. The inhibition of the ligand to metal charge-transfer process that leads to quenching of the singlet state of the sensitizing chromophore has also been defined:[184,198,216,276,277] pH sensors (e.g., incorporating [Eu(DO3AMPhenBu)] immobilized in a sol gel matrix have been reported based on this principle.[123] (Binding of the appended *N*-alkylphenanthridinium core in [Ln(DO3APhAMphenMe)]$^{4+}$ to the electron-rich GC base pairs leads to charge-transfer quenching of fluorescence from the phenanthridinium S_1 state, which is echoed by reduction in Eu emission intensity. This has been studied in oligonucleotides and DNA of varying GC content, and quenching was up to 20 times more efficient for GC over AT base pairs.[82,217]) Zinc binding to [Tb(DO3AAM-PENT)] enhances the Tb emission spectrum at pH 7.4 with a 26% change in a simulated extracellular background and with an apparent dissociation constant of 0.6 μM.[215] Protonation or metal binding of the sensitizing chromophore also may lower the energy of the singlet excited state, so that changes in excitation spectra can also characterize the reversible binding event[123] or allow selective excitation of the protonated or metal-bound species.

Second, the triplet excited state of the sensitizing chromophore may be perturbed. Its energy may be altered by protonation or metal binding, which may perturb the rate of forward or reverse energy transfer.[219,220] The aryl triplet state is sensitive to collisional quenching by molecular oxygen, so that for cases where $k_q[O_2]$ is of the same order as k_{ET}, then the Ln^{3+} emission intensity and lifetime is also a sensitive—albeit potentially complex—function of pO_2 in solution. Reports of optical oxygen sensing based on the quenching of Eu^{3+} luminescence in tris(β-diketonate) phenanthroline Eu complexes have appeared in which the lanthanide complex is immobilized in a fluoropolymer film[221,222] and the sensor operates at the air/solid interface. Terbium—phenanthridinium complexes exhibit pO_2 sensitivity in aqueous media with Stern—Volmer quenching constants of the order of 25—50 mmHg (O_2).[184] In addition, the Nd— and Yb—palladium porphyrin conjugates (Chart 8; e.g., [Yb(LnDO3Ph-PdP)]$^{3+}$) exhibit a sensitivity to dissolve oxygen as the rate of intramolecular energy transfer from the palladium porphyrin triplet to the Ln ion is rather slow, owing to their relatively long spatial separation.[74] Many other cases of pO_2 sensitivity of Ln^{3+} emission intensity have also been observed where a relatively slow energy-transfer step is found.[181]

Finally, the excited lanthanide ion itself may be quenched. Intermolecular energy transfer, for example, has been observed between the (acceptor) pH-sensitive dye bromothymol blue[223]—absorbing at 615 nm in basic media—and (donor) Eu complexes in aqueous media. Such an energy-transfer process was first applied by Mathis[6] in the 75% efficient quenching of Eu emission in Lehn's tris(bipyridyl) cryptand[186] by the protein allophycocyanine. The excited protein fluoresces at 665 nm with the time delay of the donor europium cryptate. Such a process is a key feature of commercial time-resolved homogeneous immunoassays.[235,236] More recently, using europium complex of (DTPA—COUMCF) [Chart 8], absorption at 370 nm, followed by intramolecular energy transfer led to a Eu emission that was quenched by bromothymol blue over the pH range 5—9 with a 40% modulation when immobilized in a sol—gel matrix.[224] Alternatively, the Ln^{3+} ion may be quenched by vibrational energy transfer involving energy-matched XH oscillators. Thus, the displacement of bound water molecules, e.g., by inter- or intramolecular binding anion binding, may be signaled by an enhancement of emission intensity,[78,122] an increase in the excited-state lifetime, and a change in spectral form which is most readily interpreted with Eu^{3+} complexes (see section IV.D). With chiral complexes the circular polarization of emission may be modulated, following substitution of bound water, either because of a change in complex helicity or simply by a change in the spectral form. Exemplifying the former case is the selective reversible binding of carbonate/hydrogencarbonate to [LnDO3Ph(H_2O)$_2$]$^{3+}$ in which the complex may change from a SAP geometry (40° twist angle) to a TSAP structure with a smaller twist angle in the carbonate-chelated form.[78] In an example of the latter case, binding of a

Chart 8

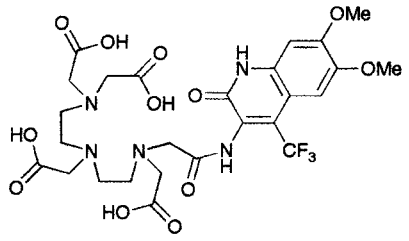

DTPACOUMCF

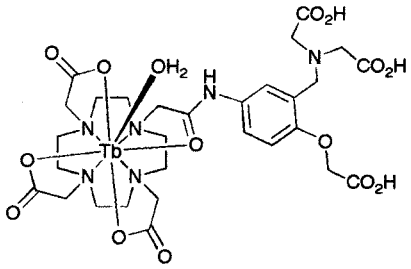

[TbDO3AM-PENT]

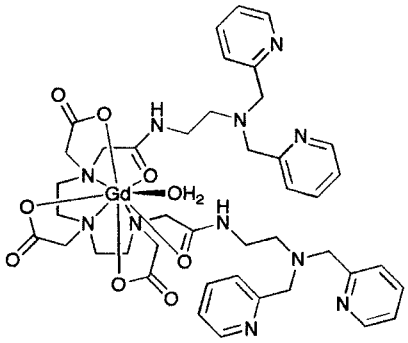

[GdDTPABPYED]

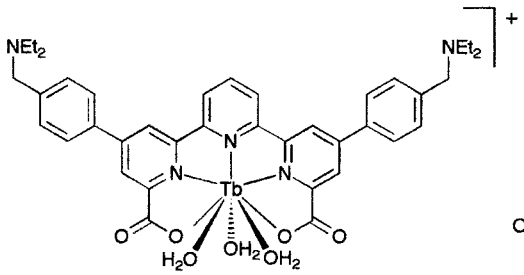

[TbTERPYAMEt]$^{+}$

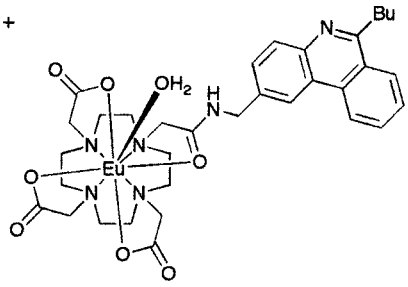

[EuDO3AAMphenBu]

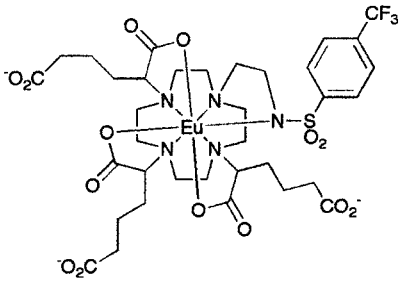

[EuaDO3AFOS]$^{4-}$

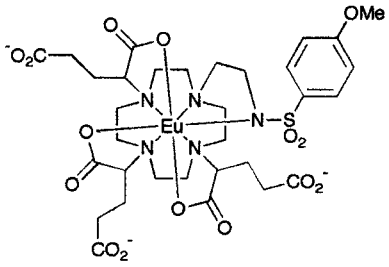

[EugDO3AMeOS]$^{4-}$

DNA phosphate group to [Ln(DO3Ph-phenMe)(H_2O)]$^{4+}$ has been observed by CPL, the CPL spectrum for the Eu complex in the presence of poly(GC), for example, resembling that obtained by independent addition of inorganic phosphate.[217]

The definition of responsive luminescent lanthanide complexes may be compared with the development in parallel of 'smart' Gd^{3+} contrast agents, wherein the overall relaxivity of the complex is a defined function of a biochemical variable such as pH, pM, or pX. Modulation of relaxivity by pH may be achieved by devising complexes in which either the complex hydration state, q, the water proton exchange rate, or the longitudinal water proton relaxation time T_{1m} is rendered a function of pH (eq 6, section IV.C). Examples of the former case involving on/off sulfonamide ligation have been reported, leading to a 48% increase in relaxivity between pH 7.4 and 6.8 in 50% human serum solution. Related cases involve pH-dependent association of hydrogencarbonate in $q = 2$ or 3 complexes.[42,78,165,225] Modulation of the water proton exchange rate has been defined involving base catalysis[34,42] or is related to protonation of a proximate ligand N or O, associated with large changes in the second hydration sphere.[125,227] Within the complex series of terms that defines T_{1m}, the pH dependence of the rotational correlation time τ_r may be picked out. Conjugates of gadolinium complexes have been reported in which a large change in the conformation and molecular volume of a macromolecule occurs, perturbing τ_r and hence the relaxivity.[226] The first example of a pM-dependent system was based on modification of well-known calcium−EGTA fluorophores:[228] binding of Ca^{2+} in the micromolar range is signaled by an increase in relaxivity from 3.3 to 5.8 mM^{-1} s^{-1}. In related work, the relaxivity of the neutral Gd complex of DTPAB-PYED was found to be fairly sensitive to variations in zinc concentration, with a maximal reduction in relaxivity of 33% for 1:1 ternary complex formation.[234]

In each of these cases it is likely that metal ion chelation perturbs the second (rather than the primary) hydration sphere.

VI. Magnetic Resonance Spectroscopy Applications

The paramagnetic properties of the lanthanides have been exploited in NMR spectroscopy for many years.[237−240] Each lanthanide ion has its own characteristic shift and relaxation properties which can affect NMR parameters of proximate nuclei to varying degrees. The lanthanides have found widespread use in the development of NMR probes for biomedical applications,[1−3,241] including the design of aqueous shift reagents for in vivo MRS and the NMR separation of enantiomers by chiral lanthanide shift reagents.[3,240] There have been numerous reviews on the theory and application of lanthanide- induced shifts and relaxation rate enhancements.[3,239,251] This section highlights some of the important basic features and reviews developments in the area. However, the theory and use of Gd contrast agents for MRI is not discussed here as this has been well documented in a number of recent reviews.[1,2,3,9]

A. Lanthanide-Induced Shifts (LIS)

There are three contributions to the LIS (Δ) for a nucleus of a ligand coordinated to a Ln^{3+} ion: the diamagnetic (Δ_d), contact (Δ_c), and pseudocontact (Δ_p) shift (eq 10).

$$\Delta = \Delta_d + \Delta_c + \Delta_p \tag{10}$$

The diamagnetic shifts are usually small and often neglected except for atoms directly coordinated to the Ln^{3+} ion. They originate from conformational changes, inductive effects, and direct field effects and can be determined directly or by interpolation from shifts induced by diamagnetic La^{3+} and Lu^{3+} ions.

Contact (or Fermi) shifts involve a through-bond transmission of the unpaired electron density at the Ln^{3+} ion to the nucleus of interest. The contact shift Δ_c (ppm) is given by eq 11, where $\langle S_z \rangle$ is the reduced value of the average spin polarization, β the Bohr magneton, k is the Boltzmann constant, γ is the gyromagnetic ratio of the nucleus in question, T is the absolute temperature, and $A/\hbar$ is the hyperfine coupling constant.

$$\Delta_c = \langle S_z \rangle F = \langle S_z \rangle \frac{\beta}{3kT\gamma}\frac{A}{\hbar}10^6 \tag{11}$$

The contact shift is usually huge for a nucleus directly bonded to the Ln^{3+} ion but decreases rapidly upon increasing the number of bonds between the Ln^{3+} and the nucleus, allowing easy identification of the donor atoms in the ligand.[3,239]

The pseudocontact contribution (or dipolar shift) is a result of a through-space interaction between the magnetic moments of the unpaired electrons of the Ln^{3+} and the nucleus under study and is expressed by eq 12.[3,239,242]

$$\Delta_p = C_D G = C_D \frac{\beta^2}{60k^2T^2}\left[\frac{\langle r^2 \rangle A_2^o (3\cos^2\theta - 1)}{r^3} + \langle r^2 \rangle A_2^2 \frac{(\sin^2\theta \cos 2\phi)}{r^3}\right] \tag{12}$$

where C_D is Bleaney's constant, $\langle r^2 \rangle A_2^o$ and $\langle r^2 \rangle A_2^2$ are second-order crystal field coefficients, r, θ, and ϕ are spherical coordinates of the observed nucleus with respect to the Ln^{3+} at the origin and with the principal axis as the z-axis. By combining C_D and the crystal field coefficients, the equation is simplified (eq 13).

$$\Delta_p = D_1 \frac{3\cos^2\theta - 1}{r^3} + D_2 \frac{\sin^2\theta \cos\phi}{r^3} \tag{13}$$

In the case of axially symmetric systems, eq 13 reduces further to eq 14

$$\Delta_p = D_1 \left[\frac{3\cos^2\theta - 1}{r^3}\right] \tag{14}$$

In fact, eq 14 is frequently used to calculate LIS in structural analysis even if the complex has no axial symmetry.[3,243] The pseudocontact contribution usually predominates for the lanthanides as the unpaired electron spin density largely resides on the Ln^{3+} ion. As the dipolar shift depends on the orientation of the resonating nucleus with respect to the Ln^{3+} ion, useful structural information may be gained.[1,11,237,239,241]

After subtraction of the diamagnetic contributions, the LIS is expressed as the paramagnetic shift, Δ'.

$$\Delta' = \Delta_c + \Delta_p = \langle S_z \rangle F + C_D G \tag{15}$$

Any contact contribution to Δ' must be separated out in order to use the dipolar term in structural analysis. The terms $\langle S_z \rangle$ and C_D are characteristic of the Ln^{3+} ion but independent of the ligand, whereas the opposite is true for F and G. Assuming that the lanthanide complexes studied are isostructural and of axial symmetry, using theoretical calculated values for $\langle S_z \rangle$ and C_D tabulated in the literature,[3,242] F and G may be determined by linear regression according to eqs 16 and 17, provided that Δ values of a ligand are known for two or more Ln^{3+} ions.

$$\frac{\Delta'}{\langle S_z \rangle} = F + \frac{C_D G}{\langle S_z \rangle} \tag{16}$$

$$\frac{\Delta'}{C_D} = \frac{\langle S_z \rangle F}{C_D} + G \tag{17}$$

Equation 16 should be used in linear regression analysis when Δ' is dominated by dipolar shifts (calculated $G/F \gg 1$), and eq 17 used when the contact contribution dominates Δ' (calculated $G/F \ll 1$).[241]

Small changes in G may reflect changes in the orientation of the ligands as the ionic radii of the lanthanides decreases along the series. These changes are magnified in eq 16, and breaks are frequently

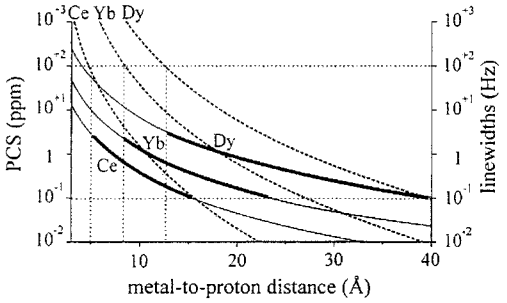

Figure 16. Useful ranges of pseudo-contact shifts (PCS) for Ce^{3+}-, Yb^{3+}-, and Dy^{3+}-containing proteins. The dashed lines indicate the observed line widths.

observed in the plots according to eq 16. As F values are not affected, the plots according to eq 17 remain linear. A significant structural change or variation in crystal field coefficients occurring across the lanthanide series will be observed as nonlinearity in plots based on both eqs 16 and 17.

The ambiguity of interpreting nonlinearity in terms of either factor is removed by the recent introduction of a 'two nuclei' (i, k) equation, which does not depend on crystal field parameters (eq 18).[273] This may be particularly useful as it is increasingly clear that crystal field coefficients may differ unpredictably, especially around the center of the series, i.e. Eu-GdTb.[274,275]

$$\frac{\delta_{ij}}{\langle S_z\rangle_j} = \left[F'_i - F'_k\frac{G'_i}{G'_k}\right] + \frac{G'_i}{G'_k}\cdot\frac{\delta_{kj}}{\langle S_z\rangle_j}$$

where

$$R_{ik} = \frac{G'_i}{G'_k} = \frac{(1 - 3\cos^2\theta_i)}{(1 - 3\cos^2\theta_h)}\cdot\frac{r_k^3}{r_i^3} \qquad (18)$$

B. Applications in Aqueous Media

There has been much interest in the use of lanthanide complexes as shift reagents in NMR to effect spectral simplification and resolution enhancement.[237,240,249] For a number of years lanthanide-induced shifts have provided angular and distance information and have found widespread use in the determination of solution structures of lanthanide chelates.[3,241] Lanthanide complexes (most often of the simple aqua ion) continue to be used as paramagnetic probes in biological studies to gain structural information on proteins, nucleotides, and amino acids.[237,238,241] For example, the lanthanide ions can often substitute the NMR-silent Ca^{2+} ion in biological systems without loss of biological activity,[244] allowing partial structural analysis of calcium-binding proteins in solution.[245,246] Ce^{3+}, Dy^{3+}, and Yb^{3+}, for example, have recently been substituted into Calbindin D_{9k}, a protein of 75 amino acids.[248] The application of these three lanthanide ions, each with very different pseudocontact shifts, can provide structural constraints for NMR−NOE analyses in shells at variable distances from the paramagnetic center (up to ~40 A) (Figure 16). The introduction of very high magnetic fields and multidimensional NMR techniques (NOE, COSY, HETCOR, EXSY) has enabled good spectral resolution and the development of accurate structural solution models of several biomolecules, without the need to employ the lanthanides. However, covalently bound LnL tags are used to orient proteins in high magnetic fields, allowing the use of residual dipolar couplings to refine the solution structures of macromolecules.[271,272]

Aqueous lanthanide complexes continue to be examined as chiral shift reagents for the NMR separation of enantiomers[240] and as shift reagents in biomedical magnetic resonance spectroscopy (MRS).[3,9,247] Although the majority of studies of chiral lanthanide complexes in the resolution of enantiomeric signals in NMR spectroscopy has been performed in organic solvents, a few water-soluble reagents have been reported.[240,250−260] Kabuto and have demonstrated that lanthanide complexes of (*R*)-PDTA (Ln = Eu), (*R*)-TPPN (Ln = Eu) and (*SS*)-BPBA (Ln = La, Ce) resolve the enantiotopic signals of a range of hydroxy-, amino-, and carboxylic acids in aqueous solution.[251−256] The magnitude of the shift difference between enantiomers ($\Delta\Delta\delta$) was small, often less than 0.1 ppm, but sufficient to determine enantiomeric purity. The $\Delta\Delta\delta$ values show a strong pH dependence. For example, separation of signals of lactic acid with (*S*)-[Eu−PDTA] was optimum at pH = 4 but was not observed at pH = 11.[252−254] The europium complex of TPPN resolved enantiomeric signals of α-amino acids even at neutral pH,[255] whereas the BPBA complexes separated the same resonances over a wider pH range.[256] All three systems afforded a good correlation between the relative signal position of the enantiomers and the absolute configuration of the substrate.

Yb^{3+} and Eu^{3+} complexes of CMOS are also capable of accomplishing NMR resolution of enantiomeric mixtures and enantiotopic nuclei of a variety of carboxylates and amino acids.[257] Enhanced spectral resolution of amino acids was reported for the Eu^{3+} complex of EDDS ($\Delta\Delta\delta$ −0.4) between pH 9−11.[258] The induced chemical shift differences were due not only to differences in adduct geometry but also in the association constants of the ternary complexes formed between [EuEDDS] and the amino acids. Superior diastereomeric shift differences were reported for the analogues of EDDS, PIPDS, and DPEDDS,[259] although they are also limited in use to a narrow pH range (~9). A new europium chiral shift reagent, TRENBMTA for α-amino acids and *N*-acyloligopeptides in aqueous solution, has been reported to give rise to enantiomeric separation at neutral pH without significant signal broadening.[260] However, it should be noted that the observed limiting chemical shift nonequivalence in each of these examples is again very small (<0.1 ppm typically) as found in so many of these aqueous chiral shift agents. Coupled with the broadness of the observed signals—often associated with chemical exchange broadening due to competing intermolecular exchange processes—this has meant that the method has found little direct application for enantiomeric purity determination in aqueous solution. On the other hand, given the large shifting ability of, say, Yb and Pr complexes, the use of well-defined water-soluble chiral complexes—such

Chart 9

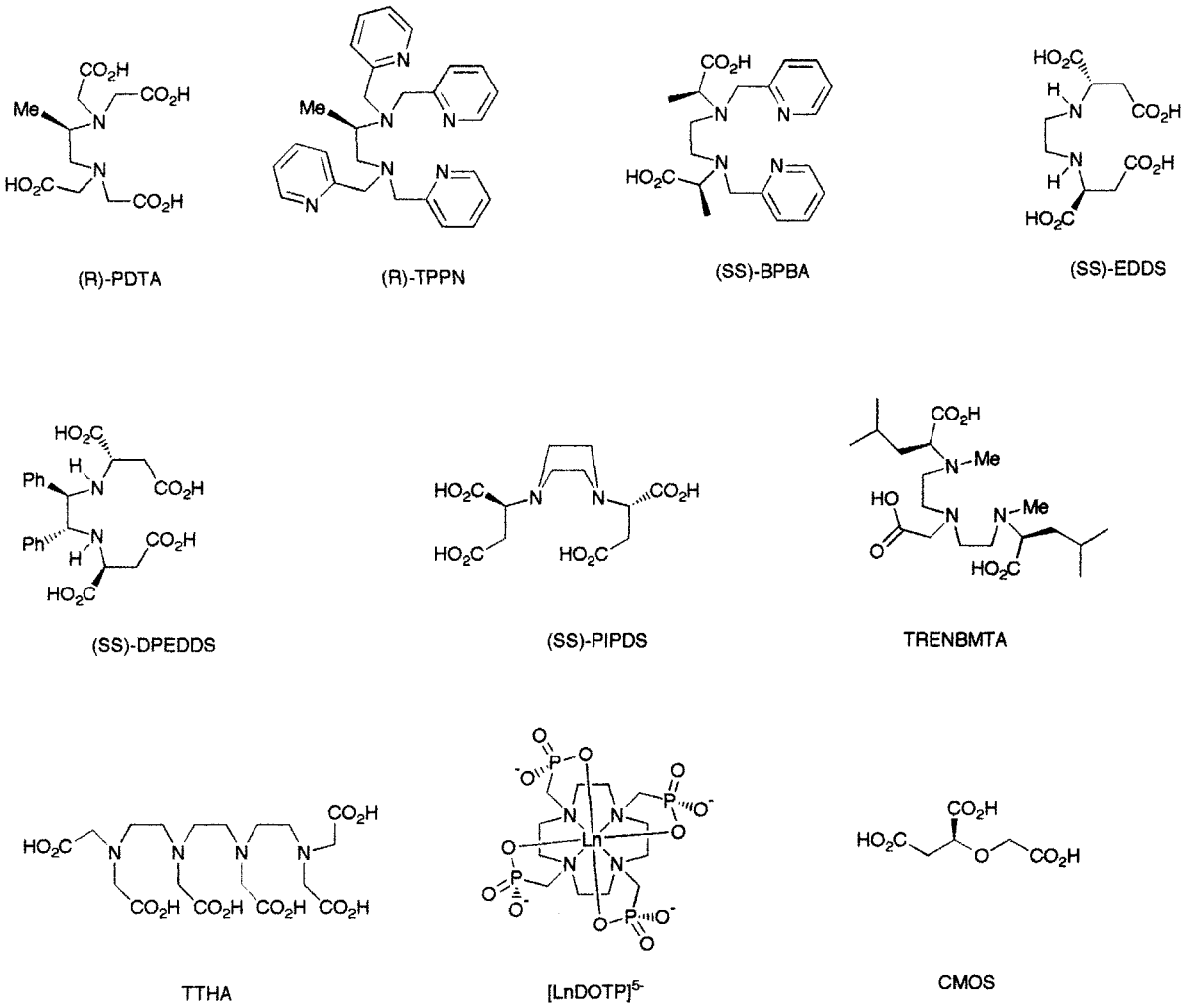

as those described in section III (based on heptadentate ligands)—offers considerable scope for the definition of more effective chiral shift reagents and—where the association constant is much larger—of chiral derivatizing agents. A first step in this direction has been reported for α-hydroxy acids, with nonequivalence of over 10 ppm for lactate complexes of [YbDO3Ph]$^{3+}$ (Chart 5).[166]

Knowledge of the distribution of biologically important anions and cations over intracellular and extracellular compartments is of considerable value in cell biology and of great potential use in medical diagnosis. Introduction of a water-soluble lanthanide shift reagent that can bind to the ion of interest and remain extracellular may induce an isotropic shift in selected nuclei, thereby allowing discrimination between intra- and extracellular ion signals. Most reports have concentrated on the use of anionic lanthanide chelates as shift reagents for alkali metals, e.g., ^{23}Na, ^{39}K, ^{7}Li, and ^{133}Cs.[3,9,237,247] These systems operate through ion-pair interactions between coordinated or pendent negatively charged groups in the chelate (e.g., carboxylate or phosphonic groups). Most favorable shifts are produced with the lanthanides with high magnetic moments and short relaxation times (i.e., Dy^{3+}, Tb^{3+}, Tm^{3+}) in complexes with high negative charge which favor a strong electrostatic interaction. Such polar species are distributed in the extracellular compartment. The ion-binding sites should be in a favorable geometry (within the so-called McConnell cone) relative to the axis of symmetry (the dipolar shift has a $3\cos^2\theta - 1/r^3$ dependence). The most effective shift reagent reported for alkali metals is the Dy^{3+}—bis(tripolyphosphate), [Dy(PPP)$_2$].[7−261] However, the [Ln(PPP)$_2$]$^{7-}$ complexes are not kinetically stable in vivo, decomposing in the presence of pyrophosphatases. There is also competition for coordination of the triphosphate by endogenous Ca^{2+} and Mg^{2+} ions.[262] [Dy(TTHA)]$^{3-}$ has a higher stability constant but is a much less efficient shift reagent than [Dy(PPP)$_2$]$^{7-}$ due to the reduced negative charge and the unfavorable spatial location of the unbound carboxylate binding sites which lie away from the paramagnetic center.[263,264] The most promising shift reagent for metal cations in vivo are the Dy^{3+} and Tm^{3+} complexes of DOTP.[265,266] The complexes are thermodynamically and kinetically very stable, resistant to dissociation over a wide pH range, and have cationic binding sites very close to the 4-fold axis of symmetry yielding maximum shifting ability. The [Tm(DOTP)]$^{4-}$ complex has been successfully used for in vivo studies of rat kidneys and produces some dramatic isotropic ^{23}Na shifts.[267] Finally, cationic lanthanide chelates have been considered as shift reagents for biological anions. [Eu(DTMA)]$^{3+}$ was found to discriminate

effectively between intra- and extracellular inorganic phosphate.[9]

Although the studies to date have highlighted the potential of lanthanide chelates as ionic shift reagents in magnetic resonance, generally the observed effects are small. Further studies are warranted focusing on the design and application of more effective complexes of greater intrinsic kinetic stability.

VII. Acknowledgements

It is a pleasure to thank Professors Mauro Botta, Lorenzo di Bari, and Ivano Bertini for the data in Figures 12, 9, and 16 as well as those cited below, especially the current and past co-workers and collaborators for their inspiration in some of the recent work described. Support from (JAKH-Senior Advanced Fellowship; HP-postdoctoral fellowship) the Royal Society (R.S.D.), and the EC COST Action D-18 (Lanthanide Chemistry for Diagnosis and Therapy) is also gratefully acknowledged.

VIII. Supporting Information

Flow chart for obtaining data set. This material is available free of charge via the Internet at http://pubs.acs.org.

IX. References

(1) *The Chemistry of Contrast Agents in Medical Magnetic Resonance Imaging*; Merbach, A. E., Toth, E. Eds.; Wiley: New York, 2001.
(2) Caravan, P.; Ellison, J. J.; McMurray, T. J.; Lauffer, R. B. *Chem. Rev.* **1999**, *99*, 2293.
(3) Peters, J. A.; Huskens, J.; Raber, D. J. *Prog. Nucl. Magn. Reson. Spectrosc.* **1996**, *28*, 283.
(4) Komiyama, M.; Takeda, N.; Shigekawa, H. *Chem. Commun.* **1999**, 1443.
(5) Hemmila, I. K. *Applications of Fluorescence in Immunoassays*; Wiley and Sons: New York, 1991.
(6) Mathis, G. *Clin. Chem.* **1995**, *41*, 1391.
(7) Parker, D. *Coord. Chem. Rev.* **2000**, *205*, 109.
(8) Parker, D.; Williams, J. A. G. *J. Chem. Soc., Dalton Trans.* **1996**, 3613.
(9) Aime, S.; Botta, M.; Fasano, M.; Terreno, E. *Chem. Soc. Rev.* **1998**, *27*, 19.
(10) Alexander, V. *Chem. Rev.* **1995**, *95*, 273.
(11) Bianchi, A.; Calabi, L.; Corona, F.; Fontana, S.; Losi, P.; Maiocchi, A.; Paleari, L.; Valtancoli, B. *Coord. Chem. Rev.* **2000**, *204*, 309.
(12) Toth, E.; Burai, L.; Merbach, A. E. *Coord. Chem. Rev.* **2001**, *216*, 363.
(13) Bakker, B. H.; Goes, M.; Hoebe, N.; van Ramesdonk, H. J.; Verhoeven, J. W.; Wertz, M. H. V.; Hofstraat, J. W. *Coord. Chem. Rev.* **2000**, *208*, 3.
(14) Mody, T. D.; Sessler, J. L. In *Supramolecular Technology*, Reinhoudt, D. N., Ed.; J. Wiley: New York, 1999; Chapter 7, pp 245−293.
(15) Mody, T. D.; Sessler, J. L. *J. Porphyrins Phthalocyanines* **2001**, *5*, 134.
(16) Allen, F. H.; Kennard, O. Cambridge Structural Database, October 2000.
(17) Chatterjee, A.; Maslen, E. N.; Watson, K. J. *Acta Crystallogr.* **1988**, *B44*, 381.
(18) Albertson, J.; Elding, I. *Acta Crystallogr.* **1977**, *B33*, 1460.
(19) Aslanov, L. A.; Ionov, V. M.; Kiekbaev, I. D. *Koord. Khim.* **1976**, *2*, 1674.
(20) Kou, H.-Z.; Yang, G.-M.; Liao, D.-Z.; Cheng, P.; Jiang, Z.-H.; Yan, S.-P.; Huang, X.-Y.; Wang, G.-L. *J. Chem. Crystallogr.* **1998**, *28*, 303.
(21) Rohovec, J.; Vojtisek, P.; Hermann, P.; Ludvik, J.; Lukes, I. *J. Chem. Soc., Dalton Trans.* **2000**, 141.
(22) Aime, S.; Batsanov, A. S.; Botta, M.; Dickins, R. S.; Faulkner, S.; Foster, C. E.; Harrison, A.; Howard, J. A. K.; Moloney, J. M.; Norman, T. J.; Parker, D.; Royle, L.; Williams, J. A. G. *J. Chem. Soc., Dalton Trans.* **1997**, 3623.
(23) Shannon, R. D. *Acta Crystallogr.* **1976**, *A32*, 751.
(24) Rohovec, J.; Vojtisek, P.; Hermann, P.; Mosinger, J.; Zák, Z.; Lukes, I. *J. Chem. Soc., Dalton Trans.* **1999**, 3585.
(25) Malandrino, G.; Benelli, C.; Castelli, G.; Fragala, I. L. *Chem. Mater.* **1998**, *10*, 3434.
(26) Rogers, R. D.; Rollins, A. N.; Elzenhouser, R. D.; Voss, E. J.; Bauer, C. B. *Inorg. Chem.* **1993**, *32*, 3451.
(27) Yan, L.; Liu, J.; Wang, X.; Yang, R.; Song, F. *Polyhedron* **1995**, *14*, 3545.
(28) Lu, W. M.; Cheng, Y. Q.; Dong, N.; Xu, C.; Chen, C. G. *Acta Crystallogr.* **1995**, *C51*, 1756.
(29) Inoue, M. B.; Inoue, M.; Fernando, Q. *Acta Crystallogr.* **1994**, *C50*, 1037.
(30) Schumann, H.; Bottger, U. A.; Weisshoff, H.; Ziemer, B.; Zschunke, A. *Eur. J. Inorg. Chem.* **1999**, 1735.
(31) Aime, S.; Botta, M.; Fasano, M.; Marques, M. P. M.; Geraldes, C. F. G. C.; Pubanz, D.; Merbach, A. E. *Inorg. Chem.* **1997**, *36*, 2059.
(32) Aime, S.; Botta, M.; Ermondi, G. *Inorg. Chem.* **1992**, *31*, 4291.
(33) Hoeft, S.; Roth, K. *Chem. Ber.* **1993**, *126*, 869.
(34) Aime, S.; Barge, A.; Bruce, J. I.; Howard, J. A. K.; Moloney, J. M.; Parker, D.; de Sousa, A. S.; Woods, M. *J. Am. Chem. Soc.* **1999**, *121*, 5762.
(35) Howard, J. A. K.; Kenwright, A. M.; Moloney, J. M.; Parker, D.; Port, M.; Navet, M.; Rousseau, O.; Woods, M. *Chem. Commun.* **1998**, 1381.
(36) Spirlet, M.; Rebizant, J.; Desreux, J. F.; Loncin, M.-F. *Inorg. Chem.* **1984**, *23*, 359.
(37) Shukla, R. B. *Magn. Reson. Ser. A* **1995**, *113*, 196.
(38) Chin, K. O. A.; Morrow, J. R.; Lake, C. H.; Churchill, M. R. *Inorg. Chem.* **1994**, *33*, 656.
(39) Morrow, J. R.; Amin, S.; Lake, C. H.; Churchill, M. R. *Inorg. Chem.* **1993**, 4566.
(40) Amin, S.; Morrow, J. R.; Lake, C. H.; Churchill, M. R. *Angew. Chem., Int. Ed. Engl.* **1994**, *33*, 773.
(41) Chappell, L. L.; Voss, D. A.; Horrocks, W. de W.; Morrow, J. R. *Inorg. Chem.* **1998**, *37*, 3989.
(42) Aime, S.; Barge, A.; Botta, M.; Parker, D.; de Sousa, A. S. *J. Am. Chem. Soc.* **1997**, *119*, 4767.
(43) Alderighi, L.; Bianchi, A.; Calabi, L.; Dapporto, P.; Giorgi, C.; Losi, P.; Paleari, L.; Paoli, D.; Rossi, P.; Valtancoli, B.; Virtuani, M. *Eur. J. Inorg. Chem.* **1998**, 1581.
(44) Aime, S.; Barge, A.; Botta, M.; de Sousa, A. S.; Parker, D. *Angew Chem., Int. Ed. Engl.* **1998**, *37*, 2673.
(45) Dickins, R. S.; Howard, J. A. K.; Lehmann, C. W.; Moloney, J. M.; Parker, D.; Peacock, R. D. *Angew. Chem., Int. Ed. Engl.* **1997**, *36*, 521.
(46) Dickins, R. S.; Howard, J. A. K.; Maupin, C. L.; Moloney, J. M.; Parker, D.; Riehl, J. P.; Siligardi, G.; Williams, J. A. G. *Chem. Eur. J.* **1999**, *5*, 1095.
(47) Aime, S.; Botta, M.; Parker, D.; Senanayake, K.; Williams, J. A. G.; Batsanov, A. S.; Howard, J. A. K. *Inorg. Chem.* **1994**, *33*, 4696.
(48) Rohovec, J.; Lukes, I.; Hermann, P. *New J. Chem.* **1999**, *23*, 1129.
(49) Kim, W. D.; Keifer, G. E.; Huskens, J.; Sherry, A. D. *Inorg. Chem.* **1997**, *36*, 4128.
(50) Aime, S.; Botta, M.; Parker, D.; Williams, J. A. G. *J. Chem. Soc., Dalton Trans.* **1996**, 17.
(51) Aime, S.; Botta, M.; Dickins, R. S.; Maupin, C. L.; Riehl, J. P.; Williams, J. A. G. *J. Chem. Soc., Dalton Trans.* **1998**, 881.
(52) Brittain, H. G. *Chirality* **1996**, *8*, 357.
(53) Riehl, J. P.; Richardson, F. S. *Methods Enzymol.* **1993**, *226*, 539.
(54) Purdie, N.; Brittain, H. G. *Analytical Applications of Circular Dichroism*; Elsevier: Amsterdam, 1994.
(55) Nakanishi, K.; Berova, N.; Wood, R. W. *Circular Dichroism, Principles and Applications*; VCH: New York, 1994.
(56) Brittain, H. G. *Photochem. Photobiol.* **1987**, *46*, 1027.
(57) Richardson, F. S. *J. Less Common Met.* **1989**, *149*, 161.
(58) Brittain, H. G. *Pract. Spectrosc.* **1991**, *12*, 179.
(59) Riehl, J. P. *Acta Phys. Pol. A* **1996**, *90*, 55.
(60) Brittain, H. G. *J. Coord. Chem.* **1989**, *20*, 331.
(61) Brittain, H. G. *Inorg. Chem.* **1980**, *19*, 2136.
(62) Peacock, R. D. *Struct. Bonding (Berlin)* **1975**, *22*, 83.
(63) Richardson, F. S. *Inorg. Chem.* **1980**, *19*, 2806.
(64) Dickins, R. S.; Howard, J. A. K.; Moloney, J. M.; Parker, D.; Peacock, R. D.; Siligardi, G. *Chem. Commun.* **1997**, 1747.
(65) Dickins, R. S.; Howard, J. A. K.; Maupin, C. L.; Moloney, J. M.; Parker, D.; Peacock, R. D.; Riehl, J. P.; Siligardi, G. *New J. Chem.* **1998**, 891.
(66) Govenlock, L. J.; Howard, J. A. K.; Moloney, J. M.; Parker, D.; Peacock, R. D.; Siligardi, G. *J. Chem. Soc., Perkin Trans. 2* **1999**, 2415.
(67) Dickins, R. S.; Howard, J. A. K.; Moloney, J. M.; Parker, D.; Siligardi, G. *Chem. Commun.* **1997**, 1747.
(68) di Bari, L.; Pintacuda, G.; Salvadori, P.; Dickins, R. S.; Parker, D. *J. Am. Chem. Soc.* **2000**, *122*, 9257.
(69) di Bari, L.; Pintacuda, G.; Salvadori, P. *J. Am. Chem. Soc.* **2000**, *122*, 5557.
(70) Coruh, N.; Riehl, J. P. *Biochemistry* **1992**, 7970.

(71) Riehl, J. P.; Caruh, N. *Eur. J. Solid State Chem*. **1991**, *28*, 263.
(72) Riehl, J. P.; Coruh, N. *Collect. Czech. Chem. Commun*. **1991**, *56*, 3028.
(73) Maupin, C. L.; Dickins, R. S.; Govenlock, L. J.; Mathieu, C. E.; Parker, D.; Williams, J. A. G.; Riehl, J. P. *J. Phys. Chem. A* **2000**, *104*, 6709.
(74) Beeby, A.; Dickins, R. S.; Fitzgerald, S.; Govenlock, L. J.; Maupin, C. L.; Parker, D.; Riehl, J. P.; Siligardi, G.; Williams, J. A. G. *Chem. Commun*. **2000**, 1183.
(75) Govenlock, L. J.; Mathieu, C. E.; Maupin, C. L.; Parker, D.; Riehl, J. P.; Siligardi, G.; Williams, J. A. G. *Chem. Commun*. **1999**, 1699.
(76) Dickins, R. S. Ph.D. Thesis, University of Durham, 1997.
(77) Dickins, R. S.; Gunnlaugsson, T.; Parker, D.; Peacock, R. D. *Chem. Commun*. **1998**, 1643.
(78) Bruce, J. I.; Dickins, R. S.; Govenlock, L. J.; Gunnlaugsson, T.; Lopinski, S.; Lowe, M. P.; Parker, D.; Peacock, R. D.; Perry, J. J. B.; Aime, S.; Botta, M. *J. Am. Chem. Soc.* **2000**, *122*, 9674.
(79) Bruce, J. I.; Parker, D.; Lopinski, S.; Peacock, R. D. *Chirality* **2002**, *14*, (June issue).
(80) Meskers, S. C. J.; Dekkers, H. P. J. M. *Spectrochim. Acta* **1999**, *55*, 1837.
(81) Meskers, S. C. J. Ph.D. Thesis, University of Leiden, 1997.
(82) Bobba, G.; Dickins, R. S.; Kean, S. D.; Mathieu, C. E.; Parker, D.; Peacock, R. D.; Siligardi, G.; Smith, M. J.; Williams, J. A. G.; Geraldes, C. F. G. C. *J. Chem. Soc., Perkin Trans. 2* **2001**, 1729.
(83) Meskers, S. C. J.; Ubbink, M.; Canters, C. W.; Dekkers, H. P. J. M. *J. Phys. Chem*. **1996**, *100*, 17957.
(84) Meskers, S. C. J.; Dekkers, H. P. J. M. *J. Phys. Chem. A* **2001**, *105*, 4589.
(85) Meskers, S. C. J.; Dekkers, H. P. J. M. *J. Am. Chem. Soc.* **1998**, *120*, 6413.
(86) Meskers, S. C. J.; Dekkers, H. P. J. M. *Spectrochim. Acta* **1999**, *55*, 1858.
(87) Moritu, M.; Hemen, M.; Ansai, T.; Rau, D. *J. Lumin*. **2000**, *87*−*89*, 976.
(88) Maupin, C. L.; Meskers, S. C. J.; Dekkers, H. P. J. M.; Riehl, J. P. *J. Phys. Chem. A* **1998**, *102*, 4450.
(89) Meskers, S. C. J.; Dekkers, H. P. J. M.; Rapenne, G.; Sauvage, J.-P. *Chem. Eur. J*. **2000**, *6*, 2129.
(90) Huskowska, E.; Maupin, C. L.; Parker, D.; Williams, J. A. G.; Riehl, J. P. *Enantiomer* **1997**, *2*, 381.
(91) Glover-Fischer, D. P.; Metcalf, D. H.; Hopkins, T. A.; Pugh, V. J.; Chisdes, S. J.; Kankare, J.; Richardson, F. S. *Inorg. Chem*. **1998**, *37*, 3026.
(92) Hilmes, G. L.; Riehl, J. P. *J. Phys. Chem*. **1983**, *87*, 3300.
(93) Luck, R. L.; Maupin, C. L.; Parker, D.; Riehl, J. P.; Williams, J. A. G. *Inorg. Chim Acta* **2001**, *317*, 331.
(94) Sarka, L.; Burai, L.; Brucher, E. *Chem. Eur. J*. **2000**, *6*, 719.
(95) Tweedle, M. F.; Hagan, J. J.; Kumar, K.; Mentha, S.; Chang, C. A. *Magn. Reson. Imaging* **1991**, *9*, 409.
(96) Harrison, A.; Walker, C. A.; Pereira, K. A.; Parker, D.; Royle, L.; Pulukkody, K.; Norman, T. J. *Magn. Reson. Imaging* **1993**, *11*, 761.
(97) Wedeking, P.; Kumar, K.; Tweedle, M. F. *Magn. Reson. Imaging* **1992**, *10*, 641.
(98) Pulukkody, K. P.; Norman, T. J.; Parker, D.; Royle, C.; Broan, C. J. *J. Chem. Soc., Perkin Trans. 2* **1993**, 605.
(99) Caravan, P.; Comuzzi, C.; Crooks, W.; McMurry, T. J.; Choppin, G. R.; Woulfe, S. R. *Inorg. Chem*. **2001**, *40*, 2170.
(100) Burai, L.; Kiraly, R.; Lazar, I.; Brucher, E. *Eur. J. Inorg. Chem*. **2001**. *3*, 813.
(101) Bianchi, A.; Calabi, L.: Giorgi, C.; Losi, P.; Mariani, P.; Padi, P.; Rossi, P.; Valtancoli, B.; Virtuani, M. *J. Chem. Soc., Dalton Trans*. **2000**, 697.
(102) Szilagyi, E.; Toth, E.; Kovacs, Z.; Platzek, J.; Raduchel, B.; Brucher, E. *Inorg. Chim. Acta* **2000**, *298*, 226.
(103) Szilagyi, E.; Brucher, E. *J. Chem. Soc., Dalton Trans*. **2000**, 2229.
(104) Desreux, J. F. *Inorg. Chem* **1980**, *19*, 1319.
(105) Forsberg, J. H.; Delaney, R. M.; Zhao, Q.; Harchas, G.; Chandran, R. *Inorg. Chem*. **1995**, *34*, 3705.
(106) Mani, F.; Morassi, R.; Stoppini, P.; Vacca, A. *J. Chem. Soc., Perkin Trans. 2* **2001**, 2116.
(107) Jacques, V.; Desreux, J. F. *Inorg. Chem*. **1994**, *33*, 4048.
(108) Woods, M.; Aime, S.; Botta, M.; Howard, J. A. K.; Moloney, J. M.; Navet, M.; Parker, D.; Port, M.; Rousseaux, O. *J. Am. Chem. Soc.* **2000**, *122*, 9781.
(109) Dunand, F. A.; Dickins, R. S.; Merbach, A. E.; Parker, D. *Chem. Eur. J*. **2001**, *7*, 5160.
(110) Dunand, F. A.; Aime, S.; Merbach, A. E. *J. Am. Chem. Soc.* **2000**, *122*, 1506.
(111) Aime, S.; Botta, M.; Ermondi, G.; Terreno, E.; Anelli, P. L.; Fedeli, F.; Uggeri, F. *Inorg. Chem*. **1996**, *35*, 2726.
(112) Kim, W. D.; Kiefer, G. E.; Huskens, J.; Sherry, A. D. *Inorg. Chem*. **1997**, *36*, 4128.
(113) Aime, S.; Botta, M.; Parker, D.; Williams, J. A. G. *J. Chem. Soc., Dalton Trans*. **1995**, 2259.
(114) Schumann, H.; Bottger, U. A.; Weisshofff, H.; Ziemer, B.; Zschunke, A. *Eur. J. Inorg. Chem*. **1999**, 1735.
(115) Peters, J. A.; Zitha-Bovens, E.; Corsi, D. M.; Geraldes, C. F. G. C. In *The Chemistry of Contrast Agents in Medical Magnetic Resonance Imaging*; Toth, E., Merbach, A. E., Eds.; Wiley: New York, 2001; Chapter 8, pp 315−381.
(116) Jenkins, B. G.; Lauffer, R. B. *Inorg. Chem*. **1988**, *27*, 4730.
(117) Geraldes, C. F. G. C.; Urbano, A. M.; Alpoim, M. C.; Hoefnagel, M. A.; Peters, J. A. *J. Chem. Soc., Chem. Commun*. **1991**, 656.
(118) Lammers, H.; Maton, F.; Pubanz, D.; Van Laren, M. W.; Van Bekkum, H.; Merbach, A. E.; Muller, R. M.; Peters, J. A. *Inorg. Chem*. **1997**, *36*, 2527.
(119) Fahrnow, A.; Petrov, O.; Platzek, J.; Raduchel, B.; Sülzle, D. *Inorg. Chem*. **1999**, *38*, 1134.
(120) Lowe, M. P.; Parker, D.; Reany, O.; Aime, S.; Botta, M.; Castellano, G.; Gianolio, E.; Pagliarin, R. *J. Am. Chem. Soc.* **2001**, *123*, 7601.
(121) Lowe, M. P.; Parker, D. *Inorg. Chim. Acta* **2001**, *317*, 163.
(122) Lowe, M. P.; Parker, D. *Chem. Commun*. **2000**, 707.
(123) Blair, S.; Lowe, M. P.; Mathieu, C. E.; Parker, D.; Senanayake, K. P. *Inorg. Chem*. **2001**, *40*, 5860.
(124) Swift, T. J.; Connick, R. E. *J. Chem. Phys*. **1962**, *37*, 307.
(125) Zhang, S.; Usu, K.; Sherry, A. D. *Angew. Chem., Int. Ed. Engl*. **1999**, *38*, 3192.
(126) Batsanov, A. S.; Beeby, A.; Bruce, J. I.; Howard, J. A. K.; Kenwright, A. M.; Parker, D. *Chem. Commun*. **1999**, 1011.
(127) Zhang, S.; Wu, K.; Biewer, H. C.; Sherry, A. D. *Inorg. Chem*. **2001**, *40*, 4284.
(128) Geier, G.; Jorgensen, C. K. *Chem. Phys. Lett*. **1971**, *9*, 263.
(129) Kostromina, N. A.; Tananaeva, N. N. *Russ. J. Inorg. Chem*. **1971**, *16*, 256.
(130) Yerly, F.; Dunand, F. A.; Toth, E.; Figueirinha, A.; Kovacs, Z.; Sherry, A. D.; Geraldes, C. F. G. C.; Merbach, A. E. *Eur. J. Inorg. Chem*. **2000**, 1001.
(131) Toth, E.; Ni Dhubhghaill, O. M.; Laurenczy, G.; Zékány, L.; Merbach, A. E. *Magn. Reson. Chem*. **1999**, *37*, 701.
(132) Latva, M.; Kankare, J.; Haapakka, J. *J. Coord. Chem*. **1996**, *38*, 85.
(133) Latva, M.; Kankare, J. *J. Coord. Chem*. **1998**, *43*, 121.
(134) Dubost, J. P.; Leger, J. M.; Langlois, M. H.; Meyer, D.; Schaefer, M. *Acad. Sci. Paris Ser. II* **1991**, *312*, 349.
(135) Corsi, D. M.; Van der Elst, L.; Muller, R. N.; van Bekkum, H.; Peters, J. A. *Chem. Eur. J*. **2001**, *7*, 1383.
(136) Aime, S.; Botta, M.; Barge, A.; Frullano, L.; Merlo, U.; Hardcastle, K. I. *J. Chem. Soc., Dalton Trans*. **2000**, 3435.
(137) Zhang, S. R.; Kovacs, Z.; Burgess, S.; Aime, S.; Terreno, E.; Sherry, A. D. *Chem. Eur. J*. **2001**, *7*, 288.
(138) Toth, E.; Pubanz, D.; Vanthey, S.; Helm, L.; Merbach, A. E. *Chem. Eur. J*. **1996**, *2*, 1607.
(139) Powell, D. H.; Ni Dhubhghaill, O. M.; Pubanz, D.; Helm, L.; Lebedev, Y.; Schloepfer, W.; Merbach, A. E. *J. Am. Chem. Soc.* **1996**, *118*, 9333.
(140) Kumar, K.; Chang, C. A.; Francesconi, L. C.; Dischino, D. D.; Malley, M. F.; Gougoutas, J. Z.; Tweedle, M. F. *Inorg. Chem*. **1994**, *33*, 3567.
(141) Lauffer, R. B.; Parmalee, D. J.; Dunham, S. U.; Ouellet, H. S.; Dolan, R. P.; Witte, S.; McMurry, T. J.; Walowitch, R. C. *Radiology* **1998**, *207*, 529.
(142) Aime, S.; Batsanov, A. S.; Botta, M.; Howard, J. A. K.; Lowe, M. P.; Parker, D. *New J. Chem*. **1999**, *23*, 668.
(143) Toth, E.; Vauthey, S.; Pubanz, D.; Merbach, A. E. *Inorg. Chem*. **1996**, *35*, 3375.
(144) Hardcastle, K. I.; Botta, M.; Fasano, M.; Digilio, G. *Eur. J. Inorg. Chem*. **2000**, 971.
(145) Botta, M. *Eur. J. Inorg. Chem*. **2000**, 399.
(146) Dickins, R. S.; Parker, D.; de Sousa, A. S.; Williams, J. A. G. *Chem. Commun*. **1996**, 697.
(147) Beeby, A.; Clarkson, I. M.; Dickins, R. S.; Faulkner, S.; Parker, D.; Royle, L.; de Sousa, A. S.; Williams, J. A. G.; Woods, M. *J. Chem. Soc., Perkin Trans. 2* **1999**, 493.
(148) Pagliarin, R.; Sisti, M.; Terreno, E. *Magn. Reson. Chem*. **1998**, *36*, 5200.
(149) Cohen, S. M.; Xu, J.; Radkov, E.; Raymond, K. N.; Botta, M.; Barge, A.; Aime, S. *Inorg. Chem*. **2000**, *39*, 5747.
(150) Aime, S.; Botta, M.; Crich, S. G.; Giovenzana, G. B.; Pagliarin, R.; Piccinini, M.; Sisti, M.; Terreno, E. *J. Biol. Inorg. Chem*. **1997**, *2*, 470.
(151) Aime, S.; Botta, M.; Frallano, L.; Geninatti Crich, S.; Giovenzana, G.; Pagliarin, R.; Palmisano, G.; Sirtori, F. R.; Sisti, M. *J. Med. Chem*. **2000**, *43*, 4017.
(152) Graeppi, N.; Powell, D. H.; Laurenczy, G.; Zekany, L.; Merbach, A. E. *Inorg. Chim. Acta* **1995**, *235*, 311.
(153) Messeri, D.; Lowe, M. P.; Parker, D.; Botta, M. *Chem. Commun*. **2001**, 2742.
(154) Aime, S.; Barge, A.; Botta, M.; Howard, J. A. K.; Lowe, M. P.; Moloney, J. M.; Parker, D.; de Sousa, A. S. *Chem. Commun*. **1999**, 1047.
(155) Vander Elst, L.; Laurent, S.; Muller, R. N. *Invest. Radiol*. **1998**, *33*, 828.

(156) Zucchi, G.; Scopellito, R.; Pittet, P. A.; Bunzli, J.-C. G.; Rogers, R. D. *J. Chem. Soc., Dalton Trans.* **1999**, 931.
(157) Aime, S.; Botta, M.; Fasano, M.; Paoletti, S.; Terreno, E. *Chem. Eur. J.* **1997**, *3*, 1499.
(158) Szilagyi, E.; Toth, E.; Brucher, E.; Merbach, A. E. *J. Chem. Soc., Dalton Trans.* **1999**, 2481.
(159) Aime, S.; Botta, M.; Fasano, M.; Crich, S. G.; Terreno, E. *J. Biol. Inorg. Chem*. **1996**, *1*, 312.
(160) Ren, J.; Springer, C. S.; Sherry, A. D. *Inorg. Chem*. **1997**, *36*, 3493.
(161) Corsi, D. M.; van Bekkum, H.; Peters, J. A. *Inorg. Chem*. **2000**, *39*, 4802.
(162) Aime, S.; Botta, M.; Fasano, M.; Terreno, E. In *The Chemistry of Contrast Agents in Medical Magnetic Resonance Imaging*; Toth E., Merbach, A. E., Eds.; Wiley: New York, 2001; Chapter 5, pp 193−242.
(163) Aime, S.; Botta, M.; Fasano, M.; Marques, M. P. M.; Geraldes, C. F. G. C.; Pubanz, D.; Merbach, A. E. *Inorg. Chem*. **1997**, *36*, 2059.
(164) Dickins, R. S.; Gunnlaugsson, T.; Parker, D.; Peacock, R. D. *Chem. Commun*. **1998**, 1643.
(165) Burai, L.; Hietopelto, V.; Kiraly, R.; Toth, E.; Brucher, E. *Magn. Reson Imaging* **1997**, *38*, 146.
(166) Dickins, R. S.; Love, C.; Puschmann, H. *Chem. Commun*. **2001**, 2308.
(167) Aime, S.; Botta, M.; Bruce, J. I.; Parker, D.; Mainero, V.; Terreno, E. *Chem. Commun*. **2001**, 115.
(168) Lammers, H.; van der Heijden, A. M.; van Bekkum, H.; Geraldes, C. F. G. C.; Peters, J. A. *Inorg. Chim. Acta* **1998**, *277*, 193.
(169) Aime, S.; Digilio, G.; Fasano, M.; Paoletti, S.; Arnelli, A.; Ascenzi, P. *Biophys. J*. **1999**, *76*, 2735.
(170) Lammers, H.; van der Heijden, A. M.; van Bekkum, H.; Geraldes, C. F. G. C.; Peters, J. A. *Inorg. Chim. Acta* **1998**, *268*, 249.
(171) Aime, S.; Botta, M.; Panero, M.; Giandi, M.; Uggeri, F. *Magn. Reson Chem*. **1991**, *29*, 923.
(172) Sherry, A. D.; Zarzycki, R.; Geraldes, C. F. G. C. *Magn. Reson. Chem*. **1994**, *32*, 361.
(173) Zitha-Bovens, E.; van Bekkum, H.; Peters, J. A.; Geraldes, C. F. G. C. *Eur. J. Inorg. Chem*. **1999**, 287.
(174) Aime, S.; Benetello, F.; Bombieri, G.; Colla, S.; Fasano, M.; Paoletti, S. *Inorg. Chim. Acta* **1997**, *254*, 63.
(175) Huskowska, E.; Riehl, J. P. *Inorg. Chem*. **1995**, *34*, 5615.
(176) Mortellaro, M. A.; Nocera, D. G. *J. Am. Chem. Soc.* **1996**, *118*, 7414.
(177) Rudzinski, C. M.; Hortmann, W. K.; Nocera, D. G. *Coord. Chem. Rev*. **1998**, *171*, 115.
(178) Ruszinski, C. M.; Engebretson, D. S.; Hartmann, W. K.; Nocera, D. G. *J. Phys. Chem. A* **1998**, *102*, 7442.
(179) Skinner, P. J.; Beeby, A.; Dickins, S.; Parker, D.; Aime, S.; Botta, M. *J. Chem. Soc., Perkin Trans. 2* **2000**, 1329.
(180) Bruce, J. I.; Lowe, M. P.; Parker, D. In *The Chemistry of Contrast Agents in Medical Magnetic Resonance Imaging*; Toth, E., Merbach, A. E., Eds.; Wiley: New York, 2001; Chapter 11, pp 437−460.
(181) Bünzli, J.-C. G.; Piguet, C. *Chem. Rev*. **2002**, *102*, 1897−1928.
(182) Ermolaev, V.; Sveshnikova, E. B. *Russ. Chem. Rev.* **1994**, *63*, 905.
(183) Beeby, A.; Dickins, R. S.; Faulkner, S.; Parker, D.; Williams, J. A. G. *Chem. Commun*. **1997**, 1747.
(184) Parker, D.; Senanayake, K.; Williams, J. A. G. *J. Chem. Soc., Perkin Trans. 2* **1998**, 2129.
(185) Selvin, P. R.; Rana, T. M.; Hearst, J. E. *J. Am. Chem. Soc.* **1994**, *116*, 6029.
(186) Alpha, B.; Lehn, J.-M.; Mathis, G. *Angew. Chem., Int. Ed. Engl*. **1987**, *26*, 266.
(187) Mukkala, V.-M.; Hetenius, M.; Hemmila, I.; Kankare, J.; Takalo, H. *Helv. Chim. Acta* **1993**, *76*, 1361.
(188) Sabbatini, N.; Guardigli, M.; Manet, I.; Ungaro, R.; Casnati, A.; Fischer, C.; Ziessel, R.; Ulrich, G. *New J. Chem*. **1995**, *19*, 137.
(189) Oude Wolbers, M. P.; van Veggel, F. C. J. M.; Snellink-Ruël, B. H. M.; Hofstraat, J. W.; Geurts, F. A. J.; Reinhoudt, D. N. *J. Chem. Soc., Perkin Trans. 2* **1998**, 2141.
(190) Dadabhoy, A.; Faulkner, S.; Sammes, P. G. *J. Chem. Soc., Perkin Trans. 2* **2000**, 2359.
(191) Beeby, A.; Bushby, L. M.; Maffeo, D.; Williams, J. A. G. *J. Chem. Soc., Perkin Trans. 2* **2000**, 1281.
(192) Werts, M. H. V.; Duin, M. A.; Hofstraat, J. W.; Verhoeven, J. *Chem. Commun*. **1999**, 799.
(193) Melby, L. R.; Rose, N. J.; Abramson, E.; Caris, J. C. *J. Am. Chem. Soc.* **1964**, *86*, 5125.
(194) Werts, M. H. V.; Woudenberg, R. H.; Emmerink, P. G.; van Gassel, R.; Hofstraat, J. W.; Verhoeven, J. W. *Angew. Chem., Int. Ed. Engl*. **2000**, *39*, 4542.
(195) Klink, S. I.; Alink, P. O.; Grave, L.; Peters, F. G. A.; Geurts, F.; van Veggel, F. C. J. M. *J. Chem. Soc., Perkin Trans. 2* **2001**, 363.
(196) Werts, M. H. V.; Verhoeven, J.; Hofstraat, J. W. *J. Chem. Soc., Perkin Trans. 2* **2000**, 433.
(197) van der Tol, E. B.; van Ramesdonk, H. J.; Verhoeven, J.; Steemers, F. J.; Kerver, E. G.; Verboom, W.; Reinhoudt, D. N. *Chem. Eur. J*. **1998**, *4*, 2315.
(198) Clarkson, I. M.; Beeby A.; Bruce, J. I.; Govenlock, L. J.; Lowe, M. P.; Mathieu, C. E.; Parker, D.; Senanayake, K. *New J. Chem*. **2000**, *24*, 377.
(199) Parker, D. In *Comprehensive Supramolecular Chemistry*; Atwood, J. E., McNicol, D. D., Davies, J. E. D., Vogtle, F., Reinhoudt, D. N., Lehn, J.-M., Eds.; Pergamon: New York, 1996; Vol. 10, pp 487−536,
(200) Sessler, J. L.; Tvermoes, N. A.; Guldi, D. M.; Mody, T. A.; Allen, W. E. *J. Phys. Chem. B* **1999**, *103*, 787.
(201) Sessler, J. L.; Tvermoes, N. A.; Guldi, D. M.; Hug, G. L.; Mody, T. L.; Magda, D. *J. Phys. Chem. B* **2001**, *105*, 1452.
(202) Salama, S.; Richardson, F. S. *Inorg. Chem*. **1980**, *84*. 512.
(203) Weber, M. J. *Phys. Rev*. **1968**, *171*, 283.
(204) Miniscalco, W. J. *J. Lightwave Technol.* **1991**, *9*, 234.
(205) Schaeffers, K. I.; Deloach, L. D.; Payne, S. A. *IEEE J. Quantum Electron*. **1996**, *32*, 741.
(206) Horrocks, W. de W.; Sudnick, D. R. *Acc. Chem. Res*. **1981**, *14*, 384.
(207) Horrocks, W. D. *Methods Enzymol*. **1993**, *226*, 495.
(208) Latva, M.; Kankare, J. *J. Coord. Chem*. **1998**, *43*, 121.
(209) Wu, S. L.; Horrocks, W. D. *Anal. Chem*. **1996**, *68*, 394.
(210) Wu, S. L.; Horrocks, W. D. *J. Chem. Soc., Dalton Trans*. **1997**, 1497.
(211) Bunzli, J.-C. G. In *Lanthanide Probes in Life, Chemical and Earth Sciences, Theory and Practices*; Bunzli, J.-C. G., Choppin, G. R., Eds.; Elsevier: Amsterdam, 1989; Vol. 7, pp 219−290.
(212) Ermolaev, V. L.; Gruzdev, V. P. *Inorg. Chim. Acta* **1984**, *95*, 179.
(213) Horrocks, W. de W.; Arkle, V. K.; Liotta, F. J.; Sudnick, D. R. *J. Am. Chem. Soc*. **1983**, *105*, 3455.
(214) de Silva, A. P.; Gunaratne, H. Q. N.; Rice, T. E. *Angew. Chem., Int. Ed. Engl*. **1996**, *35*, 2116.
(215) Reany, O.; Gunnlaugsson, T.; Parker, D. *J. Chem. Soc., Perkin Trans. 2* **2000**, 1819.
(216) Gunnlaugsson, T.; Parker, D. *Chem. Commun*. **1998**, 511.
(217) Bobba, G.; Kean, S. D.; Parker, D.; Beeby, A.; Baker, G. *J. Chem. Soc. Perkin Trans. 2* **2001**, 1738.
(218) Baxxicalupi, C.; Bencini, A.; Bianchi, A.; Giorgi, A.; Fusi, V.; Masotti, A.; Valtancoli, B.; Roque, A.; Pina, F. *Chem. Commun*. **2000**, 561.
(219) Parker, D.; Williams, J. A. G. *Chem. Commun*. **1998**, 245.
(220) Beeby, A.; Faulkner, S.; Parker, D.; Williams, J. A. G. *J. Chem. Soc., Perkin Trans. 2* **2001**, 1268.
(221) Amao, Y.; Okura, I.; Miyashita, T. *Chem. Lett*. **2000**, 934.
(222) Amao, Y.; Okura, I.; Miyashita, T. *Bull. Chem. Soc. Jpn*. **2000**, *73*, 2663.
(223) Kessler, M. A. *Anal. Chem*. **1999**, *71*, 1540.
(224) Lobnik, A.; Majcen, N.; Niederseiter, K.; Uray, G. *Sens. Actuators* **2001**, *B74*, 200.
(225) Hall, J.; Haner, R.; Aime, S.; Botta, M.; Faulkner, S.; Parker, D.; de Sousa, A. S. *New J. Chem*. **1998**, *22*, 627.
(226) Aime, S.; Botta, M.; Crich, S. G.; Giovenzana, G.; Palmisano, G.; Sisti, M. *Chem. Commun*. **1999**, 1577.
(227) Hovland, R.; Glogard, C.; Aasen, A. J.; Klaveness, J. *J. Chem. Soc., Perkin Trans. 2* **2001**, 929.
(228) Li, W.-H.; Fraser, S. E.; Meade, T. J. *J. Am. Chem. Soc.* **1999**, *121*, 1413.
(229) Ward, K. M.; Aletras, A. H.; Balaban, R. S. *J. Magn. Reson.* **2000**. *243*, 79.
(230) Zhang, S. R.; Winter, P.; Wu, K. C.; Sherry, A. D. *J. Am. Chem. Soc.* **2001**, *123*, 1517.
(231) Terreno, E.; Aime, S.; Barge, S.; Castelli, D. D.; Niesen, F. U. *J. Inorg. Biochem*. **2001**, *86*, 452.
(232) Desreux, J. F.; Humblet, V.; Hermann, M.; Jacques, V.; Paris, J.; Ranganathan, R. S.; Sauvage,. C.; Thonon, D.; Tweedle, M. F. *J. Inorg. Biochem*. **2001**, *86*, 41.
(233) Edlin, C. D.; Faulkner, S.; Parker, D.; Wilkinson, M. P.; Woods, M.; Lin, J.; Lasri, E.; Neth, F.; Port, M. *New J. Chem*. **1998**, *22*, 1359−64.
(234) Hanaoka, K.; Kikuchi, K.; Uromo, Y.; Nagano, T. *J. Chem. Soc., Perkin Trans. 2* **2001**, 1840.
(235) Alpha-Bazin, B.; Bazin, H.; Boissy, L.; Mathis, G. *Anal. Biochem*. **2000**, *286*, 1840.
(236) Mathis, G.; Socquet, F.; Viguier, M.; Darbouret, B. *Anticancer Res*. **1997**, *17*, 3011.
(237) Sherry, A. D.; Geraldes, C. F. G. C. In *Lanthanide Probes in Life, Chemical and Earth Sciences*; Bunzli, J.-C. G., Choppin, G. R., Eds.; Elsevier: Amsterdam, 1989; pp 93−126.
(238) Evans, C. H. *Biochemistry of Lanthanides*; Plenum: New York, 1990; Vol. 8.
(239) Bertini, I.; Luchinat, C. H. *Coord. Chem. Rev*. **1996**, *150*, 1.
(240) Wenzel, T. G. *NMR Shift Reagents*; CRC Press: Boca Raton, 1987.
(241) Geraldes, C. F. G. C. In *NMR in Supramolecular Chemistry*; Pans, M., Ed.; Kluwer: Netherlands, 1999; pp 133−154.
(242) Bleaney, B. *J. Magn. Reson*. **1972**, *8*, 91.

(243) Briggs, J. M.; Moss, G. P.; Randall, E. W.; Sales, K. D. *J. Chem. Soc., Chem. Commun.* **1972**, 1180.
(244) Martin, R. B. In *Calcium in Biology*; Spiro, T. G., Ed.; John Wiley: New York, 1983; Chapter 6.
(245) Lee, L.; Sykes, B. D. *Biochemistry* **1981**, *20*, 1156.
(246) Williams, T. C.; Corson, D. C.; Sykes, B. D. *J. Am. Chem. Soc.* **1984**, *100*, 5698.
(247) Sherry, A. D. In *Magnetic Resonance and the Kidney: Experimental and Clinical Applications*; Endre, Z. H., Ed.; Marcel Dekker: New York, 1996.
(248) Allegrozzi, M.; Bertini, I.; Janik, M. B. L.; Lee, Y. M.; Liu, G.; Luchinat, C. *J. Am. Chem. Soc.* **2000**, *122*, 4154.
(249) Horrocks, W. de W. In *NMR of Paramagnetic Molecules, Principles and Applications*; La Mar, G. N., Holm, R. H., Horrocks, W. de W., Eds.; Academic Press: London, 1973; Chapter 12.
(250) Reuben, J. *J. Chem. Soc., Chem. Commun.* **1979**, 68.
(251) Reuben, J. *J. Am. Chem. Soc.* **1980**, *102*, 2232.
(252) Kabuto, K.; Sasaki, Y. *J. Chem. Soc., Chem. Commun.* **1984**, 316.
(253) Kabuto, K.; Sasaki, Y. *J. Chem. Soc., Chem. Commun.* **1987**, 670.
(254) Kabuto, K.; Sasaki, Y. *Chem. Lett.* **1989**, 385.
(255) Hazama, R.; Umakoshi, K.; Kabuto, C.; Kabuto, K.; Sasaki. Y. *Chem. Commun.* **1996**, 15.
(256) Ogasawara, K.; Omata, K.; Kabuto, K.; Hasegawa, T.; Kojima, Y.; Sasaki, Y. *Org. Lett.* **2000**, *2*, 3543.
(257) Peters, J. A.; Vijverberg, C. A. M.; Kieboom, A. P. G.; van Bekkum, H. *Tetrahedron Lett.* **1983**, *24*, 3141.
(258) Kido, J.; Okamoto, Y.; Brittain, H. G. *J. Org. Chem.* **1991**, *56*, 1412.
(259) Hulst, R.; de Vries, N. K.; Feringa, B. L. *J. Org. Chem.* **1994**, *59*, 7453.
(260) Watanabe, M.; Hasegawa, T.; Mayake, H.; Kojima, Y. *Chem. Letts.* **2001**, 4.
(261) Gupta, R. K.; Gupta, P. *J. Magn. Reson.* **1982**, *47*, 344.
(262) Ren, J.; Springer, C. S.; Sherry, A. D. *Inorg. Chem.* **1997**, *36*, 3493.
(263) Pike, M. M.; Springer, C. S. *J. Magn. Reson.* **1982**, *46*, 348.
(264) Szklaruk, J.; Maracek, J. F.; Springer, A. L.; Springer, C. S. *Inorg. Chem.* **1990**, *29*, 660.
(265) Sherry, A. D.; Malloy, C. R.; Jeffrey, F. M. H.; Cacheris, W. P.; Geraldes, C. F. G. C. *J. Magn. Reson.* **1988**, *76*, 528.
(266) Buster, D. C.; Castro, M. M. C. A.; Geraldes, C. F. G. C.; Sherry, A. D.; Siemens, T. C. *Magn. Reson. Med.* **1990**, *15*, 25.
(267) Seshan, V.; Germann, M. J.; Preisig, P.; Malloy, C. R.; Sherry, A. D.; Bansal, N. *Magn. Reson. Med.* **1995**, *34*, 25.
(268) Piszczek, G.; Maliwal, B. P.; Gryczynski, I.; Dattelbaum, J.; Lakowicz, J. R. *J. Fluoresc.* **2001**, *11*, 101.
(269) Kimpe, K.; D'Olieslager, W.; Gorlier-Walrand, C.; Figuerinha, A.; Kovacs, Z.; Geraldes, C. F. G. C. *J. Alloys Compd.* **2001**, *323*, 828.
(270) Aime, S.; Barge, A.; Botta, M.; Fedel, F.; Mortilaro, A.; Parker, D.; Puschmann, H. *Chem. Commun.* **2002**, 1120.
(271) Bertini, I.; Donaire, A.; Jiminez, B.; Luchinat, C.; Parigi, G.; Piccoli, M.; Poggi, L. *J. Biomol. NMR* **2001**, *21*, 85.
(272) Prosser, R. S.; Shiyanovskaya, I. V. *Concepts Magn. Reson.* **2001**, *13*, 19.
(273) Platon, C.; Avecilla, F.; de Blas, A.; Geraldes, C. F. G. C.; Rodriguez-Blas, T.; Adams, H.; Mahia, J. *Inorg. Chem.* **1999**, *38*, 3190.
(274) Hopkins, T. A.; Metcalf, D. H.; Richardson, F. S. *Inorg. Chem.* **1998**, *37*, 1401.
(275) Rigault, S.; Piguet, C. *J. Am. Chem. Soc.* **2000**, *122*, 9304.
(276) Gunnlaugsson, T. *Tetrahedron Lett.* **2001**, *42*, 8901.
(277) Gunnlaugsson, T.; MacDonaill, D. A.; Parker, D. *J. Am. Chem. Soc.* **2001**, *123*, 12866.
(278) Bretonniere, Y.; Mazzanti, M.; Pecaut, J.; Dunand, F.; Merbach, A. E. *Inorg. Chem.* **2001**, *40*, 6737.
(279) Bruce, J. I.; Parker, D.; Tozer, D. J. *Chem. Commun.* **2001**, 2250.
(280) Bobba, G.; Frias, J.-C.; Parker, D. *Chem. Commun.* **2002**, 890.

CR010452+